

https://dspace.org/

The development of a supercritical extraction method to extract zero valent gold

Henderson, Marc Simon

2022
https://hdl.handle.net/10539/34899

Downloaded from a DSpace repository. https://dspace.org/



UNIVERSITY OF THE
WITWATERSRAND,
JOHANNESBURG

The development of a supercritical extraction method to extract zero valent gold.

MSc Research Dissertation

Prepared by

Marc Simon Henderson

1362073

Submitted to

School of Chemical and Metallurgical Engineering, Faculty of Engineering and the Built Environment, University of the Witwatersrand, Johannesburg, South Africa

Supervisors:

Mr Paul Den Hoed, Prof Herman Potgieter and Prof Lizelle Van Dyk

March 2022

University of the Witwatersrand, Johannesburg, South Africa

Faculty of Engineering and the Built Environment

School of Chemical and Metallurgical Engineering

Plagiarism Declaration

I, Marc Simon Henderson hereby declare the following:

I. I am aware that plagiarism (the use of someone else's work without their permission and/or without acknowledging the original source) is wrong.

II. I confirm that the work submitted for assessment for the above course is my own unaided work except where I have explicitly indicated otherwise.

III. I have followed the required conventions in referencing the thoughts and ideas of others.

IV. I understand that the University of the Witwatersrand may take disciplinary action against me if there is a belief that this is not my own unaided work or that I have failed to acknowledge the source of the ideas or words in my writing.

Signature:  Date: 30 March 2022

Abstract

South Africa's easily accessible, high grade gold ores are on the decline and as a result it is more expensive to mine the deeper, low grade ores. Companies such as DRD Gold have identified secondary gold deposits that now are economically feasible to process. The advantages of mining old tailings around the Witwatersrand basin are that the major processing costs such as crushing and grinding have already been incurred.

These secondary deposits contain free surface gold particles as well as gold which is locked up in refractory silicate and sulphide minerals (i.e. pyrite and quartz). The free gold particles can easily be removed through conventional hydrometallurgical processes such as cyanidation and carbon in leach. DRD Gold recovers around 60% of the gold from these tailings (grade of the tailings is typically around 0.31 g/t). To tap into the remaining 40%, supercritical CO_2 extraction has been proposed.

The supercritical fluid (SCF) is created by taking CO_2 to conditions above its critical temperature and pressure (>31°C and >73.8 Bar). The properties of a SCF are ideal for extracting valuable minerals as the CO_2 is able to penetrate into the ore due to its gas like diffusivity and the high pressures within the reactor. However CO_2 is non polar and thus a ligand is required to extract the gold. A fluorinated β-diketone (hexafluoroacetylacetone (HFA)), non-fluorinated β-diketone (acetylacetone (AcAc)) and an ionic liquid (betaine-bis(trifluoromethylsulfonyl)imide ([Hbet][TF_2N])) were selected as the ligands of interest for this research. To determine what ligand-oxidant combination had the most promising results, the ligands were mixed with either nitric acid (HNO_3) or hydrogen peroxide (H_2O_2). It was determined that the AcAc-HNO_3 system achieved the greatest gold extraction.

The following conditions were investigated to determine what effect they had on the amount of gold that could be extracted from a pure gold button; temperature (80-100 °C), concentration of HNO_3 (0-6.34 M), molar ratio of ligand to oxidant and volumetric ratio of ligand to oxidant. It was determined that the AcAc-HNO_3 system exhibited the most promising gold extraction results after an 8-hour extraction period. The gold was in excess so no meaningful percentage extraction could be calculated, however, the process was able to extract 64.65 mg of Au. This occurred at 100°C, 100 Bar, using a 1:1 molar ratio of AcAc to HNO_3 (6.34 M), the total volume of the oxidant-ligand

mixture was 23 mL, in a reactor fitted with a Hastelloy liner. It was found that corrosion in the form of co-leaching of Fe, Cr and Ni occurred for all extraction mixtures. The replacement of the Hastelloy liner with a Teflon liner showed decreased gold extraction pointing to a possible positive kinetic effect of these metals on the extraction reaction.

The newly developed method was used to treat tailings from the DRD Gold ERGO plant, and it was observed that the process could extract an additional 48.38% of the gold present in the ERGO plant tailing.

Acknowledgements

Firstly I would like to thank DRD Gold for sponsoring this research, without their generous contributions to the department of chemical and metallurgical engineering at Wits, this type of research would not be possible.

Thank you Prof Herman Potgieter for giving me the opportunity to complete my MSc and for always ensuring that I always had the required financial support. Thanks for your advice and support when we encountered setbacks as well as the discussions we had around the project when trying to find ways forward as well as guiding me during the write up of this thesis.

Thank you Paul den Hoed for always making time to help, whether it be to set up my experimental equipment, fix broken equipment, arranging for the collection of samples and for assisting with analyses. Most of all thank you for the countless hours that you spent helping me order my thoughts during the research as well as the write up and for teaching me how to tackle a problem from different perspectives.

Thank you Prof van Dyk for the valuable discussions we had and for your guidance during my MSc. Your insights and advice when writing up this thesis were invaluable, and as a result I have learnt how to think more critically about problems in general.

I would like to thank my mother and brother for all their support and for being there for me when things were not going as planned. Thanks for always lending an ear when I needed to discuss my research and for proof reading so much of my work.

Table of Contents

Plagiarism Declaration i

Abstract ii

Acknowledgements iv

List of Figures viii

List of Tables xii

Nomenclature and Abbreviations xiii

1 Introduction 1

1.1 Background 1

1.2 Problem statement 3

1.4 Research objectives 4

1.5 Research questions 5

1.6 Lay-out of dissertation 5

2 Literature Review 6

2.1 Witwatersrand Gold Ore Mineralogy 6

2.2 Chemistry of Gold 7

2.3 Pre-treatment processes 9

2.3.1 Roasting 10

2.3.2 Pressure Oxidation 11

2.3.3 Biological Oxidation 13

2.3.4 Microwaves 15

2.4 Leaching Processes 17

2.4.1 Cyanidation 17

2.4.2 Halide Leaching 20

2.4.3 Thiourea Leaching 22

2.4.4 Thiosulfate leaching 23

2.5 Supercritical Fluids 25

2.6 Ligands and their use for SFE 27
2.6.1 Dithiocarbamates 27
2.6.2 β-diketones 31
2.6.3 Organophosphorus 36
2.6.4 Macrocyclic compounds 41
2.7 Other metal extraction experiments 46
2.7.1 Gold Extraction using SCFs and different ligands 46
2.7.2 Plutonium and Uranium Extraction 47
2.7.3 E-waste Recycling 48
2.8 Summary 51
3 Experimental 52
3.1 Gold bearing materials 52
3.1.1 Tailings from gold processing at ERGO 52
3.1.2 Pure gold nugget 53
3.2 Experimental apparatus and operating procedure 53
3.3 Chemicals used and Reagent Preparations 56
3.4 Analytical Techniques Used 57
3.4.1 XRF Major 57
3.4.2 XRF Trace 57
3.4.3 XRD 58
3.4.4 Micro-Raman spectroscopy 58
3.4.5 AAS 58
3.4.6 ICP-OES and ICP-MS 58
3.5 Supercritical Gold Extraction Experiments 60
3.5.1 Initial extractions in [Hbet][TF_2N], TBP-HNO_3 and $ScCO_2$ 60
3.5.2 Evaluation of different gold extraction solutions in supercritical CO_2 60
3.5.3 Extraction of Gold from DRD Gold Ergo tailing 62

4 Results and Discussion 63

4.1 Characterisation of the Ergo tailings sample 63

4.2 Feasibility of gold extraction using [Hbet][TF_2N], TBP-HNO_3 and $ScCO_2$ 69

4.3 Developing a new SFE process without using Tributyl phosphate (TBP) 72

4.4 Examining what effect changing operating parameters has on Au extraction. . 82

4.5 Extraction of gold from gold tailings using an AcAc-HNO_3 -$ScCO_2$ system 88

5 Conclusion 91

5.1 To develop a method to analyse the pregnant leach solution produced in Mawire's (2019) extraction method. 91

5.2 To determine whether the extraction method proposed by Mawire (2019) is safe. 91

5.3 To determine if there is an alternative oxidant to the TBP-HNO_3 adduct used in Mawire's (2019) work and if so, investigate the extraction of gold in supercritical CO_2 utilising a new reagent mixture. 92

5.4 To determine if there is a ligand that can extract more gold than [Hbet][Tf_2N] and HFA. 92

5.5 To determine, by applying a more fundamental approach (using pure gold instead of tailings), under what conditions zero valent gold is extracted using supercritical fluids. 92

5.6 To apply the new method to a DRD Gold tailings sample. 93

5.7 Thoughts on the hypothesis. 93

5.8 Recommendations for future research 93

6 References 95

List of Figures

Figure 1.1: South African gold production from 1990-2019 (CEIC, 2020). 1

Figure 1.2: The ERGO operation (DRDGold, 2019).....2

Figure 2.1: Eh vs pH diagram for gold (Xue & Osseo-Asare, 1985).....7

Figure 2.2: Linear geometry of an aurous gold complex (Lorösch, 2001). 9

Figure 2.3: Square planar geometry of an auric gold complex(Lorösch, 2001). 9

Figure 2.4: Eh-pH diagram for Au-CN-H2O system (Xue & Osseo-Asare, 1985). 18

Figure 2.5: CN- ions lost to the formation of HCN at varying pH's (Marsden & House, 2006). 19

Figure 2.6: Steps involved in the dissolution of gold (Marsden & House, 2006).....20

Figure 2.7: CO_2 phase diagram (Glennon et al., 1999). 26

Figure 2.8: General structure of a dithiocarbamates (Ding et al., 2017). 27

Figure 2.9: Keto-enol tautomerism in β-diketones (Özel et al., 1997).....32

Figure 2.10: Enol vs Enolate form in β-diketones (Ding et al., 2017).....32

Figure 2.11:General chemical structures of different organophosphorus reagents (Ding et al., 2017; Erkey, 2000; Wai & Wang, 1997). 37

Figure 2.12: Crown ethers along with their associated cavity sizes (Steed, 2001). 42

Figure 2.13: Common crown ethers (Wang & Zhuang, 2020). 42

Figure 2.14: Different conformations of unsubstituted calix[4]arenes (Wang & Zhuang, 2020). 44

Figure 2.15: Tetragold complex (Silwa & Deska, 2008). 45

Figure 2.16: Fluorinated calixarene derivatives with lower rim sulphur donor atoms (Glennon et al., 1999). 45

Figure 2.17: Experimental setup that Mawire (2019) used. 47

Figure 2.18: Experimental set up used by Pitchaiah et al. (2019). Carbon dioxide cylinder (1), molecular sieve filter (2), carbon dioxide pump (3), co-solvent reservoir (4), co-solvent pump (5), six way valve (6), heat exchanger (7), high pressure extraction

vessel (8), oven (9), back pressure regulator (10) and collection vessel (11) (Pitchaiah et al., 2019).....48

Figure 2.19: Experimental setup used by Liu et al. (2016). 49

Figure 2.20: Experimental setup used by Argenta et al. (2017). Carbon dioxide cylinder (1), cooling bath (2), high pressure pump (3), extractor (4), heating bath (5), extracted sample (6) (Argenta et al., 2017).....50

Figure 3.1: Supercritical fluid extraction experimental setup, adapted from Mawire (2019).....54

Figure 3.2: Supercritical fluid reactor, adapted from Mawire (2019). 54

Figure 4.1: XRD diffractogram of the DRD Gold plant tailings [Cobalt anode - wavelength of 1.79 Å, 2 Theta range: 5-80 degrees and steps 0.0274 degrees]. 65

Figure 4.2: Micro-Raman spectra of three particles of pyrite (A−D). Figure A contains the identified pyrite spectrum. The blue, green and red spectra were produced from the pyrite particles identified in Figures B, C and D respectively (see the arrows). The pink spectrum is a reference pyrite sample from the RRUFF data base.....66

Figure 4.3: Molecular structure of crystalline precipitate (Trimethylammonioacetic acid nitrate). 71

Figure 4.4: Possible transport steps in the SFE process. 73

Figure 4.5: SFE of Au in different oxidants (20 mL HNO_3 or H_2O_2) and 3 mL of the ligands (Acetylacetone(AcAc), hexafluoroacetylacetone (HFA) and betaine bis(trifluoromethylsulfonyl)imide ([Hbet][TF_2N])) at 100 Bar, 80℃ for 8 h. 75

Figure 4 6: Metals extracted using AcAc/HFA with different oxidants after 8 hours at 100 Bar and 80℃. 78

Figure 4.7: AcAc-HNO_3 (20 mL of 6.34 HNO_3 and 3 mL AcAc) metal extraction over a temperature range (80-100℃) for 8 hr at 100 Bar.....79

Figure 4.8: AcAc-H_2O_2 (20 mL of 6.34 H_2O_2 and 3 mL AcAc) metal extraction over a temperature range (80-100℃) for 8 hr at 100 Bar.....80

Figure 4.9: HFA-HNO_3 (20 mL of 6.34 HNO_3 and 3 mL HFA) metal extraction over a temperature range (80-100℃) for 8 hr at 100 Bar (Au is in mg*100 so that the difference can be seen). 81

Figure 4.10: HFA-H_2O_2 (20 mL of 6.34 H_2O_2 and 3 mL HFA) metal extraction over a temperature range (80-100℃) for 8 hr at 100 Bar (Au is in mg*100 so that the difference can be seen). 81

Figure 4.11: Au extracted when varying the volumetric ratio of AcAc to HNO_3 (6.34 M) at 100 Bar and 100℃ for 8 hours. 83

Figure 4.12: Cr, Fe and Ni extracted when varying the ratio of AcAc to HNO_3 at 100 Bar and 100℃ for 8 hours. 83

Figure 4.13: Corrosion of the Hastelloy bucket. 84

Figure 4.14: Corrosion of the stainless steel reactor. 85

Figure 4.15: Metals extracted when using a Hastelloy bucket vs a Teflon liner at 100 Bar and 100℃ for 8 hours. 86

Figure 4.16: Au extracted when changing the molar ratio of AcAc to HNO_3 at 100 Bar and 100℃ for 8 hours. 87

Figure 4.17: The effect of HNO_3 concentration on the extraction of Au at 100 Bar and 100℃ for 8 hours. 88

List of Tables

Table 2.1: Substances and their critical points (Knez et al., 2019). 26

Table 2.2: Different dithiocarbamates (Adapted from: Ashraf-Khorassani et al., 1997a; Ding et al., 2017; Wai & Wang, 1997). 28

Table 2.3: Solubility Results from Laintz et al. (1997). 29

Table 2.4: Metal extraction results from Wai et al. (1996). 30

Table 2.5: Solubility results from Wai et al. (1996). 31

Table 2.6: Chemical structures for common β-diketones (Ashraf-Khorassani et al., 1997a; Ding et al., 2017; Erkey, 2000; Wai & Wang, 1997). 31

Table 2.7: Solubility results of some metal β-diketones from Ashrat-Khorassani et al. (1997b) 33

Table 2.8: Extraction efficiency results from Ashrat-Khorassani et al. (1997b). 33

Table 2.9: Extraction efficiencies for fluorinated β-diketones (Wai et al., 1996). 34

Table 2.10: Extraction of Co using different ligands (Özel et al., 1997). 35

Table 2.11: Co extraction using varying amounts of HFAA (Özel et al., 1997) 35

Table 2.12: Chemical names, abbreviations and R groups for organophosphorus reagents. (Ding et al., 2017; Erkey, 2000; Wai & Wang, 1997). 37

Table 2.13: Metal Extraction using different chelating agents and modifiers (Ghoreishi et al., 2016). 39

Table 2.14: Continuation of Table 2.13. 39

Table 2.15: The findings from Liu et al. (2016). 50

Table 3.1: Instrument settings used for ICP-MS and ICP-OES. 59

Table 3.2: Gold extraction in [Hbet][TF2N], TBP-HNO_3 and $ScCO_2$. 60

Table 3.3: Screening experiments of the different ligand-oxidant systems. 61

Table 3.4: Experiments to determine the effect that changing temperature has on the system. 61

Table 4.1: Chemical composition of tailings†. 63

Table 4.2: XRF trace element analysis†. 64

Table 4.3: Au in the sample of DRD Gold tailings tested.....67

Table 4.4: Surface area of gold particles assuming a set mass and that particles are spherical.....74

Table 4.5: Metal analysis of the tailings residue at experimental conditions 100°C, 100 Bar, 8 hours and 23 mL ligand-oxidant solution (1:1 molar ratio).....89

Nomenclature and Abbreviations

Notation/Unit	Meaning
$ScCO_2$	Supercritical carbon dioxide
SFE	Supercritical fluid extraction
SCF	Supercritical Fluid
TBP	Tributyl phosphate
TBP-HNO_3	Tributyl phosphate nitric acid adduct
AcAc	Acetylacetone
HFA	Hexafluoroacetylacetone
[Hbet][TF_2N]	Betaine-bis(trifluoromethylsulfonyl)imide
HNO_3	Nitric acid
H_2O_2	Hydrogen peroxide
β-diketone	Beta-diketone
ICP-MS	Inductively coupled plasma –mass spectrometry
ICP-OES	Inductively coupled plasma atomic emission spectroscopy
AAS	Atomic absorption spectroscopy
XRF	X-ray fluorescence
XRD	X-ray diffraction
μRS	Micro-Raman spectroscopy
LOI	Loss on ignition
MSDS	Safety data sheet
Au^+	Gold with a valency of plus 1
Au^{3+}	Gold with a valency of plus 3
Au^0	Zero valent gold
Mtpm	Million tonnes per month

1 Introduction

1.1 Background

The mining industry is of great economic importance to South Africa. In 2019 the mining industry contributed R360.90 billion to the country's gross domestic product (GDP) (Minerals Council South Africa, 2020). In particular, gold mining has played a crucial role in the development of South Africa and contributed R72.60 billion to the GDP in 2019 (Minerals Council South Africa, 2020). In 1884, prospectors discovered gold in what is known today as the Witwatersrand basin, an area which holds the largest known gold deposit in the world (Minerals Council South Africa, 2020). The discovery of gold in the Witwatersrand basin led to the development of Johannesburg, which is known as the city of gold. The South African gold industry was responsible for producing around 30% of the world's gold in 1899 (Britannica, 2020). This increased to 66.6% by 1981 resulting in South Africa becoming the world's largest gold producer (Nicoli, 1995). Figure 1.1 has been drawn using data from the census and economic information centre (CEIC, 2020), and illustrates South Africa's gold production rates over the last 30 years.

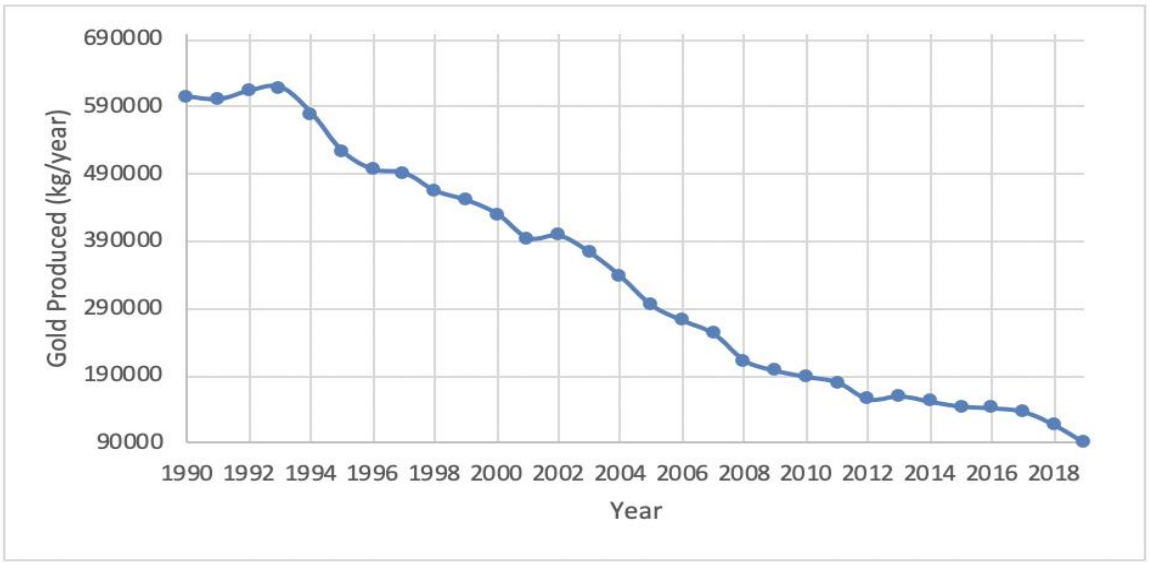


Figure 1.1: South African gold production from 1990-2019 (CEIC, 2020).

There is a decreasing trend (see Figure 1.1) in gold production, which can be attributed to a decrease in high grade ore and the rising costs of mining (Nicoli, 1995). The rising costs are due to the fact that mining companies are having to go deeper underground to find gold for mining (as mines age). Gold mining companies have identified a secondary source of gold that is cheaper to mine, i.e. old mine tailings. Tailings refer to the waste material that is produced by mines and is ore that has had most of the valuable minerals extracted. These tailings are still a viable source of gold as the mining and main processing costs have already been incurred (Muir et al., 2005). For example, the blasting and mine transportation costs alone account for 40% of the production costs (Heiser, 2014).

Anglo American commissioned a plant in 1997 called the ERGO plant to recover gold and uranium from old mine tailings (Heiser, 2014). The aforementioned tailings are from mining activities that occurred on the Witwatersrand basin during the early 1900s and mid 1960s (Muir et al., 2005). The ERGO plant (see Figure 1.2) can process 1.8 Mtpm of ore (DRDGold, 2019). The material is fed to the plant via pipelines as the tailings are reclaimed through high pressure hydromechanical mining (DRDGold, 2019).

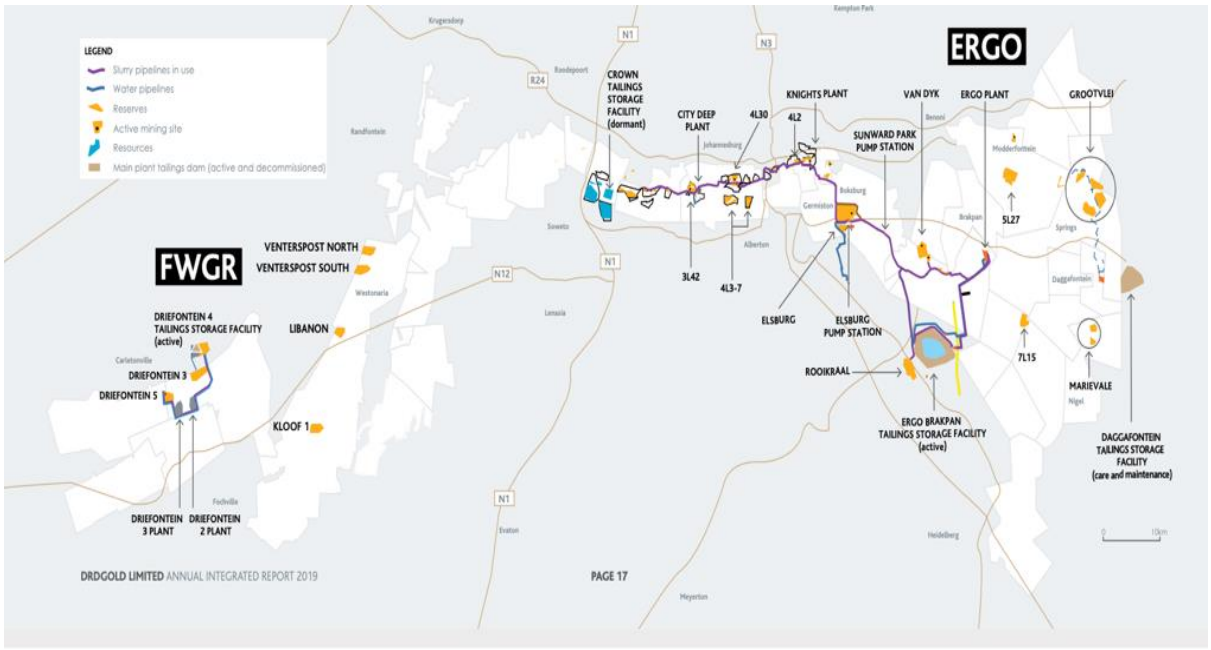


Figure 1.2: The ERGO operation (DRDGold, 2019).

According to DRD Gold (2019) the plant feed contains the same minerals as those found in the Witwatersrand basin, namely quartz (70-80%), mica (10%), chlorite and chloritoid (9-18%), pyrite (1-2%), Au (<100 ppm), U(<100 ppm), Zr (<100 ppm) and Cr(<100 ppm). The tailings originally underwent sulphide flotation and fine grinding (flotation concentrate) followed by high and or low grade (flotation tailings) carbon in leach to remove the gold from the slurry (DRDGold, 2019). However, recently the flotation, flotation grinding and high grade carbon in leach/carbon in pulp (CIL/CIP) circuits were all closed down. The reason for closing the above-mentioned circuits was that the plant costs versus the gold recovery were not economical. At present the tailings are pumped to the plant where its slurry density is adjusted before sending the material directly to CIL. The process utilizes zinc precipitation to recover the gold from the leach solution instead of electrowinning as the base metal concentration in solution is high and affects the electrowinning process. Consequently, zinc precipitation is a better option as it is not sensitive to the base metal concentration (DRDGold, 2019).

The grade of the tailings entering the plant are reported to be 0.31 g/t (DRDGold, 2019). The yield of the Ergo plant was reported to be 0.194 g/t and the total gold production from the plant was 4493 kg for 2019 (DRDGold, 2019). This means that the gold recovery is around 60%, with the remaining gold most likely trapped in refractory minerals and thus unrecoverable. The ERGO operation is losing as much as 40% of the gold to its plant tailings. There is clearly a need for a process which can extract additional gold locked up in the refractory minerals. The DRD Gold research group at the University of the Witwatersrand is exploring different technologies for the recovery of the gold from the ERGO tailings.

Supercritical fluid extraction of gold has been proposed by Mawire (2019) and preliminary studies have shown promise in the extraction of gold from this low grade refractory ore. As this work was preliminary, the research is ongoing in the group and forms the basis of this research.

1.2 Problem statement

Preliminary research into the supercritical extraction of gold, from DRD gold tailing samples, screened different extractants and has shown that up to 82% gold extraction is achievable with betaine-bis(trifluoromethylsulfonyl)imide ([Hbet][TF_2N]) in a TBP-

HNO_3 adduct (Mawire, 2019). Additional optimization work with [Hbet][TF_2N] showed a dependence of gold extraction on the temperature, pressure and the amount of solids loaded into the reactor. Experimental analysis of gold in solution posed a problem with the formation of a bi-phasic pregnant solution and results of the gold extraction could only be calculated based on gold analysis of the solid residue (Mawire, 2019). This poses a challenge when doing metal accounting in a plant. Additionally, no work was done to describe the mechanisms of extraction and little consideration were given to the health and safety of the proposed process.

1.3 Research hypothesis

It is expected that the SFE processes proposed in this research will be able to extract gold which is locked up in refractory minerals in a safe and efficient manner.

1.4 Research objectives

The objectives for the research are as follow:

- To develop a method to analyse the pregnant leach solution produced in Mawire's (2019) extraction method.
- To determine whether the proposed extraction method is safe.
- To determine if there is an alternative oxidant to the TBP-HNO_3 adduct used in Mawire's process and if so, investigate the extraction of gold in supercritical CO_2 utilizing a new reagent mixture.
- To determine if there is a ligand that can extract more gold than [Hbet][TF_2N] and HFA.
- To determine, by applying a more fundamental approach (using pure gold instead of tailing), under what conditions zero valent gold is extracted using supercritical fluids. This will be achieved by studying the influence of operating conditions.
- To apply the new method to a DRD Gold sample.

1.5 Research questions

The research questions that will be answered are as follow:

- Is the extraction method developed by Mawire (2019) safe?
- Can the pregnant leach solution be analysed with ease?
- If the answer to the first two questions is no, is there an acid (either polar or non-polar) that can replace the TBP-HNO_3 adduct?
- If one considers an alternative to the fluorinated β-diketones (i.e HFA), such as a non-fluorinated β-diketone (i.e. acetylacetone), is there a marked difference in gold extracted?
- If an alternative process is proposed, will it be capable of extracting zero valent gold and what effect does changing the ligand used, operating temperature, acid concentration and material of construction (of the reactor) have on the amount of gold extracted?
- What molar ratio of ligand to acid is required to extract the greatest amount of gold and what does this tell one about the possible reaction that is taking place?
- If an alternative process is proposed, can it be used to extract gold from the DRD Gold tailings? If so, what gold extractions can be achieved?

1.6 Lay-out of dissertation

Chapter 1 gives the background, motivation, and the objectives of the research. Chapter 2 contains a review of the current literature and includes a general discussion on the Witwatersrand gold ore mineralogy, the chemistry of gold, as well as the pretreatment and leaching techniques used in the gold mining industry. The literature review then focuses on what supercritical fluids are, the types of ligands suitable for use in the supercritical fluid extraction (SFE) process and finally describes research that has been conducted around the use of supercritical fluids for metal extraction. Chapter 3 covers the samples and reagents used and describes the experimental procedures that were followed. Chapter 4 presents and discusses the results. Finally, chapter 5 contains the conclusions from the research as well as propose future research questions that could add value to this body of work.

2 Literature Review

2.1 Witwatersrand Gold Ore Mineralogy

The mineralogy of an ore dictates the mineral processing and extraction techniques required to recover the minerals of interest. Gold deposits occur in two forms: as gold ores or placer deposits (Harris, 1990). Ore deposits describe a naturally occurring collection of valuable minerals (i.e., minerals of economic importance) and gangue minerals (Lurie, 2013). Placer deposits result from the weathering of ore deposits, leading to an accumulation of a stable metals/minerals within an area (Lurie, 2013). The gold deposits found within the Witwatersrand supergroup are referred to as buried placer deposits (Lurie, 2013). The ore mineralogy found within the Witwatersrand supergroup is complex and can be divided into two main groups, namely the Central Rand Group and the West Rand Group (Lurie, 2013). The lithologies of the two groups are made up of conglomerates, quartzite and shale (Lurie, 2013; Nwaila et al., 2013).

Gold found in the Witwatersrand reefs (mineral deposits), is present within conglomerates (Pretorius, 1974) which consists of rounded pebbles and a complex matrix of minerals. The rounded pebbles are mainly made up of quartz and other minerals such as pyrite, shale, jasper and schist (Janisch, 1986; Nwaila et al., 2013). These pebbles, despite accounting for around 70% of the conglomerates' volume, do not contain any minerals of interest (i.e., no gold, uranium, silver etc) (Janisch, 1986).

The complex matrix of the conglomerates contains the minerals of interest. The matrix is quartzitic in nature and contains sericite, sulphide minerals (i.e., pyrite), chlorite, muscovite and pyrophyllite (Janisch, 1986; Nwaila et al., 2013). Janisch (1986) reported the conglomerate composition as composing of quartz (70 -90%), sericite along with chlorite, pyrophyllite and chloritoid (10-30%), pyrite (3-4%), other sulphide minerals (1-2%), heavy detrital minerals (1-2%) and uriniferous kerogen (1%). The gold occurs as native gold particles which are usually associated with pyrite, quartz or uranite, but it can also present as an alloy with silver (electrum) (Nwaila et al., 2013; Pretorius, 1974). Gold present as free gold, electrum or in oxides is generally easily accessible through conventional leaching processes. Whereas, gold that is associated with

refractory sulphide minerals and quartz is more difficult/expensive to extract using conventional leaching techniques.

2.2 Chemistry of Gold

Gold is a precious metal and it is the most noble of all the metallic elements (Yannopoulos, 1991). Gold's inertness means that it cannot be dissolved easily in aqueous solutions that do not contain oxidants as it is not attacked/oxidized by strong acids such as HF, H_2SO_4, HNO_3 and HCl. This also applies to alkalis (Lorösch, 2001). Gold is also resistant to attack by sulphur or oxygen at high temperatures (Yannopoulos, 1991). Figure 2.1 depicts an Eh-pH diagram of the Au-H_2O system which illustrates just how stable gold is (Xue & Osseo-Asare, 1985).

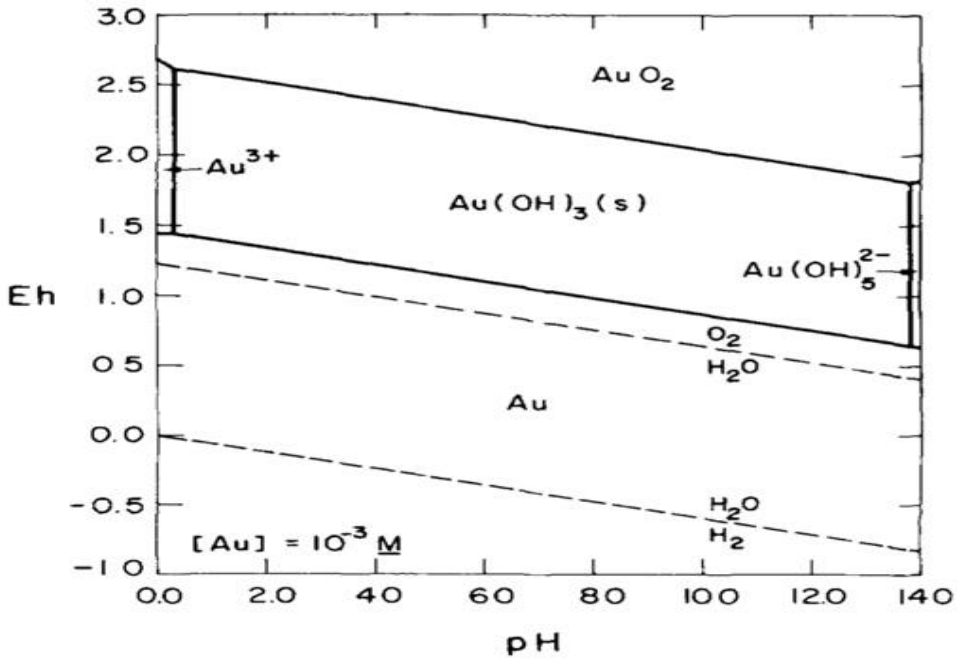


Figure 2.1: Eh vs pH diagram for gold (Xue & Osseo-Asare, 1985).

As mentioned above, gold is generally unreactive. However, there are a few instances where it can react with other substances. Halogens cause reactions with gold and the stabilities of the gold complexes formed tend to have the following trend: $I^- > Br^- > Cl^- > F^-$ (Friend & Wise, 1964; Lorösch, 2001). Gold can also react in chloride solutions, cyanide solutions or in solutions that produce chlorine (Glennon et al., 1999). Examples of the above-mentioned reactions are as follows:

- When gold reacts with bromine, this reaction is exothermic and occurs spontaneously at room temperature (Yannopoulos, 1991):

$$3Br_{2\,(l)} + 2Au_{\,(s)} \rightarrow Au_2Br_{6\,(s)} \quad (1)$$

- Aqua regia (chloride solution) attacks gold (Yannopoulos, 1991):

$$Au_{(s)} + HNO_{3\,(aq)} + 4HCl_{(aq)} \rightarrow H(AuCl_4)_{(aq)} + 2H_2O_{(l)} + NO_{(g)} \quad (2)$$

- The dissolution of gold in a cyanide solution is possible when the system is aerated or contains hydrogen peroxide (Glennon et al., 1999). This reaction is referred to as the Elsner equation (Yannopoulos, 1991):

$$4Au_{(s)} + 8NaCN_{(aq)} + O_{2\,(g)} + 2H_2O_{(l)} \rightarrow 4Na(Au(CN)_2)_{(aq)} + 4NaOH_{(aq)} \quad (3)$$

Gold complexes can be formed in solution as either aurous (Au^+) or auric (Au^{3+}) (Lorösch, 2001; Nicol et al., 1987). However, neither of these oxidation states are stable in an aqueous solution and therefore they have to be stabilized through the addition of suitable complexing agents/ligands (Nicol et al., 1987). The aurous and auric states do not occur as Au^+ and Au^{3+} ions in solution, they occur as hydrated complexes, i.e. they are bonded to water molecules (Nicol et al., 1987). However, if stronger ligands are present in solution, then the Au^+ and Au^{3+} ions will substitute the water molecules for the stronger ligands.

It has been mentioned above that the Au^+ and Au^{3+} ions are stabilized through the addition of ligands and this is due to the fact that ligands provide the electron lone pairs that the gold needs to complete its outer electron shell (Lorösch, 2001). H_2O, NH_2, CN^- and OH^- are examples of some basic ligands (Nicol et al., 1987).

The aurous and auric states are known as β-type metal ions. This means that as the electronegativity of the ligand used increases, so does the stability of the complexes that form (Nicol et al., 1987). The aurous oxidation state forms very stable complexes

when so called "soft" ligands containing sulphur and phosphorous are used (Glennon et al., 1999). When a ligand is referred to as soft, it simply means that it a soft Lewis base. Cyanide, thiourea, thiocyanate and thiosulphate are all examples of "soft" ligands (Lorösch, 2001). The aurous oxidation state has a $4f^{14}5d^{10}$ electron configuration (closed shell) and the complexes formed tend to have a linear geometry (Lorösch, 2001; Nicol et al., 1987). Figure 2.2 illustrates the linear geometry of the aurous complex that is formed with cyanide ($Au(CN)_2^-$).

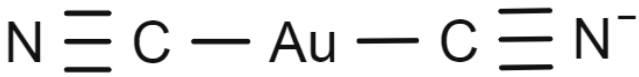


Figure 2.2: Linear geometry of an aurous gold complex (Lorösch, 2001).

The auric oxidation state forms very stable complexes with "hard" Lewis bases and thus can form complexes with both the "hard" and "soft" ligands (Nicol et al., 1987). Thus Au^{3+} can form complexes with ligands such as F^-, NH_3 and Cl^- (Lorösch, 2001; Nicol et al., 1987). The valence electron configuration of Au^{3+} is $4f^{14}5d^8$ and the complexes formed tend to be square planar, so they have a co-ordination number of 4 (Lorösch, 2001). Figure 2.3 illustrates this geometry:

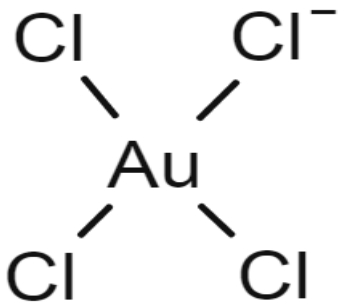


Figure 2.3: Square planar geometry of an auric gold complex(Lorösch, 2001).

2.3 Pre-treatment processes

The leaching of Au ores that contain sulfide minerals and carbonaceous material proves to be problematic. These ores are referred to as refractory. The main problems associated with the leaching of refractory Au ores are the poor Au recoveries along with the large amounts of lixiviant that is consumed (Marsden & House, 2006). These refractory ores thus need to undergo pretreatment processes such as pressure oxidation, biological oxidation, microwave degradation or roasting (Marsden &

House, 2006; Yannopoulos, 1991). The processes mentioned above can be classified as either hydrometallurgical or pyrometallurgical processes. They are used to make the refractory ores more amenable to leaching processes (Marsden & House, 2006; Yannopoulos, 1991).

2.3.1 Roasting

Roasting is a pyrometallurgical pretreatment technique that is used when treating refractory ores or concentrates (Marsden & House, 2006; Yannopoulos, 1991). The aim of roasting refractory ores is to liberate precious metals which are encapsulated by sulfide minerals, as well as to remove any carbonaceous materials (Altinkaya, 2008; Yannopoulos, 1991). The pretreatment of refractory gold ores and concentrates before cyanide leaching has long been achieved through roasting processes (La Brooy et al., 1994; Yannopoulos, 1991). This is due to the cost effectiveness of roasting. However, roasting produces sulphur dioxide (SO_2), which is harmful to the environment. Strict environmental regulations for SO_2 emissions have thus required the use of costly equipment to control the SO_2 emissions (La Brooy et al., 1994). The production of SO_2 can be seen in Equation 4.

There are many different types of roasting processes, depending on the oxidant used. Roasting is done at high temperatures with an oxidant such as air or pure O_2 (Marsden & House, 2006). The temperature at which roasting is conducted is very important (Marsden & House, 2006). If the temperature is too low, below 450^{o}C, then the oxidation rates will not be acceptable (Marsden & House, 2006). On the other hand, if the temperatures are too high, 700-750^{o}C, this may cause flash roasting (Marsden & House, 2006; Yannopoulos, 1991). Flash roasting results in calcine fusing (Yannopoulos, 1991). The calcine fusion is not ideal as it can cause gold encapsulation, resulting in lower gold recoveries during leaching (Yannopoulos, 1991).

The desired product of roasting is an iron oxide calcine, which is porous and ideally hematite should be formed (Marsden & House, 2006; Yannopoulos, 1991). The formation of hematite is important as it has finer grains than magnetite, which improves gold particle exposure (Yannopoulos, 1991). During roasting, the fine gold particles within the sulfide minerals migrate towards the grain boundaries (Marsden

& House, 2006). The porous iron oxide calcines formed along with its lowered amounts of carbonaceous material, makes leaching processes more efficient (Marsden & House, 2006).

The oxidation of minerals such as pyrite and arsenopyrite are exothermic (Yannopoulos, 1991), and this is ideal as it provides heat to the roasting system. If an ore contains large amounts of pyrite, then the roasting temperature is between 650 and 700°C (La Brooy et al., 1994). Any pyrite that is converted into hematite does so through Equation 4 (La Brooy et al., 1994; Yannopoulos, 1991).

$$4FeS_{2\,(s)} + 11O_{2\,(g)} \rightarrow 2Fe_2O_{3\,(s)} + 8SO_{2\,(g)} \quad (4)$$

2.3.2 Pressure Oxidation

Pressure oxidation is an aqueous hydrometallurgical pretreatment technique, which is used to treat refractory ores before they undergo leaching (Fraser et al., 1991). Pressure oxidation, like roasting, is a well-established pretreatment method in industry (La Brooy et al., 1994). The process is carried out in an autoclave as it requires high temperatures and pressures. This means that pressure oxidation is costly in terms of both the equipment required and the operating conditions (Marsden & House, 2006). The advantage of using pressure oxidation is that it can oxidise more than 90 percent of the sulfide minerals (Marsden & House, 2006).

Pressure oxidation can be conducted at low or high pressures. Low pressure oxidation is used when the ore is moderately refractory (Marsden & House, 2006). Moderately refractory ore means that the Au is not intimately associated with the sulfide minerals (Marsden & House, 2006). The process only achieves partial sulfide oxidation due to the low solubility of O_2 in water, under atmospheric conditions (Marsden & House, 2006). This process is therefore a cheaper alternative to high pressure oxidation as it can be done in an agitated tank at pH's between 8 and 11 (Marsden & House, 2006). These higher pH's don't cause highly corrosive environments as seen when high pressure acidic oxidation is used.

High pressure oxidation is done in an autoclave and can either be performed under acidic or alkaline conditions. High pressure acidic oxidation is generally used for refractory ores that have high sulfur contents (Marsden & House, 2006). The oxidation is conducted at pH's lower than 2 (La Brooy et al., 1994). The use of oxygen at high temperatures and pressures results in rapid oxidation of the sulfide minerals (Marsden & House, 2006). The temperature at which the oxidation is done is very important. At low temperatures (100-170°C), elemental sulfur is produced when oxidising sulfide minerals such as pyrite and pyrrhotite (La Brooy et al., 1994; Marsden & House, 2006). The oxidation of the above-mentioned minerals below 170°C can be represented by Equations 5 and 6 (Marsden & House, 2006).

$$2FeS_{2\,(s)} + O_{2\,(g)} + 4H^{+}{}_{(aq)} \rightleftharpoons 2Fe^{2+}{}_{(aq)} + 4S_{(s)} + 2H_2O_{(l)} \quad (5)$$

$$2Fe_7S_{8\,(s)} + 7O_{2\,(g)} + 28H^{+}{}_{(aq)} \rightleftharpoons 14Fe^{2+}{}_{(aq)} + 16S_{(s)} + 14H_2O_{(l)} \quad (6)$$

The production of elemental sulphur is not ideal as it can coat the gold particles. Such passivation of the gold particles thus reduces the Au dissolution during leaching processes. However, if the temperature is maintained above 170°C, then the elemental sulphur is oxidized to a sulfate (La Brooy et al., 1994; Marsden & House, 2006). The sulphur is oxidized according to Equation 7 (Marsden & House, 2006).

$$2S_{(s)} + 3O_{2\,(g)} + 2H_2O_{(l)} \rightleftharpoons 4H^{+}{}_{(aq)} + 24SO_4^{2-}{}_{(aq)} \quad (7)$$

In practice, the optimum operating conditions are pressures between 11 and 32 Bar at temperatures between 170 and 225°C (La Brooy et al., 1994). The oxidation of pyrite and pyrrhotite at these higher temperatures can thus be represented by Equations 8 and 9 (Marsden & House, 2006).

$$2FeS_{2\,(s)} + 7O_{2\,(g)} + 2H_2O_{(l)} \rightleftharpoons 2FeSO_{4\,(aq)} + 2H_2SO_{4\,(aq)} \quad (8)$$

$$2Fe_7S_{8\,(s)} + 31O_{2\,(g)} + 2H_2O_{(l)} \rightleftharpoons 14FeSO_{4\,(aq)} + 2H_2SO_{4\,(aq)} \quad (9)$$

High pressure acidic oxidation is however expensive. The required high pressures, acidic reaction conditions and the exothermic nature of the above-mentioned reactions necessitate the use of special materials of construction along with good temperature and pressure control. Titanium, a high cost metal, is often used as a material of construction for high pressure oxidation process equipment (Yannopoulos, 1991).

High pressure non-acidic oxidation is very similar to high pressure acidic oxidation, except that it is conducted under neutral to slightly alkaline conditions (La Brooy et al., 1994). This process is only suitable for ores which contain low amounts of sulfide minerals, but high amounts of carbonates (La Brooy et al., 1994). The carbonates are lixiviant consuming and thus are removed before leaching (Marsden & House, 2006). This process is cheaper when compared to high pressure acidic oxidation as the plant costs are lower, however the Au recovery rate is lower (La Brooy et al., 1994).

2.3.3 Biological Oxidation

Biological oxidation is a hydrometallurgical pretreatment technique. It can be used when treating low grade, refractory ores, and tailings (de Carvalho et al., 2019; Kaksonen et al., 2014). This oxidation process involves the use of microorganisms for the degradation of refractory iron and sulfide minerals (Altinkaya et al., 2018; Yannopoulos, 1991). It is an environmentally friendly and cost-effective process, which is typically used in heap, dump, or agitated leaching tanks (Altinkaya et al., 2018; de Carvalho et al., 2019; Syed, 2012). When compared to roasting and pressure oxidation, it is the cheapest pretreatment technique for treating low grade sulfide ores (La Brooy et al., 1994). One of the reasons for biological oxidation being cheap is that it does not produce SO_2 like roasting processes (de Carvalho et al., 2019). This means that there is no need for expensive gas capturing technologies.

Low-grade gold ores may contain iron-sulfide minerals such as pyrite (FeS_2), arsenopyrite (FeAsS), chalcopyrite ($CuFeS_2$) or pyrrhotite (FeS/Fe_7S_8) (de Carvalho et al., 2019; Yannopoulos, 1991). The sulfide minerals are associated with gold particles, as the gold is encapsulated by these minerals (de Carvalho et al., 2019; Yannopoulos, 1991). As mentioned before, this makes the dissolution of gold through typical

leaching processes very difficult. However, certain microorganisms can oxidise these minerals, releasing the Au (Yannopoulos, 1991).

The oxidation of the sulfide and iron minerals provide the microorganisms with energy (Marsden & House, 2006). This is achieved by oxidising ferrous iron (Fe^{2+}) to ferric iron (Fe^{3+}) and the sulfide minerals into H_2SO_4 (Altinkaya et al., 2018). Some of the oxidation reactions for pyrite and arsenopyrite when using microorganisms can be seen in Equations 10-15 (Marsden & House, 2006; Yannopoulos, 1991):

$$2FeS_{2\,(s)} + 7O_{2\,(g)} + 2H_2O_{(l)} \rightarrow 2FeSO_{4\,(aq)} + 2H_2SO_{4\,(aq)} \quad (10)$$

$$2FeS_{2\,(s)} + O_{2\,(g)} + 2H_2SO_{4\,(aq)} \rightarrow 2FeSO_{4\,(aq)} + 2H_2O_{\,(l)} + 4S_{\,(s)} \quad (11)$$

$$4FeAsS_{(s)} + 13O_{2\,(g)} + 6H_2O_{\,(l)} \rightarrow 4FeSO_{4\,(aq)} + 4H_3AsO_{4\,(aq)} \quad (12)$$

$$4FeSO_{4\,(aq)} + O_{2\,(g)} + 2H_2SO_{4\,(aq)} \rightarrow 2Fe_2(SO_4)_{3\,(aq)} + 2H_2O_{\,(l)} \quad (13)$$

$$2H_3AsO_{3\,(aq)} + O_{2\,(g)} \rightarrow 2H_3AsO_{4\,(aq)} \quad (14)$$

$$2S_{\,(s)} + 3O_{2\,(g)} + 2H_2O_{\,(l)} \rightarrow 2H_2SO_{4\,(aq)} \quad (15)$$

Biological oxidation is conducted at low pH's, around pH 1-1.8, as these acidic conditions allow for the microorganisms to oxidise the sulfide minerals (La Brooy et al., 1994; Marsden & House, 2006). The oxidation of the sulfide minerals above are exothermic reactions (Yannopoulos, 1991).

There are different types of microorganisms which can be used for biological oxidation at different temperatures (Marsden & House, 2006). Mesophilic bacteria are a class of microorganism which can be found around mining sites that contain sulfide minerals (Altinkaya et al., 2018; Yannopoulos, 1991). The *thio-oxidans* and *ferro-oxidans* of the *thiobacillus* group are used to treat sulfide ores at ambient temperatures (35-

45°C) (Marsden & House, 2006; Yannopoulos, 1991). There are also microorganisms which can be used for treating ores at high temperatures, these are known as thermophiles (Marsden & House, 2006; Yannopoulos, 1991). The thermophiles are divided into two groups, moderate and extreme thermophiles (Marsden & House, 2006).

The moderate thermophiles describe microorganisms which can be used at temperatures between 45 and 65°C (Marsden & House, 2006). However, if the biological oxidation takes place at temperatures between 65 and 85°C, then they are referred to as extreme thermophiles (Marsden & House, 2006; Yannopoulos, 1991). These high temperatures are ideal when trying to increase the oxidation rates of sulfide minerals.

The oxidation of sulfide minerals is the fastest at grain boundaries and cracks (Marsden & House, 2006). Thus, only partial oxidation is required to expose the Au as gold preferably deposits around these sites (La Brooy et al., 1994; Marsden & House, 2006). The partial oxidation results in sulfide minerals, which are more porous (Marsden & House, 2006). This, as mentioned in the other pretreatment techniques, leads to a lower consumption of lixiviant during leaching and better Au dissolution (Kaksonen et al., 2014).

2.3.4 Microwaves

Mine tailings have undergone costly milling and grinding processes. However, some Au is still locked up in the sulfide minerals. Instead of regrinding the tailings, microwave pretreatment can be used. Microwave pretreatment is a pyrometallurgical processing technique that can be used to directly oxidise sulfide minerals or carbonaceous material, as well as improve ore grindability (Marsden & House, 2006).

Microwaves effect minerals differently, depending on their dielectric and magnetic properties (Nanthakumar et al., 2007). Sulfide minerals can absorb microwaves when irradiated, and this is due to their dielectric properties (Marsden & House, 2006; Nanthakumar et al., 2007). Most oxides and carbonates, such as quarts, act as insulators and thus do not absorb the microwaves (Marsden & House, 2006;

Nanthakumar et al., 2007). The differences in the rates of heating of the different minerals, lead to thermal stresses within the ore (Olubambi, 2009). These thermal stresses cause crack propagation along the different mineral grain boundaries (Olubambi, 2009), thus improving gold liberation (Amankwah & Ofori-Sarpong, 2011).

Olubambi (2009), as well as Amankwah and Orfori-Sarpong (2011), investigated the effect that microwaves have on the leachability and grindability of ores. Olubambi (2009) considered the effect that microwave pretreatment has on the biological leaching of low-grade sulfur ores. He concluded that the metal extraction was higher when using microwaved ore samples for biological leaching as opposed to that when using virgin ore samples. It was also determined that the pH of the leaching system was lower when using the microwaved ore. Olubambi (2009) attributed the more acidic conditions to an increase in the number of electrochemical sites within the ore. The increased electrochemical sites, coupled with lower amounts of sulfur, lead to better metal dissolution. The decreased sulfur amounts occur if enough oxygen is present during the microwave irradiation (Marsden & House, 2006). This allows for the sulfides to be directly oxidised, forming SO_2 gas (Marsden & House, 2006). This gas formation also leads to the formation of cracks, due to the expansion of the gas (Marsden & House, 2006).

Amankwah and Orfori-Sarpong (2011) evaluated the effect that microwaves have on the grindability and cyanide leachability of gold ores. The findings were similar to those observed in Olubambi's (2009) study. The leaching rate was seen to increase when using microwave pretreatment. The leaching rates observed were substantially different. The microwaved samples achieved 95% metal extraction in 12 hours, whereas the untreated ore took 22 hours to reach the same level of extraction. The strength of the ore also decreased by 31.2% when microwaved.

Overall, the microwave pretreatment is an exciting technology, as it could be used to improve the leachability of low-grade gold tailings and decrease lixiviant consumption.

2.4 Leaching Processes

In the pretreatment section above, leaching has been mentioned as a means for metal dissolution from an ore. There are many different types of lixiviants that can be used for the dissolution of gold. However, the cyanidation process is still the most widely used as it its main reagent, cyanide, is relatively cheap. Halide, thiosulfate and thiourea leaching are possible alternatives to cyanidation. The aforementioned leaching processes will be described below:

2.4.1 Cyanidation

It has already been mentioned that cyanide can be used for the dissolution of gold (Au). Cyanide is a relatively cheap regent, while still being very effective in the dissolution of Au (Marsden & House, 2006) and thus it is ideal for treating low grade gold ores. Cyanide leaching uses cyanide in the form of a salt e.g. NaCN, KCN or $Ca(CN)_2$ (Marsden & House, 2006). However, NaCN and KCN are the more commonly used cyanide salts as they have good solubilities in water (Marsden & House, 2006). When the aurous (Au^+) or auric (Au^{3+}) states were described above, it was seen that they form complexes with linear and square planar geometries, respectively. It was also mentioned that if a ligand such as CN^- is present in solution, that the Au^+ and Au^{3+} ions will form complexes. The complexes formed are $Au(CN)_2^-$ and $Au(CN)_4^-$. The aurous complex ($Au(CN)_2^-$) is the more stable complex (Marsden & House, 2006). The stability of $Au(CN)_2^-$ can be seen in the Eh-pH diagram (see Figure 2.4) as it is present over a wide pH range (Xue & Osseo-Asare, 1985).

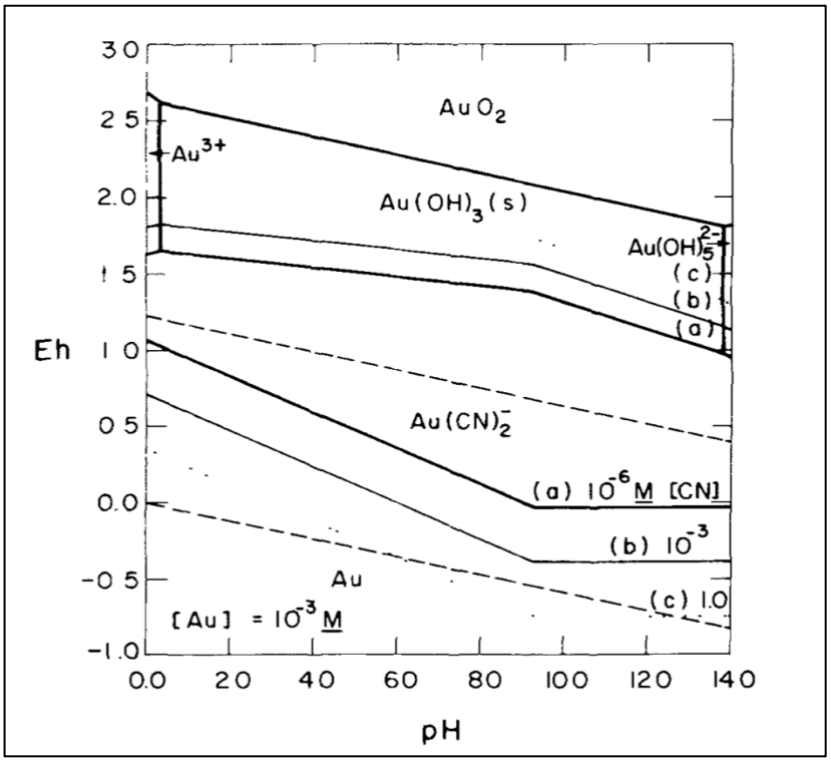


Figure 2.4: Eh-pH diagram for Au-CN-H2O system (Xue & Osseo-Asare, 1985).

The alkalinity of the cyanide solution should be carefully controlled as the CN^- ions hydrolyse in H_2O, producing HCN (Yannopoulos, 1991). The issue with the production of HCN (besides its health risks) is that it leads to the formation of an insoluble gold complex called AuCN (Yannopoulos, 1991). Marsden and House (2006) state that to minimise the formation of HCN, the pH of the leaching system must be kept above pH 10. Yannopoulos (1991) suggests that the ideal pH range is between pH 11 and 12.

Figure 2.5 illustrates that large amounts of the CN^- ions that can be lost to the formation of HCN, which decreases the dissolution rate of gold (Marsden & House, 2006).

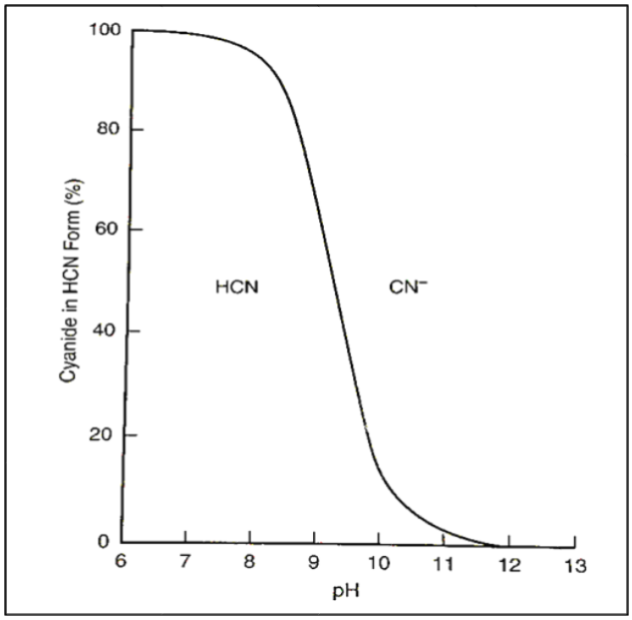


Figure 2.5: CN- ions lost to the formation of HCN at varying pH's (Marsden & House, 2006).

Thus, the dissolution of gold requires an aerated, alkaline cyanide solution. Elsner's equation mentioned above (Equation 3) is one of the theories proposed for the dissolution of gold using cyanide (Marsden & House, 2006; Yannopoulos, 1991). It has been suggested that Elsner's equation, although stoichiometrically correct, does not consider all the possible cathodic reactions that occur (Marsden & House, 2006). Yannopoulos describes the above theory as the hydrogen peroxide theory, and this theory describes the dissolution of gold through the following reactions:

$$2Au_{(s)} + 4CN^-_{(aq)} + O_{2\,(g)} + 2H_2O_{\,(l)} \rightleftharpoons 2Au(CN)^-_{2\,(aq)} + H_2O_{2\,(aq)} + 2OH^-_{(aq)} \quad (16)$$

$$2Au_{(s)} + 4CN^-_{(aq)} + H_2O_{2\,(g)} \rightleftharpoons 2Au(CN)^-_{2\,(aq)} + 2OH^-_{(aq)} \quad (17)$$

The second reaction (Equation 17) depicts the dissolution of gold using hydrogen peroxide (H_2O_2). However, this reaction is minor as too much H_2O_2 leads to the formation of CNO^- ions, which reduce gold dissolution (Yannopoulos, 1991). The dissolution of gold is a heterogeneous reaction as it involves a solid (gold ore) and a lixiviant (cyanide solution). The steps of this reaction are as follow:

1. The first step is for the reactants (CN^- and O_2) to diffuse through the diffusion layer surrounding the gold ore.
2. The reactants then diffuse through any product layer before it can reach unreacted surfaces.
3. Once the reactants reach the unreacted surfaces, there is a chemical reaction that takes place at the surface. This results in the production of H_2O_2, OH^- and $Au(CN)_2^-$.
4. These products then diffuse through the product layer and then the diffusion layer, into the bulk cyanide solution.

Figure 2.6 illustrates the above steps for the dissolution of gold (Marsden & House, 2006).

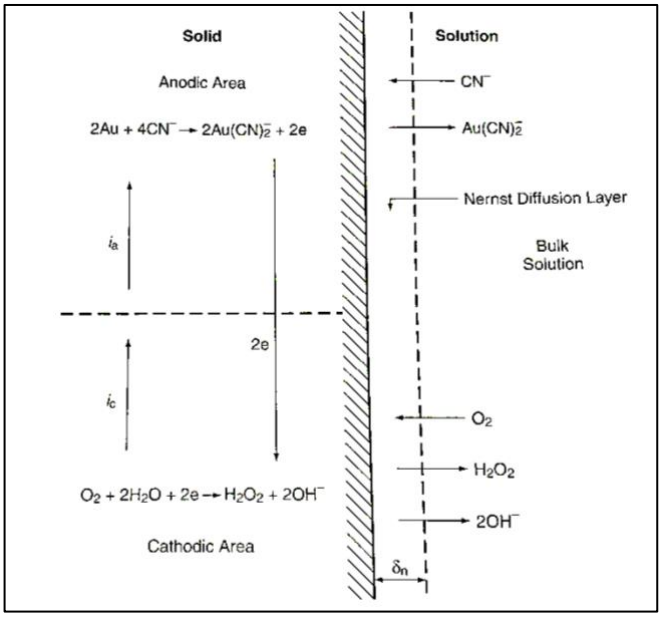


Figure 2.6: Steps involved in the dissolution of gold (Marsden & House, 2006).

2.4.2 Halide Leaching

Halide leaching of gold was established long before the advent of the cyanidation process (Lorösch, 2001). As mentioned before, most iodides, bromides, and chlorides in conjunction with a suitable oxidising agent have the ability to dissolve gold (Yannopoulos, 1991). The most common halide used for gold dissolution was chlorine in a process known as chlorination. Chlorination can be used to treat gold ores, which contain sulfides or fine gold particles (Marsden & House, 2006). The halides can

dissolve any sulfide minerals, allowing for the liberation of gold which is locked in sulfide minerals (Lorösch, 2001).

Chlorination involves the use of strong oxidising agents such as chlorine (Cl_2) or chloride ions (Cl^-) (Marsden & House, 2006). The Cl_2 gas is very soluble in water and reacts as follows (Marsden & House, 2006).

$$Cl_{2\,(g)} \rightleftharpoons Cl_{2\,(aq)} \tag{18}$$

$$Cl_{2\,(aq)} + H_2O_{\,(l)} \rightleftharpoons HCl_{\,(aq)} + HOCl_{\,(aq)} \tag{19}$$

The dissolution of gold in chlorine is faster than in the cyanide solutions (La Brooy et al., 1994). The reason for the increased dissolution rate is that Cl_2 is more soluble in water than O_2 is (Marsden & House, 2006). The acids that are formed in Equation 19 are hydrochloric acid (strong acid) and hypochlorous acid (weak acid), which are both oxidising agents (Marsden & House, 2006). At a pH less than or equal to 1, the active oxidant that is involved in the gold dissolution is chlorine (Lorösch, 2001). However, as the pH increases, the Cl_2 disproportionates according to Equation 19. When the pH rises above 5, then HOCl becomes the active oxidant (La Brooy et al., 1994; Lorösch, 2001).

The oxidising agents formed above can oxidise sulfide minerals such as pyrite (FeS_2). This means that it can be used to treat ores which have some sulfide minerals. However, this can make the use of chlorine uneconomical as there is a high reagent consumption, leading to high costs (La Brooy et al., 1994; Marsden & House, 2006). The formation of gold-halide complexes when the halide is the active oxidant, can be seen in the following equation (Lorösch, 2001):

$$2Au_{\,(s)} + 3X_2 + 2X^- \rightleftharpoons 2AuX_4^- \tag{20}$$

If the active oxidant is a hypohalogenic acid (e.g. HOCl), then the dissolution equation becomes (Lorösch, 2001):

$$2Au_{(s)} + 3HOX + 5X^- \rightleftharpoons 2AuX_4^- + 3H_2O \quad (21)$$

The reason for chlorination not being used in industry, is that it cannot be used for the economical leaching of refractory ores. This is due to the fact that the sulfides increase the reagent consumption (La Brooy et al., 1994). This high consumption rate and acidic conditions lead to high operating costs (La Brooy et al., 1994; Lorösch, 2001).

2.4.3 Thiourea Leaching

Thiourea is an organic compound with the chemical formula, NH_2CSNH_2 (Marsden & House, 2006). Thiourea leaching can be used for treating gold ores which are refractory or consume large amounts of cyanide (Marsden & House, 2006). The above is achieved through the use of acidic thiourea solutions which are at a pH of 1-2 (La Brooy et al., 1994). The stable complex formed under the aforementioned conditions is called bis(thiourea)gold(I) (Lorösch, 2001). The formation of the stable complex is represented by Equation 22:

$$Au_{(s)} + 2CS(NH_2)_2 \rightleftharpoons Au(CS(NH_2)_2)_2^+ + e^- \quad E^0 = 0.38\ V \quad (22)$$

The advantages of using thiourea over cyanide are that it is non-toxic and if it enters the environment, it acts as a fertilizer (Marsden & House, 2006). However, it may also be carcinogenic, it is more expensive than cyanide and is consumed in large amounts during the leaching process (La Brooy et al., 1994; Yannopoulos, 1991). The rate of gold dissolution is very slow when using O_2 as an oxidant and thus a stronger oxidant, such as Fe^{3+}, is required (Marsden & House, 2006).

The reason for the high consumption rate of thiourea is that it is easily oxidized into formamidine disulfide under the required leaching conditions (Lorösch, 2001; Yannopoulos, 1991). This reaction can be seen in Equation 23 (Yannopoulos, 1991):

$$2CS(NH_2)_2 \rightleftharpoons NH_2(NH)CSSC(NH)NH_2 + 2H^+ + 2e^- \quad (23)$$

The rate at which formamidine disulfide is produced, is dependent on the oxidant used (Marsden & House, 2006). Formamidine disulfide is a more effective oxidant than Fe^{3+} (Marsden & House, 2006). Thus, it is ideal for the leaching process as it increases the dissolution rate of gold (Lorösch, 2001; Yannopoulos, 1991). The dissolution of gold using formamidine disulfide is as follows (Marsden & House, 2006):

$$2Au + 2CS(NH_2)_2 + NH_2(NH)CSSC(NH)NH_2 + 2H^+ \rightleftharpoons 2Au(CS(NH_2)_2)_2^+ \quad (24)$$

However, the formamidine disulfide can disproportionate into thiourea and a sulfinic compound (Marsden & House, 2006). This reaction is undesirable as it is irreversible and produces elemental sulfur (S) (Marsden & House, 2006; Lorösch, 2001). The S can coat exposed gold particles which prevents them from being leached (Yannopoulos, 1991), thus decreasing the gold dissolution rate. However, this can be limited/reduced through the addition of SO_2 (Marsden & House, 2006; Yannopoulos, 1991), resulting is less passivation of the gold.

2.4.4 Thiosulfate leaching

Thiosulfate leaching can be used to recover gold from its ore or concentrate (Marsden & House, 2006). The chemical formula of thiosulfate is $S_2O_3^{2-}$ (Lorösch, 2001). The sulfide ion in thiosulfate means that thiosulfate has the ability to form strong complexes with precious and base metals (Lorösch, 2001). It has previously been mentioned that Au^+ forms very stable complexes with "soft" ligands, and thiosulfate is one of these ligands. The stable aurous gold complex formed can be seen in Equation 25 (Marsden & House, 2006):

$$Au + 2S_2O_3^{2-} \rightleftharpoons Au(S_2O_3)_2^{3-} + e^- \qquad E^o = 0.15\ V \quad (25)$$

Cyanidation requires the use of O_2 as an oxidant. However, for thiosulfate leaching, if O_2 is used as an oxidant then the rate of Au dissolution is very slow (Marsden & House, 2006; Lorösch, 2001). The rate of Au dissolution can be increased through the use of a stronger oxidant such as Cu^{2+} or Fe^{3+}(Lorösch, 2001; Yannopoulos, 1991). The above is true when there is ammonia (NH_3) present in the system as it helps to stabilize the Cu by forming copper(II)tetramine ($Cu(NH_3)_4^{2+}$) (Marsden & House, 2006). This can be seen in Equation 26 (Marsden & House, 2006).

$$Au + 5S_2O_3^{2-} + \mathrm{Cu(NH_3)_4^{2+}} \rightleftharpoons Au(S_2O_3)_2^{3-} + 4NH_3 + Cu(S_2O_3)_3^{5-} \qquad (26)$$

The addition of the Cu ions can increase the dissolution rate of gold by 20 times (La Brooy et al., 1994). The ammoniacal thiosulfate leaching process is conducted between pH 9 and 11, as this region allows for the formation of the stable gold-thiosulfate complex, $Au(S_2O_3)_2^{-3}$ (Marsden & House, 2006; Lorösch, 2001). If the pH falls below 9, copper(II)triamine ($Cu(NH_3)_3^{+}$) is formed, which decreases the dissolution rate of gold (Marsden & House, 2006).

The leaching rate of gold in ammoniacal thiosulfate is one order of magnitude greater than that in the cyanidation process (Lorösch, 2001). However, once again cyanidation remains the process of choice, as it is a cheaper process because large amounts of thiosulfate are consumed during the leaching process.

2.5 Supercritical Fluids

A supercritical fluid (SCF) is any substance whose temperature and pressure exceeds that of the substance's critical temperature and pressure (Sengers, 2000). The properties of a SCF are special as they are an intermediate between those of a liquid and a gas. This means that SCFs have high diffusivities and low viscosities due to their gas-like nature (Knez et al., 2019). However, SCFs also have liquid-like densities, this means that they can act as solvents (Knez et al., 2019). The density of a SCF can be varied by changing the temperature and pressure of the SCF. This means that one can have a solvent of variable solvent strength (Prabhat, Rao, Kumar & Tomar, 2016). There are many different commercially available extraction techniques that can be used to recover metal ions from pregnant leach solutions. These include ion exchange, solvent extraction, electrowinning and precipitation. More recently, SCFs have been explored as possible extraction media (Prabhat et al., 2016) for the recovery of metals from liquids or solids. This process is known as supercritical fluid extraction.

The main problem with using SCFs for metal ion extraction is that the extraction process is very inefficient (Lin et al., 1995). The inefficiencies are due to the weak solute-solvent interactions, as well as the required charge neutralization (Lin et al., 1995). An example that illustrates the aforementioned inefficiencies is when supercritical carbon dioxide ($ScCO_2$) is used as a solvent. The CO_2 is a non-polar molecule and therefore experiences difficulties extracting the metal ions (Prabhat et al., 2016). To solve the poor extraction/inefficiencies problem, ligands are used as they bond to the metal ions. There are many different SCFs that can be used. Some are favoured over others due to environmental advantages or simply the feasibility of reaching the critical temperatures and pressures. Table 2.1 contains some substances which can be used as SCFs along with the critical temperatures and pressures of each substance (Knez et al., 2019).

Table 2.1: Substances and their critical points (Knez et al., 2019).

Substance	Critical Temperature (°C)	Critical Pressure (Bar)
Ar (Argon)	-122.5	48.6
CHF_3 (Fluoroform)	25.9	48.2
CO_2 (Carbon dioxide)	31.1	73.8
SF_6 (Sulphur hexafluoride)	45.5	37.6
C_3H_8 (Propane)	96.7	42.5
C_2H_6O (Dimethyl ether)	126.9	54.0
H_2O (Water)	374.0	220.6

The two most commonly used SCFs are CO_2 and H_2O (Joung et al., 2000; Knez et al., 2019). This is due to the environmentally friendly characteristics exhibited by each. They are sustainable, non-toxic, non-flammable, cost effective and non-carcinogenic (Joung et al., 2000; Knez et al., 2019). Figures 2.7 illustrate the CO_2 phase diagram along with its critical point (Glennon et al., 1999).

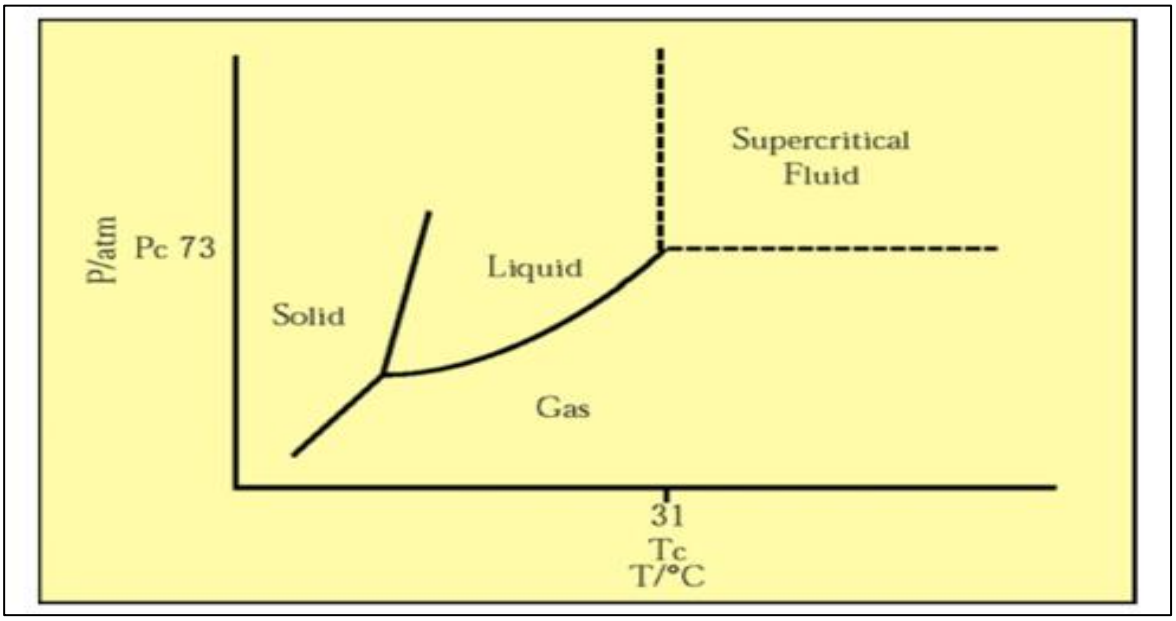


Figure 2.7: CO_2 phase diagram (Glennon et al., 1999).

However, $ScCO_2$ and ScH_2O are used for different applications. $ScCO_2$ is most commonly used during supercritical fluid extraction (SFE) (Knez et al., 2019), whereas ScH_2O is used for processes involving supercritical water oxidation (SCWO) or supercritical water gasification (SCWG) (Knez et al., 2019). SCWG is a technique that can be used to treat organic wastes such as sewage sludge (Yan et al., in press) to allow for the production of syn gas (a combination of H_2, CH_4, CO_2 and CO). This gas can

be used for energy generation (Yan et al., in press). Meng et al. (2016) researched the sulphur transferal in coal during the SCWG process, and found that SCWG removed sulphur from the sulphate minerals and pyrite minerals, and also produced less SO_2 than traditional coal pyrolysis.

2.6 Ligands and their use for SFE

Through the review of literature, it is clear that 4 classes of ligands, in particular, have been the focus of many studies. These classes are: dithiocarbamates, β-diketones, organophosphorus and macrocyclic compounds. It is important to identify possible ligands that can be used for the economical SFE of gold. This will be achieved through the evaluation of different ligands found in the 4 classes mentioned above. Modifiers, which have been proven to increase the solubilities of the different ligands in $ScCO_2$, will also be identified.

2.6.1 Dithiocarbamates

Dithiocarbamates are very similar to carbamates. However, they differ as the dithiocarbamates have sulphur atoms instead of oxygen atoms, with the general formula of R_2NCS_2X (Wai & Wang, 1997). The R represents an alkyl group and the X is a cation such as an alkali metal , ammonium or alkyl ammonium ions (Wai & Wang, 1997). The general structure of a dithiocarbamates without an attached cation is shown in Figure 2.8 (Ding et al, 2017).

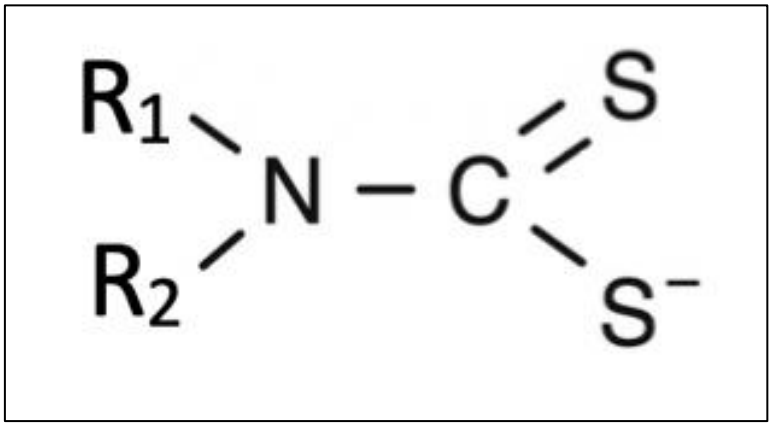


Figure 2.8: General structure of a dithiocarbamates (Ding et al., 2017).

These ligands are chelating extractants, which have very high metal extraction capabilities. Thus they are widely used in analytical chemistry (Erkey, 2000) and for

preconcentrating trace elements through the use of solvent extraction (Wai & Wang, 1997). Diethyldithiocarbamate (DDC) is one of the more commonly used dithiocarbamates, as it has been reported to extract over 40 different metal species from aqueous solutions when using solvent extraction (Wai & Wang, 1997). These are commonly used as salts of the acid (Smart et al., 1997), e.g. sodium diethyldithiocarbamate (NaDDC).

The main disadvantage of dithiocarbamates is their lack of solubility in water and especially in acidic environments (Wai & Wang, 1997). This problem can become more apparent when using $ScCO_2$, as the CO_2 and water interact to form carbonic acid which dissociates in water (Ding et al., 2017; Wai & Wang, 1997). This increases the acidity of the system (Ding et al., 2017; Wai & Wang, 1997), which leads to the decomposition of dithiocarbamates. The solution to this is to use large amounts of dithiocarbamates for the SFE of metal species as it ensures that high extraction efficiencies can be reached (Ding et al., 2017; Wai & Wang, 1997). Table 2.2 gives examples of typical dithiocarbamates (Ashraf-Khorassani et al., 1997a; Ding et al., 2017; Wai & Wang, 1997).

Table 2.2: Different dithiocarbamates (Adapted from: Ashraf-Khorassani et al., 1997a; Ding et al., 2017; Wai & Wang, 1997).

Chemical Name	Abbreviation	Where R =
Diethyldithiocarbamate	DDC	$-C_2H_5$
Bis(trifluoroethyl)dithiocarbamate	FDDC	$-CH_2CF_3$
Lithium-bis(trifluoroethyl)dithiocarbamate	LiFDDC	$-CH_2CF_3(Li^+)$
Dipropyldithiocarbamate	P3DC	$-C_3H_7$
Dibutyldithiocarbamate	BDC	$-C_4H_9$
Dipentyldithiocarbamate	P5DC	$-C_5H_{11}$
Dihexyldithiocarbamate	HDC	$-C_6H_{13}$
Pyrrolidinedithiocarbamate	PDC	$-CH_2(CH_2)_2CH_2$

It must be noted that the solubility of DDC in $ScCO_2$ is very low and thus it cannot be used for SFE (Ding et al., 2017). The solution to the insolubility of DDC is fluorination (Wai & Wang, 1997), which enhances its solubility in $ScCO_2$. This is done by substituting the hydrogen on the ethyl substituent by fluorine (Laintz et al., 1991).

Laintz et al. (1991) conducted a study which investigated the solubilities of different metal-DDC and metal-FDDC dithiocarbamates in $ScCO_2$. The results obtained in the aforementioned literature can be found in Table 2.3. Laintz and co-workers found that the Na salt of the ligand only showed a slight increase in solubility when it was fluorinated. However, it can also be seen that the solubilities of metal chelates such as Cu, Ni and Co increased significantly. The findings for the solubility of $Bi(DDC)_3$ and $Bi(FDDC)_3$ show that fluorination decreased the ligands' solubility. However, this was only at the tested pressure (100 atm). When the pressure increased to 150 atm, so did the solubility. Laintz and co-workers concluded that fluorination of metal dithiocarbamates can increase their solubilities in CO_2 by as much as 2-3 orders of magnitude.

Table 2.3: Solubility Results from Laintz et al. (1997).

Metal-Dithiocarbamate	Solubility (mol/L)	Increase in solubility (FDDC/DDC)
Na(FDDC)	$(4.7 \pm 0.3) \times 10^{-4}$	3.1
Na(DDC)	$(1.5 \pm 0.1) \times 10^{-4}$	
$Cu(FDDC)_2$	$(9.1 \pm 0.3) \times 10^{-4}$	830
$Cu(DDC)_2$	$(1.1 \pm 0.2) \times 10^{-6}$	
$Ni(FDDC)_2$	$(7.2 \pm 1.0) \times 10^{-4}$	850
$Ni(DDC)_2$	$(8.5 \pm 1.0) \times 10^{-7}$	
$Co(FDDC)_3$	$(8.0 \pm 0.6) \times 10^{-4}$	330
$Co(DDC)_3$	$(2.4 \pm 0.4) \times 10^{-6}$	
$Bi(FDDC)_3$	$< 10^{-7}$	-
$Bi(DDC)_3$	$(1.3 \pm 0.1) \times 10^{-6}$	
$Bi(FDDC)_3$	$(7.3 \pm 1.0) \times 10^{-4}$	81 (Calculated for 150 atm)
$Bi(DDC)_3$	$(9.0 \pm 0.6) \times 10^{-6}$	

Wai et al. (1996) evaluated the use of dithiocarbamates and β-diketones for the extraction of Cd, Pb and Hg from spiked filter paper and sand samples using $ScCO_2$. Wai and co-workers' findings for the β-diketones will be discussed later. Wai et al. (1996) used 4 different dithiocarbamates, namely, lithium bis(trifluoroethyl)dithiocarbamates (LiFDDC), diethylammonium diethyldithiocarbamate (Et_2NH_2DDC), sodium diethyldithiocarbamate (NaDDC) and ammonium pyrrolidinedithiocarbamate (APDC). Wai and his co-workers' results can be found in Table 2.4. The samples used were produced by spiking 300 mg of sand with 5 μg of each metal and then 50 mg of the desired ligand was used.

Table 2.4: Metal extraction results from Wai et al. (1996).

Chelating agent	At 100 atm and 45°C			At 250 atm and 45°C			At 200 atm and 60°C		
	Sand samples			Sand samples			Spiked filter paper samples		
	Cd^{2+} (%)	Pb^{2+} (%)	Hg^{2+} (%)	Cd^{2+} (%)	Pb^{2+} (%)	Hg^{2+} (%)	Cd^{2+} (%)	Pb^{2+} (%)	Hg^{2+} (%)
LiFDDC (pure CO_2)	90	84	92	92	91	93	91	83	95
	92	81	93	91	90	94	90	88	95
Et_2NH_2DDC (pure CO_2)	61	70	75	66	81	91	29	62	94
	58	71	78	70	80	93	30	64	95
NaDDC (pure CO_2)	35	40	60	81	86	95	38	68	91
	36	43	55	82	85	92	36	71	94
APDC (pure CO_2)	16	18	24	21	42	27	4	9	13
	10	20	21	17	44	24	6	11	18
LiFDDC (CO_2 +5% Methanol)	92	91	94	97	97	97	96	96	96
	90	89	90	96	95	98	96	95	97
Et_2NH_2DDC (CO_2 +5% Methanol)	80	92	97	85	83	90	72	92	96
	88	86	89	83	93	95	70	90	95
NaDDC (CO_2 +5% Methanol)	53	84	89	92	91	97	75	91	92
	52	83	84	87	90	96	71	90	91
APDC (CO_2 +5% Methanol)	32	53	47	53	65	54	16	51	35
	34	52	43	52	63	59	18	49	44

The results (see Table 2.4) illustrate that all of the ligands were able to achieve metal extraction. It can be seen that LiFDDC was the most effective when using pure CO_2, followed by: Et_2NH_2DDC>NaDDC>APDC. When CO_2 is modified with 5% methanol, the recoveries observed for each ligand also increase. The extraction efficiency of Et_2NH_2DDC in the modified CO_2 is far greater than in the pure CO_2, it is in fact comparable to that of LiFDDC in the modified CO_2. This is an important finding, as it emphasises that the solubilities of ligands in CO_2 can be increased through the use of appropriate modifiers. Wai and co-workers' findings show that the 5% methanol addition resulted in 2-5 times higher solubilities for the ligands in CO_2. It was also determined that with an increase in pressure, that the extraction efficiencies increase. However, the best combination is the use of modified CO_2 at high pressures. The aforementioned solubility results can be found in Table 2.5 .

Table 2.5: Solubility results from Wai et al. (1996).

Chelating agent	SCF	Solubility (mol/L) at 60°C and 200 atm
Et_2NH_2DDC	CO_2	6×10^{-2}
		2×10^{-2}
Et_2NH_2DDC	CO_2 + 5% methanol	24×10^{-2}
		17×10^{-2}
NaDDC	CO_2	0.2×10^{-2}
		0.1×10^{-2}
NaDDC	CO_2 + 5% methanol	0.4×10^{-2}
		0.3×10^{-2}
APDC	CO_2	0.02×10^{-2}
		0.02×10^{-2}
APDC	CO_2 + 5% methanol	0.04×10^{-2}
		0.04×10^{-2}

The LiFDDC was synthesized and therefore only three of the four ligands are commercially available, namely Et_2NH_2DD, NaDDC and APDC. This means that further research can be conducted using Et_2NH_2DD as it showed good extraction efficiencies. The above research conducted by Wai and co-workers concluded that diethyldithiocarbamates can be used as chelating agents for the extraction of transition metal ions from solids.

2.6.2 β-diketones

β-diketones can best be described as a molecule in which two ketones are joined together by a single carbon atom (Mawire, 2019). These ligands are also chelating extractants and are commonly used when divalent transition metals are being extracted (Ding et al., 2017). Some of the most commonly used β-diketones include, acetylacetone (AcAc), trifluoroacetylacetone (TFAA), hexafluoroacetylacetone (HFA) and thenoyltrifluoroacetone (TTA). Table 2.6 gives the chemical structures for common β-diketones.

Table 2.6: Chemical structures for common β-diketones (Ashraf-Khorassani et al., 1997a; Ding et al., 2017; Erkey, 2000; Wai & Wang, 1997).

Chemical Name	Abbreviation	Where R_1 =	Where R_2 =
Acetylacetone	AcAc	$-CH_3$	$-CH_3$
Trifluoroacetylacetone	TFAA	$-CH_3$	$-CF_3$
Hexafluoroacetylacetone	HFA	$-CF_3$	$-CF_3$
Heptafluorobutanoylpivaroylmethane	FOD	$-C(CH_3)_3$	$-C_3F_7$

Thenoyltrifluoroacetone	TTA		-CF_3

They generally exist in one of two equilibrium states, namely the keto and enol states (Ding et al., 2017). This equilibrium is established through keto-enol tautomerism (Özel et al., 1997; Smart et al., 1997) which is depicted in Figure 2.9.

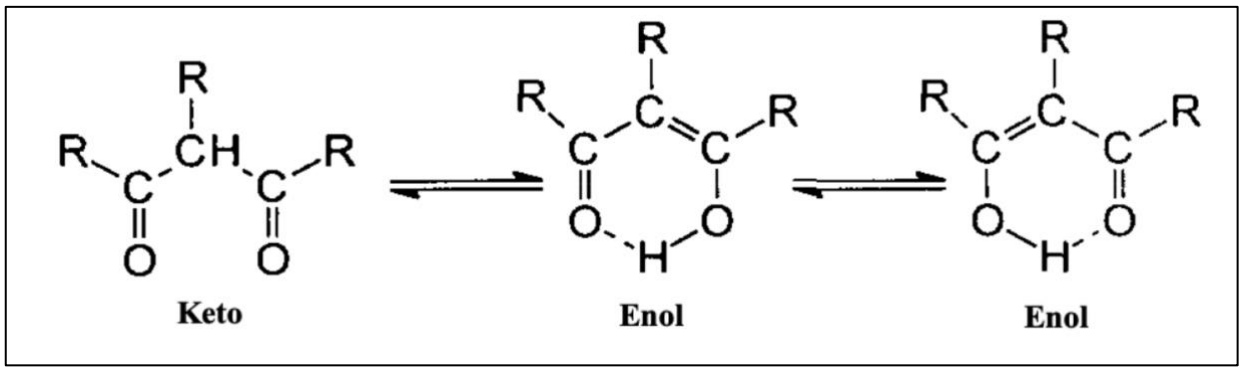


Figure 2.9: Keto-enol tautomerism in β-diketones (Özel et al., 1997).

β-diketones use cationic exchange to extract metals (Ding et al., 2017). Furthermore, they react with the metal ions by way of the enolate ions, forming neutral complexes (Ding et al., 2017; Wai & Wang, 1997). Figure 2.10 illustrates the enolate form.

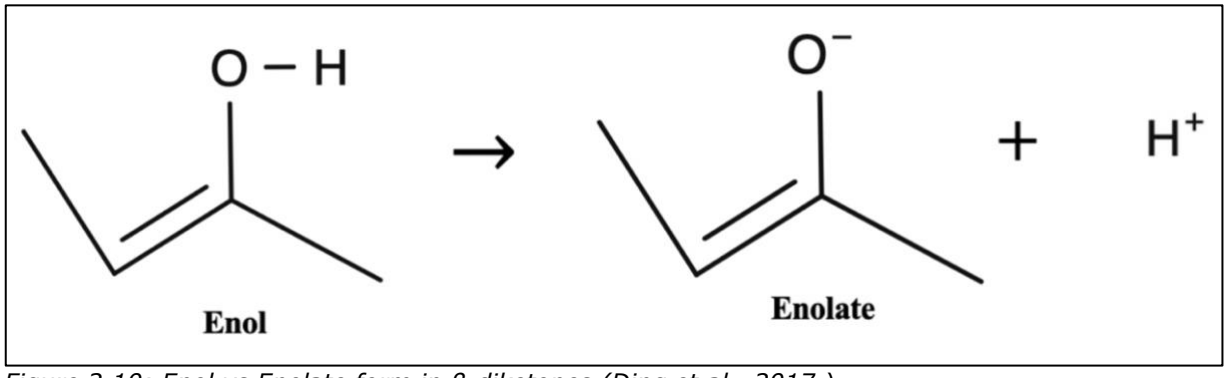


Figure 2.10: Enol vs Enolate form in β-diketones (Ding et al., 2017).

There is a similarity between β-diketones and dithiocarbamates, and both their solubilities in $ScCO_2$ can be increased through fluorination (Ding et al., 2017). However, the fluorinated β-diketones are only found in the enol state and not in the keto state (Ding et al., 2017). Very little work has been done on the solubilities of β-diketones in $ScCO_2$.

Ashrat-Khorassani et al. (1997b) investigated the solubilities of different metal hexafluoroacetylacetone (HFAA) and metal acetylacetone (Acac) chelates in $ScCO_2$. The aforementioned metal chelates are as follows: $Ni(HFAA)_2$, $Cu(HFAA)_2$ and $Cr(HFAA)_3$, as well as $Ni(Acac)_2$, $Cu(Acac)_2$ and $Cr(Acac)_3$. Ashrat-Khorassani and co-workers could not measure the solubilities of $Ni(Acac)_2$ and $Cu(Acac)_2$ due to their low solubilities in $ScCO_2$. Ashrat-Khorassani and co-workers' experiments were conducted at 200 and 400 atm and 60°C. The solubility results can be found in Table 2.7.

Table 2.7: Solubility results of some metal β-diketones from Ashrat-Khorassani et al. (1997b).

Metal β-diketone	Solubility in $ScCO_2$ at 200 atm and 60°C (mole/L)	Solubility in $ScCO_2$ at 400 atm and 60°C (mole/L)
$Ni(HFAA)_2$	$(8.0 \pm 0.1) \times 10^{-3}$	$(9.9 \pm 0.2) \times 10^{-3}$
$Cu(HFAA)_2$	$(8.7 \pm 0.2) \times 10^{-2}$	$(8.5 \pm 0.1) \times 10^{-2}$
$Cr(HFAA)_3$	$>8.0 \times 10^{-2}$	$>8.2 \times 10^{-2}$
$Cr(Acac)_3$	$(2.0 \pm 0.04) \times 10^{-3}$	$(3.5 \pm 0.2) \times 10^{-3}$

The results (see Table 2.7) illustrate that the solubilities of the fluorinated acetylacetone chelates are higher than the non-fluorinated acetylacetone chelates. The increase in solubility is at least one order of magnitude (Ashrat-Khorassani et al.,1997b).

Ashrat-Khorassani and co-workers also evaluated the extraction efficiencies of the different metal complexes from an aqueous matrix. Ashrat-Khorassani and co-workers compared $Cr(Acac)_3$ to $Ni(Acac)_2$ and $Cu(Acac)_2$. $Cr(Acac)_3$ had a far higher solubility in $ScCO_2$ and thus it yielded higher extraction efficiencies when compared to $Ni(Acac)_2$ and $Cu(Acac)_2$. It can also be seen that the metal-HFAA chelates are more soluble in $ScCO_2$ than the metal-FDDC chelates. However, the inverse is true for the observed extraction efficiencies. Ashrat-Khorassani and co-workers concluded that by fluorinating the ligands, the volatility and solubility of the complexes increased, which led to improved extraction efficiencies (see Table 2.8).

Table 2.8: Extraction efficiency results from Ashrat-Khorassani et al. (1997b).

Metal β-diketone	%Recovery at 200 atm and 60°C	%Recovery at 400 atm and 60°C
$Cr(Acac)_3$	66	82

$Cr(HFAA)_3$	61	52
$Cu(Acac)_2$	12	9
$Cu(HFAA)_2$	49	51
$Ni(Acac)_2$	2	1.5
$Ni(HFAA)_2$	6.4	11

It has already been mentioned in the dithiocarbamates section (see section 2.6.1) that Wai et al. (1996) used β-diketones as chelating agents for the extraction of Cd, Pd and Hg from solid samples using $ScCO_2$. Wai and co-workers used three commercially available β-diketone, namely TFAA, TTA and HFAA. The extraction efficiencies for each fluorinated β-diketone can be found in Table 2.9.

Table 2.9: Extraction efficiencies for fluorinated β-diketones (Wai et al., 1996).

Chelating agent	At 100 atm and 45°C			At 250 atm and 45°C		
	Sand samples (300 mg spiked with 5 μg of each metal ion)			Sand samples (300 mg spiked with 5 μg of each metal ion)		
	Cd^{2+} (%)	Pb^{2+} (%)	Hg^{2+} (%)	Cd^{2+} (%)	Pb^{2+} (%)	Hg^{2+} (%)
TFAA(50 μL)	65	71	72	76	70	85
pure CO_2	51	68	63	65	66	83
TTA (100 mg)	21	51	50	67	70	72
pure CO_2	24	62	56	58	74	75
HFAA (50 μL)	62	68	67	69	65	66
pure CO_2	77	71	62	60	68	73
TFAA (50 μL)	93	88	91	95	72	94
CO_2 +5% Methanol	84	80	82	90	68	93
TTA (100 mg)	77	75	86	96	86	96
CO_2 +5% Methanol	82	80	92	93	81	91
HFAA (50 μL)	82	87	92	96	77	74
CO_2 +5% Methanol	67	81	93	95	74	82

Wai and co-workers' results (see Table 2.9) illustrate that fluorinated β-diketone such as TFAA, TTA and HFAA are effective at extracting transition metals such as Cd^{2+}, Pb^{2+} and Hg^{2+}. It is clear from the results that there is a sharp increase in the extraction of metal ions when using CO_2 modified with 5% methanol.

Özel et al. (1997) considered the extraction of cobalt from the surface of stainless steel using β-diketones. The β-diketones used were Acac and HFAA, which will help to compare the extraction efficiencies of fluorinated and non-fluorinated β-diketone.

Table 2.10: Extraction of Co using different ligands (Özel et al., 1997).

CO_2 with different ligands	Percentage Co extracted (%)
No Ligand	0.1±0.1
Acac	0.9±0.8
HFAA	78.3±3.7

Özel and co-workers' findings (see Table 2.10) illustrate that almost no Co is extracted when using no ligand or Acac. However, this changes when HFAA is used as the Co extraction increases to 78%. Özel and co-workers (1997) attributed the differences in extraction efficiencies between Acac and HFAA to the following:

- HFAA has a higher thermal stability, which means that it is less likely to undergo thermal degradation during SFE.
- The CF_3 groups found in HFAA result in a more acidic ligand (4 orders of magnitude more acidic). This means that HFAA is able to extract metal ions under more acidic conditions. This is important for SFE processes because, as mentioned before, the CO_2 reacts with water, generating carbonic acid.

Özel and co-workers (1997) further investigated the effect that using different amounts of HFAA would have on the Co extraction. The reason behind this test is that under supercritical extraction conditions, ligands and metal complexes may undergo degradation due to the high temperatures. The results for this experiment are provided in Table 2.11.

Table 2.11: Co extraction using varying amounts of HFAA (Özel et al., 1997).

Amount of HFAA used (μmol)	Percentage Co extracted (%)
100	78.3±3.7
350	90.7±4.9
700	90.5±6.4

Özel and co-workers' findings (see Table 2.11) show that metal extraction recoveries can be increased dramatically through the use of excess amounts of ligands. This is due to the fact that the excess amounts of ligands present in the system help compensate for any ligand or metal complex degradation that may take place.

Wang and Wai (2005) considered the dissolution and extraction of base and precious metals such as copper (Cu), gold (Au) and palladium (Pd) in $ScCO_2$, using a fluorinated β-diketone. These zero-valent metals require an oxidant to be dissolved. The oxidant used by Wang and Wai (2005) was HNO_3. The problem with just using HNO_3 is that it is insoluble in CO_2. Thus the oxidant had to be complexed with a CO_2 soluble Lewis base such as tributyl phosphate (TBP), which allows for the oxidant to be carried into the $ScCO_2$. Wang and Wai (2005) reported that the complex formed has the following general formula: $TBP(HNO_3)_X(H_2O)_Y$. It was found that $TBP(HNO_3)_1(H_2O)_{0.4}$ was required for the dissolution of Pd. However, lower amounts of HNO_3 are required for the dissolution of Au and Cu, and this could be done using $TBP(HNO_3)_{0.7}(H_2O)_{0.7}$. At 40^{o}C and 110 atm, the $TBP(HNO_3)_{0.7}(H_2O)_{0.7}$ complex was reported to have a solubility of 1.7 mol% in $ScCO_2$.

The source of Cu was a Cu coated silicon (128 nm thick) wafer. It was found that all the copper could be removed from the wafer in just 4 minutes when using the $TBP(HNO_3)_{0.7}(H_2O)_{0.7}$ complex in $ScCO_2$ at 40^{o}C and 200 atm. Wang and Wai (2005) then conducted the same experiment with only TBP. This showed that no Cu was extracted and thus proves that the oxidant plays a vital role in the extraction of zero-valent metals. The source of Pd was a Pd coated silicon wafer. It has already been mentioned that much larger amounts of HNO_3 are needed to be present in the complex to achieve dissolution. The extraction and dissolution of gold was achieved using Au plated central processing unit (CPU) pins. Wang and Wai (2005) found that the Au could be dissolved quickly in $ScCO_2$ when using the same TBP-HNO_3 complex that is mentioned in the Cu extraction experiments. The Au experiments found that dissolution of Au in $ScCO_2$ (150 atm at 40^{o}C) is around 5-10 times faster than that experienced when using liquid CO_2 (150 atm at 24^{o}C).

Wang and Wai (2005) showed that even if the required oxidant is not/poorly soluble in $ScCO_2$, that the oxidant can be transferred into the $ScCO_2$ through the use of a CO_2 soluble Lewis base. Their experiments illustrate that fluorinated β-diketones and suitable oxidant-complexes can be used for the SFE of zero-valent metals.

2.6.3 Organophosphorus

Organophosphorus reagents have been extensively used in extraction processes such as solvent extraction. They are organic compounds that contain a central phosphorus atom. A commonly used organophosphorus reagent is tributyl phosphate (TBP), which is typically used for processing nuclear waste (Ding et al., 2017). One of the most famous processes that uses TBP is the PUREX process (Wuhua et al., 2010). However, organophosphorus reagents have also been used to extract rare earth metals such as neodymium and cerium (Wuhua et al., 2010) and actinides (Wai & Wang, 1997). The great advantage of using organophosphorus reagents is that they have good miscibility in CO_2 (Ding et al., 2017) and are commercially available (Wai & Wang, 1997). The sulphur containing organophosphorus ligands such as Cyanex301 and Cyanex302 are stable in acidic conditions, have high solubilities in CO_2 and, due to their widespread use, are cheap (Ding et al., 2017).

Table 2.12 contains some of the more commonly used organophosphorus reagents and the structural formula for the different organophosphorus reagents are listed in Figure 2.11.

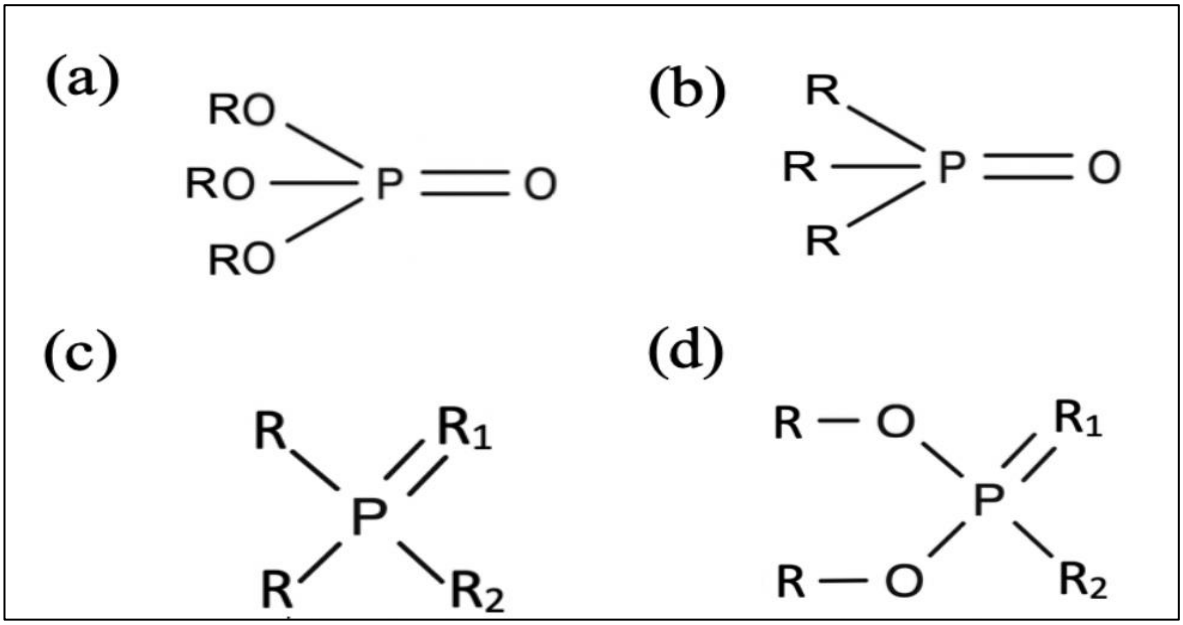


Figure 2.11:General chemical structures of different organophosphorus reagents (Ding et al., 2017; Erkey, 2000; Wai & Wang, 1997).

Table 2.12: Chemical names, abbreviations and R groups for organophosphorus reagents. (Ding et al., 2017; Erkey, 2000; Wai & Wang, 1997).

Chemical Name	Abbreviation	Refer to Figure 11	Where R, R_1 and R_2 =
Tributylphosphate	TBP	a	R = n-C_4H_9

Tributylphosphine oxide	TBPO	b	R = n-C_4H_9
Trioctylphosphine oxide	TOPO	b	R = n-C_8H_{17}
Triphenylphosphine oxide	TPPO	b	R = n-C_6H_5
Bis(2,4,4-trimethypentyl)dithiophosphinic acid	Cyanex301	c	R = $(CH_3)_3CCH_2CH(CH_3)CH_2$- R_1 = S R_2 =SH
Bis(2,4,4-trimethypentyl)monophosphinic acid	Cyanex302	c	R = $(CH_3)_3CCH_2CH(CH_3)CH_2$- R_1 = S R_2 =OH
Bis(2,4,4-trimethypentyl)phosphinic acid	Cyanex272	c	R = $(CH_3)_3CCH_2CH(CH_3)CH_2$- R_1 = O R_2 =OH
Di(2-ethylhexyl)phosphoric acid	D2EHPA	d	R = $CH_3(CH_2)_2CH(CH_2CH_3)CH_2$ - R_1 = O R_2 =OH

Prabhat et al. (2016) investigated SFE of uranium (U) from crude sodium diuranate. The adduct used for the dissolution and extraction of the U was TBP-HNO_3. The dissolution and TBP-complexation equations for the crude sodium diuranate can be described through the following equations:

$$Na_2U_2O_{7\,(s)} + 6HNO_{3\,(aq)} = 2UO_2(NO_3)_{2\,(aq)} + 2NaNO_{3\,(aq)} + 3H_2O_{\,(l)} \qquad (27)$$

$$UO_2(NO_3)_{2\,(aq)} + 2TBP_{(org)} = UO_2(NO_3)_2.2TBP_{(org)} \qquad (28)$$

The optimum conditions found by Prabhat et al. (2016) for the processing of 200 mg of their crude sodium diuranate (SDU) were: temperature = 49.85^oC, pressure = 152 Bar, and 1 mL of TBP-HNO_3 with 20 minute static time (time taken for the SDU dissolution and U complexation) and collection times (time taken to collect the extract in a collection vessel).

Their work also covered the effect that changes in pressure and temperature had on the extraction of U. They concluded that as pressure increased (keeping temperature constant at 59.85^oC), that the solvating strength of $ScCO_2$ increased, leading to an

increase in the U extraction efficiency, but only up until 152 Bars. When the temperature was varied between 39.85°C and 79.85°C (constant pressure of 202.70 Bar), there was very little effect on the extraction efficiency. This was attributed to a proportional increase in the volatility of the $ScCO_2$ with a decreasing $ScCO_2$ density.

Ghoreishi et al. (2016) investigated the extraction of toxic heavy metals (Hafnium, Uranium, Zirconium and Cadmium) from a solid matrix using different chelating agents and modifiers. The chelating agents used by Ghoreishi and co-workers are as follows: ethylenediaminetetra acetic acid (EDTA), TOPO, Cyanex272, Cyanex 301 and Cyanex302. The aforementioned agents were used with methanol, acetone, acetylacetone, acetonitrile and methyl isobutyl ketone (MIBK). The experiments were run at 22 MPa, 70°C for 50 minutes. Tables 2.13 and 2.14 contain Ghoreishi and co-workers' findings.

Table 2.13: Metal Extraction using different chelating agents and modifiers (Ghoreishi et al., 2016).

Chelating agent	Percentage extraction using different modifiers (%)											
	Methanol				Acetylacetone				MIBK			
	Zr (%)	Hf (%)	U (%)	Cd (%)	Zr (%)	Hf (%)	U (%)	Cd (%)	Zr (%)	Hf (%)	U (%)	Cd (%)
EDTA	73.2	73.3	80	78.6	69.6	73.9	78.9	75.5	61.1	74.4	73.6	66.5
TOPO	90	85.5	84.4	93.7	89.9	85.6	82	90.7	84.9	85.6	75.4	81.6
Cyanex272	93.3	93.3	89.7	99	92.3	93.5	87.6	96	86.4	93.6	81.4	86.9
Cyanex301	91.5	93.8	90.7	98.3	89.7	94.1	89	95.3	83	94.4	83	86.2
Cyanex302	84.8	87.1	87.5	91.5	82.2	87.6	86.1	88.4	74.5	88	80.5	79.4

Table 2.14: Continuation of Table 2.13.

Chelating agent	Percentage extraction using different modifiers							
	Acetone				Acetonitrile			
	Zr (%)	Hf (%)	U (%)	Cd (%)	Zr (%)	Hf (%)	U (%)	Cd (%)
EDTA	64.4	71.9	69.3	66.5	71.7	72.6	76.8	75.5
TOPO	75.3	85.2	76.3	81.6	85.1	85.4	82.5	90.7
Cyanex272	80.3	92.7	81	86.9	89.2	93	87.4	96
Cyanex301	80.3	93	81.3	86.2	88.4	93.4	88.2	95.3
Cyanex302	75.3	86.1	77.5	79.4	82.6	86.6	84.6	88.4

The results (see Tables 2.13 and 2.14) show that Cyanex272 and Cyanex301 were the most effective chelating agents for the different ligand-modifier combinations. It was also reported that EDTA was the least effective, as it always exhibited the lowest metal extraction amounts, no matter the ligand-modifier combination. Ghoreishi and co-

workers decided that the Cyanex272-methanol system was the optimum combination of ligand-modifier. Thus further experiments were conducted to determine the optimum operating parameters. Ghoreishi and co-workers concluded that the optimum parameters for metal extraction occur at 80^{o}C, 26 MPa and 70 minutes. The extraction efficiencies reported by Ghoreishi and co-workers are 100% of the Zr, Hf and Cd, while 99.1% for U was achieved.

It has been mentioned before that organophosphorus reagents can be used to extract rare earth metals. Wuhau et al. (2010) used organophosphorus complexes modified with HNO_3 and H_2O to extract rare earth elements in $ScCO_2$. The metals (Neodymium and Cerium) were extracted from their oxides, namely Nd_2O_3 and CeO_2. Wuhau and co-workers used two organophosphorus complexes, namely TBP-HNO_3 and TROP-HNO_3. Wuhau et al. (2010) describes TROP as a mixture of 4 trialkylphosphine oxides, known in industry as Cyanex923. Wuhau and co-workers conducted static and dynamic tests, where the static tests simply refer to SFE processes in which the volume of the extractant is fixed. In contrast, dynamic conditions described a system in which the extraction mixture was fed into the extraction vessel at a constant rate.

The first SFE process involves using 0.5 g of Nd_2O_3 with varying amounts of TBP-HNO_3 (4, 6, 8 and 10 mL), and was run at 15 MPa, 50^{o}C at 2 hours static time. Wuhau and co-workers found that the volume of TBP-HNO_3 used, strongly influenced the extraction efficiencies. When using 8 mL of TBP-HNO_3, they could achieve 62.45% Nd extraction. However, if they added 20 mL of pure TBP-HNO_3, they could recover as much as 94.69% of the Nd after the 2 hour period. This is attributed to the fact that Nd^{3+} easily dissolves in water.

The H^+ concentration in the TBP-HNO_3 complex was also evaluated by varying the [H^+] between 2.10 and 5.55 mol/L at 15 MPa and 50^{o}C. Wuhau and co-workers found that when the [H^+] was increased, there was an increase in the Nd extraction for low acidity. However, when the [H^+] was increased past 4.54 mol/L, the solubility of the TBP-HNO_3 complex in $ScCO_2$ decreased. The decreased solubility led to a decrease in Nd extraction. For the dynamic extraction of Nd using TBP-HNO_3, it was found that a complex with a lower acidity (2.52 mol/L) was optimum, leading to 97.68% recovery.

It must be noted that Wuhau and co-workers found that increasing the pressure of the system can increase the solubility of the acidic TBP-HNO_3 complex. The extraction efficiencies for the static extraction of Nd using TROP-HNO_3 was found to be very low (<10%). Wuhau and co-workers attributed the low extraction efficiencies to TROP-HNO_3 having a high polarity, which means that it is poorly soluble in $ScCO_2$ or to the Nd-TROP complex being poorly soluble in $ScCO_2$. Wuhau et al. stated that it is difficult to extract Ce using TROP-HNO_3 as it was observed that TBP-HNO_3 extracted less than 1%, apparently because HNO_3 does not dissolve CeO_2 effectively.

The experiments conducted by Wuhau et al. (2010) and Ghoreishi et al. (2016) illustrate that the extraction efficiencies of different chelating agents can be increased by suitable modifier selection as well as changes in complex acidity.

2.6.4 Macrocyclic compounds

Macrocyclic compounds are a class of organic compounds that have a cavity/cyclic structure (Ding et al., 2017). Two well studied macrocyclic classes are the crown ethers and calixarenes (Smart et al., 1997; Wai & Wang, 1997). The aforementioned classes are selective ligands which can form metal complexes (Wai & Wang, 1997).

2.6.4.1 Crown esters

Crown esters are cyclic compounds, which contain multiple ether groups connected in a ring structure (Wai & Wang, 1997; Wang & Zhuang, 2020). There are many different types of crown ethers as additional functional groups can be added to the crown structure (Wang & Zhuang, 2020). The extraction of the metal ions is dependent on the macrocyclic compounds' cavity size (Ding et al., 2017; Smart et al., 1997; Wai & Wang, 1997). Figure 2.12 illustrates some crown ethers along with their associated cavity sizes (Steed, 2001).

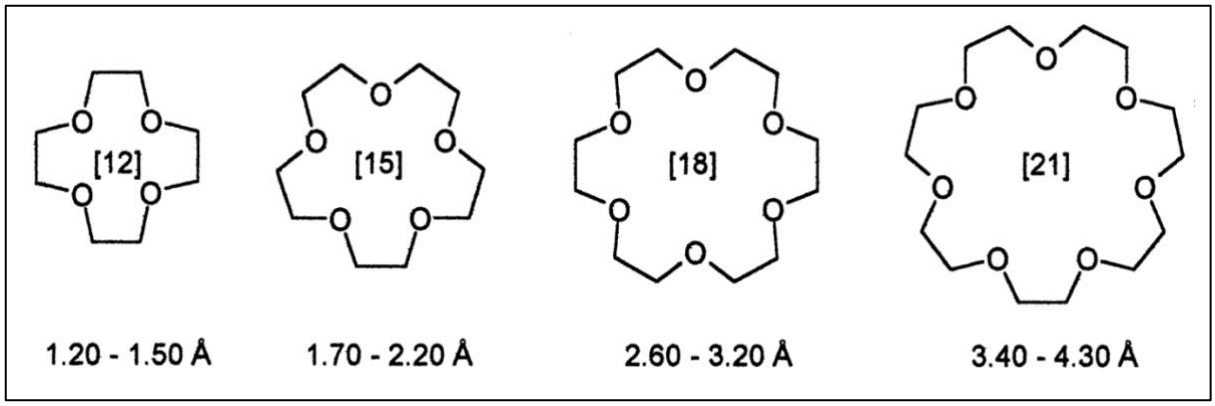


Figure 2.12: Crown ethers along with their associated cavity sizes (Steed, 2001).

The metal complexes formed by crown ethers are positively charged (Ding et al., 2017). Due to the non-polar nature of CO_2, positively charged complexes experience solubility issues in the CO_2. To overcome this solubility problem, one of two things can be done, the first option is to use counteranions such as pentadecafluoro-n-octanoic acid (PFOA) or tetraethylammonium perfluoro-1-octanesulfonate (TPFOS) (Ding et al., 2017). The second option is to modify the structure of the crown ether by attaching a negatively charged functional group (Smart et al., 1997). Wai and Wang (1997) reviewed many different sources of literature. They found that the solubilities of crown ethers, such as triazolocrowns, can be increased by an order of magnitude when 5% methanol is added to the CO_2 (Wai & Wang, 1997). Figure 2.13 from Wang and Zhuang (2020) depict some of the common crown ethers.

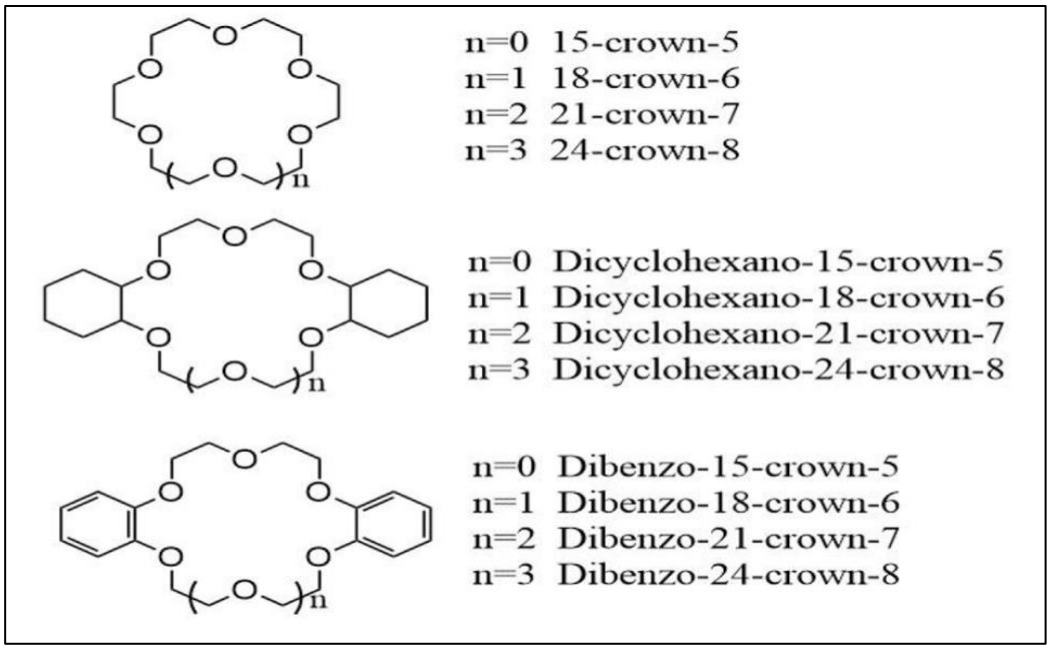


Figure 2.13: Common crown ethers (Wang & Zhuang, 2020).

Shamispur et al. (2001) investigated the solubilities of large crown ethers in $ScCO_2$. The crown ethers that were tested are as follows: dibenzo-24-crown-8 (DB24C8), dibenzo-27-crown-9 (DB27C9) and dibenzo-30-crown-10 (DB30C10). Shamispur and co-workers tested the solubility of DB24C8 at pressures between 120-440 atm and temperatures of 35, 45, 55 and 65°C. The solubilities of DB27C9 and DB30C10 were tested at pressures between 120-480 atm and temperatures of 35, 45, 55, 65 and 75°C.

Shamispur and co-workers found that when pressure was increased at a constant temperature, that the crown ethers became more soluble in $ScCO_2$. They found that for all three crown ethers tested, that there is a point (pressure = 160 atm) at which any increases in the temperature or pressure of the system leads to increased solubilities. However, below 160 atm only increases in pressure result in increased solubilities. Shamispur and co-workers determined that crown ethers with lower vapour pressures and smaller molecular weights are more soluble in $ScCO_2$ when compared to those with higher molecular weights and vapour pressures.

Hongwu et al. (1991) evaluated the use of solvent extraction involving a crown ether (B15C5) as a means to extract Au^{3+} from an aqueous solution. Hongwu and co-workers considered the addition of metal ions to the aqueous solution in an attempt to increase the Au^{3+} extraction efficiency. This is due to the fact that in the absence of a metal, the extraction of $AuCl_4^-$ is low, as it is difficult to form a B15C5 cationic complex. Hongwu and co-workers determined that K^+ was the most effective metal ion for increasing the extraction of gold. They attributed the increase in extraction efficiency to the formation of a hydrophobic complex. The complex cation formed can be seen in the following reaction:

$$nB15C5 + K^+ \rightleftharpoons K^+(B15C5)_n \quad n = 1 - 2 \tag{29}$$

Hongwu and co-workers determined that the extraction equilibrium for the aforementioned solvent extraction process can be represented as follows:

$$mAuCl_{4\,(aq)}^- + mK^+{}_{(aq)} + nB15C5_{(Organic)} \rightleftharpoons [K^+{}_m(B15C5)_n(AuCl_4)_m]_{(Organic)} \tag{30}$$

It was concluded that Au^{3+} can be extracted in industry using the above process. This is due to the selective co-ordination seen between B15C5 and K^+, which leads to the reduction of unwanted cations or hydrophilic anions from reporting to the organic phase during the solvent extraction process.

2.6.4.2 Calixarene derivatives

Calixarene derivatives have a vase like structure with aromatic building blocks (Smart et al., 1997) e.g. the calix[4]arene derivatives. The calix[4]arene derivatives are molecules which are made up of 4 aromatic blocks, namely the phenol group and these are bridged with methylene groups (Smart et al., 1997). These ligands are chelating agents that contain lipophilic and metal co-ordinating moieties (Wai & Wang, 1997). The upper rim is the lipophilic moiety whereas the lower rim is the metal co-ordinating moiety (Wai & Wang, 1997). Wang and Zhuang (2020) state that unsubstituted calix[4]arene can have four different conformations (see Figure 2.14).

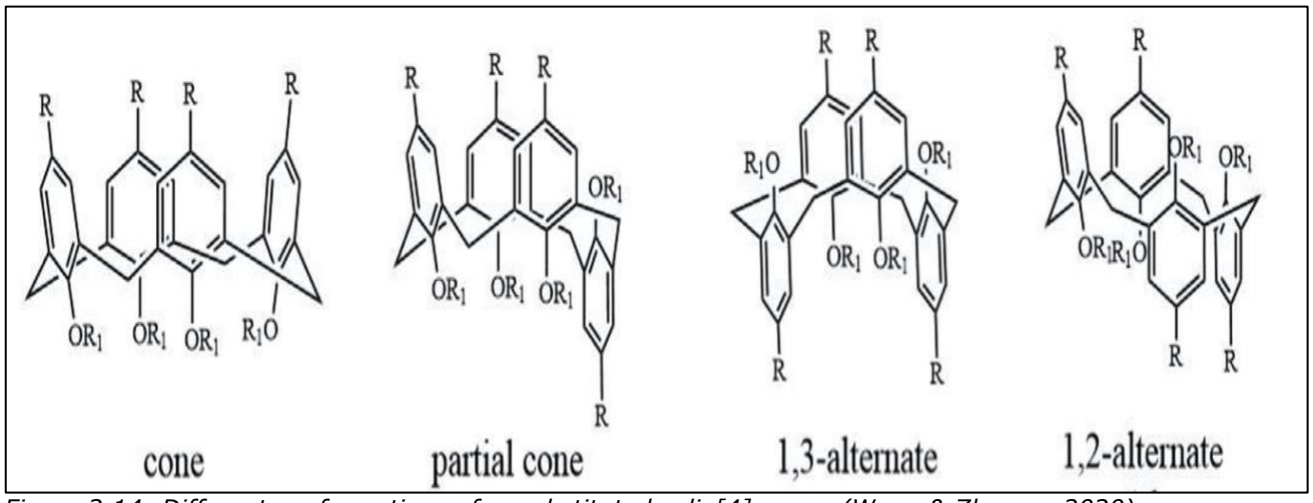


Figure 2.14: Different conformations of unsubstituted calix[4]arenes (Wang & Zhuang, 2020).

Silwa and Deska (2008) published a paper which described the different calixarene complexes that can be formed with soft metal ions. Figure 2.15 is a tetragold complex that Silwa and Deska (2008) produced by reacting a calixarene with four AuCl(tetrahydrothiophene) molecules [AuCl(THT)]. The aforementioned figure has been included as it depicts the metal co-ordinating moiety nicely (Silwa & Deska, 2008).

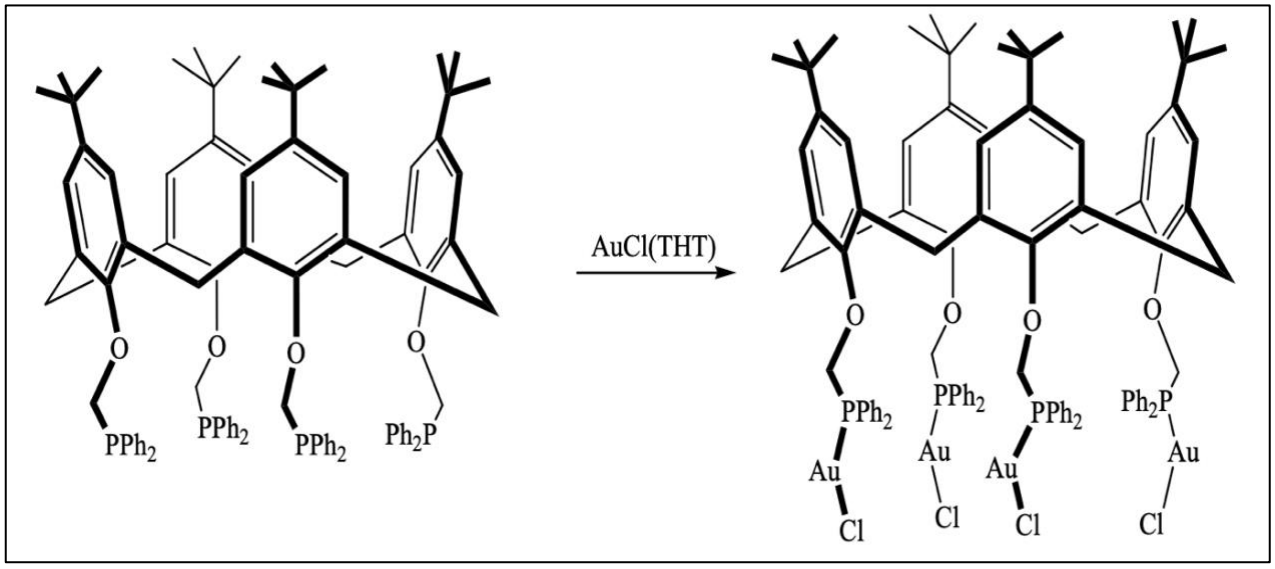


Figure 2.15: Tetragold complex (Silwa & Deska, 2008).

Glennon et al. (1999) investigated the extraction of gold using $ScCO_2$ which contained synthesized ligands, namely fluorinated calixarene derivatives with lower rim sulfur donor atoms. The synthesized ligands were reported by Glennon and co-workers to have the following chemical structures (see Figure 2.16):

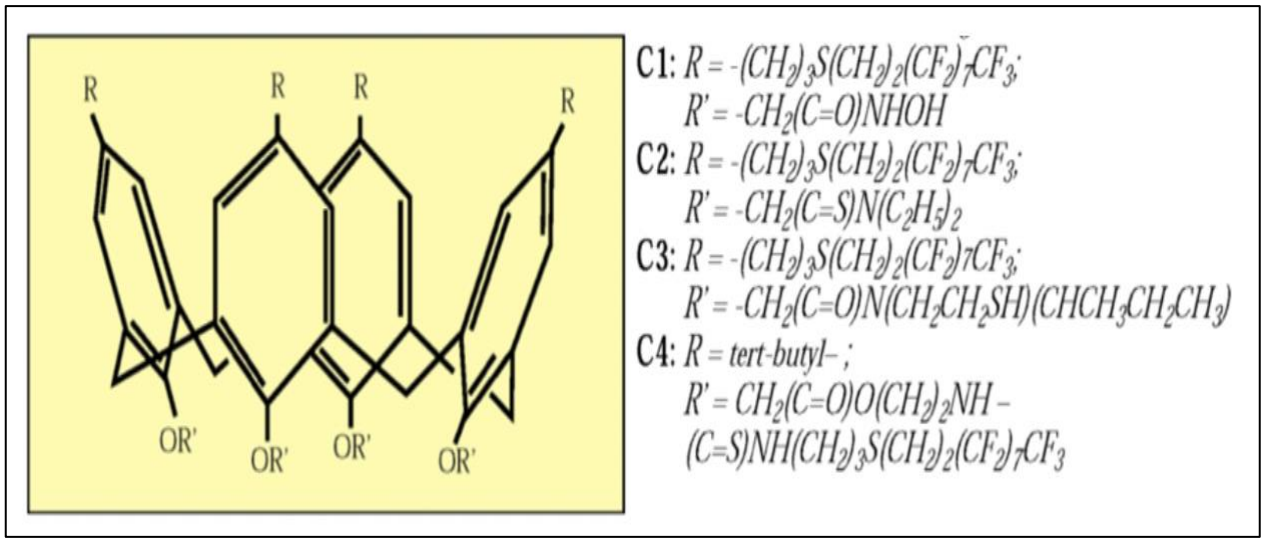


Figure 2.16: Fluorinated calixarene derivatives with lower rim sulphur donor atoms (Glennon et al., 1999).

The extraction of gold was done by spiking Au^{3+} on a piece of filter paper, which was then placed, along with the ligand, into a glass tube. The tube was subsequently placed into the reaction vessel for the extraction to occur. Once the reaction was completed,

the extraction vessel was vented into a collection vessel, which contained either dimethyl sulfoxide (DMSO) or methyl iso-butyl ketone (MIBK).

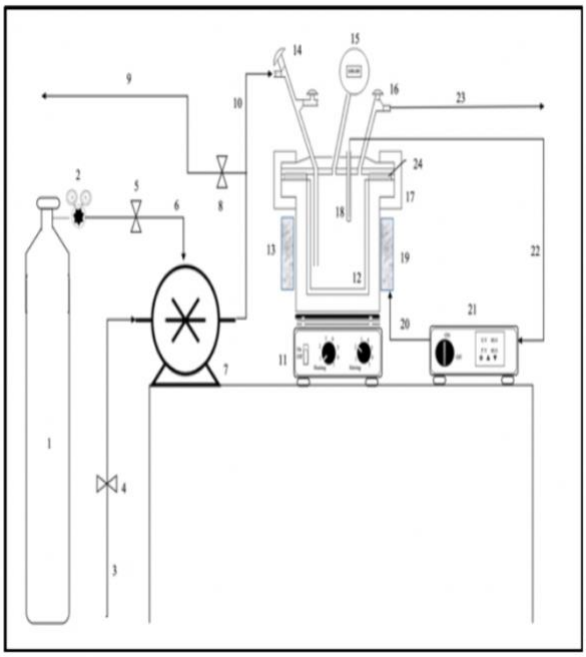
The work indicated that no gold was extracted for the ligand named "C1". The conditions under which the SCE took place was evaluated, and the optimum temperature was found to be 60^{o}C. The optimum pressure at this temperature was then found to be 405.30 Bars. It was concluded that the extraction of gold from the filter paper was the highest when using ligand C4 at 60^{o}C and 400 atm, as all of the C4 added in the extraction vessel had been removed. It was also determined that no gold can be extracted when zero valent gold is used under these conditions. To make zero valent gold extraction possible, there needs to be an oxidant present.

2.7 Other metal extraction experiments

This section will describe a few more SFE processes that have been conducted using many different ligand classes and their experimental setups.

2.7.1 Gold Extraction using SCFs and different ligands

Mawire (2019) developed a SFE process for the extraction of gold from refectory gold ore tailings. He identified 5 possible ligands that can be used in conjunction with $ScCO_2$ and an oxidant that are capable of leaching the gold from the refectory tailings into solution. The ligands that were identified are as follows: 3-(trifluoromethyl)-phenyl-thiourea (TPT), betaine-bis(trifluoromothylsulfonyl)imide ([Hbet][TF_2N]), 1,1-trifluoro-2,4-pentanedione (TTA), 4-methyl-4H-1,2,4 triazole-3-thiol (MHTT) and hexafluoroacetylacetone (HFA). Two adducts were used as oxidants, namely TBP-HNO_3 and TBP-H_2O_2. The experiments involved placing the gold tailings, ligands and TBP-HNO_3/TBP-H_2O_2 into a Hastelloy basket which is a removable liner inside of the reactor. The experiments ran for 6, 12, 18 and 24 hour periods at 100 Bars and 40^{o}C. At the end of each time interval, the CO_2 was vented and the contents of the reactor filtered. The experimental set up used by Mawire (2019) is shown in Figure 2.17.



1 CO_2 Cylinder	13 Pump outlet line
2 High-pressure regulator	14 Reactor gas inlet
3 Compressed air line	15 Pressure gauge
4 Compressed air control valve	16 Reactor gas outlet
5 CO_2 control valve	17 Reactor body clamps
6 CO_2 feed line	18 Thermo-well
7 Maximator air driven pump	19 Heating Jacket
8 Vent line valve	20 Controller response to heating jacket
9 Vent line	21 Temperature controller
10 High-pressure CO_2 feed line to reactor	22 Thermocouple to the controller
11 Magnetic stirrer plate	23 Depressurizing line
12 Hastelloy removable liner	24 O-rings

Figure 2.17: Experimental setup that Mawire (2019) used.

Mawire (2019) reported having a biphasic liquid form that created difficulties with analysis. To circumvent this problem, he dried the solid residue and digested it using a combination of HNO_3, HCl and H_3BO_3. The solution was then diluted and analysed using an atomic absorption spectrometer. It was found that both of the aforementioned oxidants were suitable, with the maximum gold extraction for the TBP-HNO_3 (after 6 hours) and TBP-H_2O_2 (after 4 hours) of 82% and 75%, respectively. The ligands were classified according to their gold extracting abilities after an 18-hour extraction period, and the order was found to be: ([Hbet][TF_2N]) > HFAA > MHTT >TTA > TBP.

2.7.2 Plutonium and Uranium Extraction

Pitchaiah et al. (2019) developed a SFE process as an alternative to the plutonium-uranium extraction (PUREX) process, which reprocesses spent nuclear fuel. Pitchaiah's et al. (2019) research was a first of its kind as it considered the SFE of U and plutonium (Pu) from pyrochemical salt matrices. The SFE involved three different ligands, namely trioctylmethylammonium chloride (TOMAC), acetylacetone (AcAc) and tributyl phosphate (TBP). The U and Pu were extracted from UCl_3-LiCl-KCl/UO_2Cl_2-NaCl-CsCl and $PuCl_3$-LiCl-KCl, respectively. The SFE process followed by Pitchaiah et al. (2019) is very similar to that followed by Prabhat et al. (2016), except

that the collection media used was a mixture of chloroform and 0.01 N HNO_3 for the U-complex and n-propanol and 0.1 N HNO_3 for the Pu-complex. The SFE process that Pitchaiah et al. (2019) used is shown in Figure 2.18.

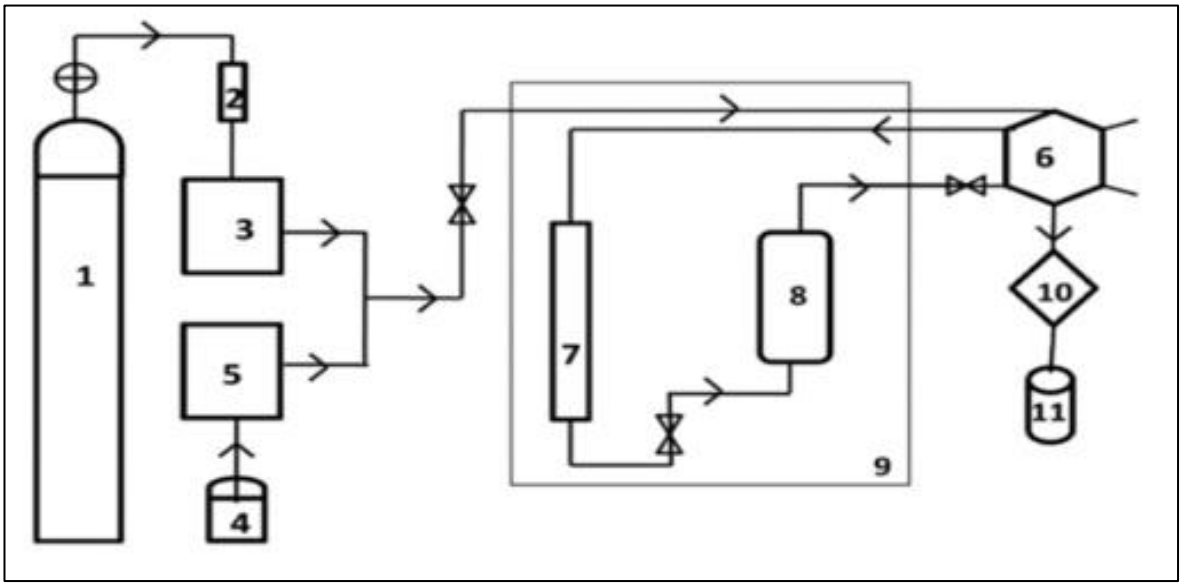


Figure 2.18: Experimental set up used by Pitchaiah et al. (2019). Carbon dioxide cylinder (1), molecular sieve filter (2), carbon dioxide pump (3), co-solvent reservoir (4), co-solvent pump (5), six way valve (6), heat exchanger (7), high pressure extraction vessel (8), oven (9), back pressure regulator (10) and collection vessel (11) (Pitchaiah et al., 2019).

Pitchaiah et al. (2019) found that U could almost be completely extracted when the optimum conditions were 1 N HNO_3, pressure = 200 Bar, temperature = 49.85^oC and n-proponol was used as a co-solvent. However, it was observed that under the above optimum conditions the Pu extraction was much lower. This inefficiency was solved by Pitchaiah et al. (2019) through increasing the static extraction time of the SFE process. This yielded 80% Pu extraction. This work is important as it shows that it is possible to replace current industrial processes with SFE processes, which lead to lower amounts of secondary liquid waste generation.

2.7.3 E-waste Recycling

The recycling of e-waste is a vibrant area of research for the future, as our society discards more and more e-waste as we become more technologically advanced. The recycling of e-waste is generally accomplished through the use of hydrometallurgical and pyrometallurgical processes. These processes are not always environmentally friendly. There is much research being done on the possible applications of superfluid's as a means to recover valuable metals from e-waste. These studies range

from the processing of discarded electronic printed circuit boards to the recycling of liquid crystal displays (LCDs) from cell phones.

Liu et al. (2016) developed a SFE process for the direct extraction of palladium (Pd) and silver (Ag) from used PCBs. The process involves the combination of SCWO and SFE processes. The reason for Liu et al. (2016) using SCWO, was to concentrate the Pd and Ag present before utilising SFE. This was achieved by operating at a temperature of 425^{o}C for 60 minutes and at a solid liquid ratio of 6.25 g/L. Once the SCWO step was completed, the residue was washed, dried and the base metals were removed through the use of a 0.1 M HCl solution at room temperature (25^{o}C) for 10 minutes.

This preconcentration step designed by Liu and co-workers lead to enrichment factors of 5.3 and 4.8 for Pd and Ag, respectively. The SFE process used 0.1 g of the PCB concentrate along with KI-I_2 dissolved in different co-solvents (water/ethanol/acetone). The complexes formed in the reaction vessel were then separated from the solvents through the use of a vacuum rotary evaporator. The experimental set up for extraction and separation processes described above is schematically presented in Figure 2.19.

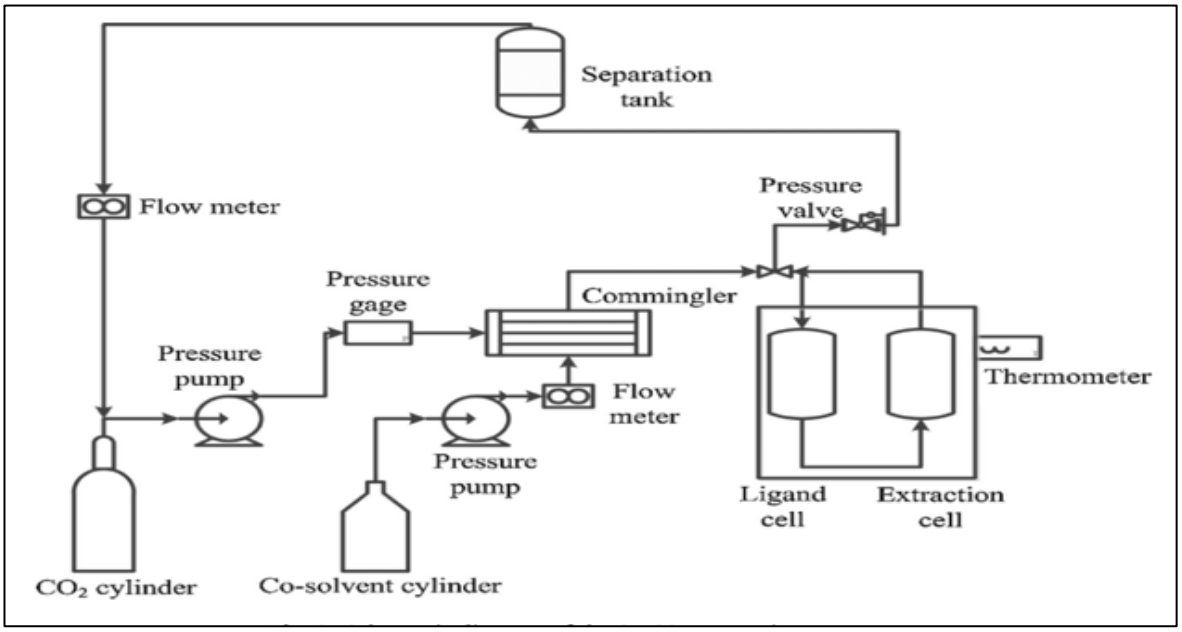


Figure 2.19: Experimental setup used by Liu et al. (2016).

Liu et al. (2016) concluded that it is feasible to extract precious metals from waste. The results of their work is summarised in Table 2.15. It appears as if the acetone-KI-I_2 co-solvent was the most effective at extracting Ag and Pd.

Table 2.15: The findings from Liu et al. (2016).

Co-solvent Used	Pd Extraction (%)	Ag Extraction (%)
No co-solvent	< 4.00	< 4.00
Water	23.30	28.70
Ethanol	68.50	55.60
Acetone	85.90	89.30

Argenta et al. (2017) developed an environmentally friendly method for the recycling of used LCDs from cell phones. This was done through the use of SCFs (see Figure 2.20) and organic acids to extract indium (In) from the LCDs. Argenta et al. (2017) tested the efficiencies of atmospheric leaching against that of SFE. Both processes involved the use of citric and malic acid as well as H_2O_2. Argenta and co-workers established that the optimum conditions for the atmospheric leaching of the LCDs involved using 1 M malic acid at 90°C for 120 minutes with 5% H_2O_2 and a solid to liquid ratio of 1:20. The above leaching conditions yielded an extraction of 74.5%. When citric acid was used, it was lower at 70.9%. These results led to them using only malic acid in the SFE process. They found that the efficiency of In extraction increased to 94.60% in just 30 minutes at a temperature of 100°C, a pressure of 150 Bar, and a solid to liquid ratio of 1:20 with 5% H_2O_2 as oxidant.

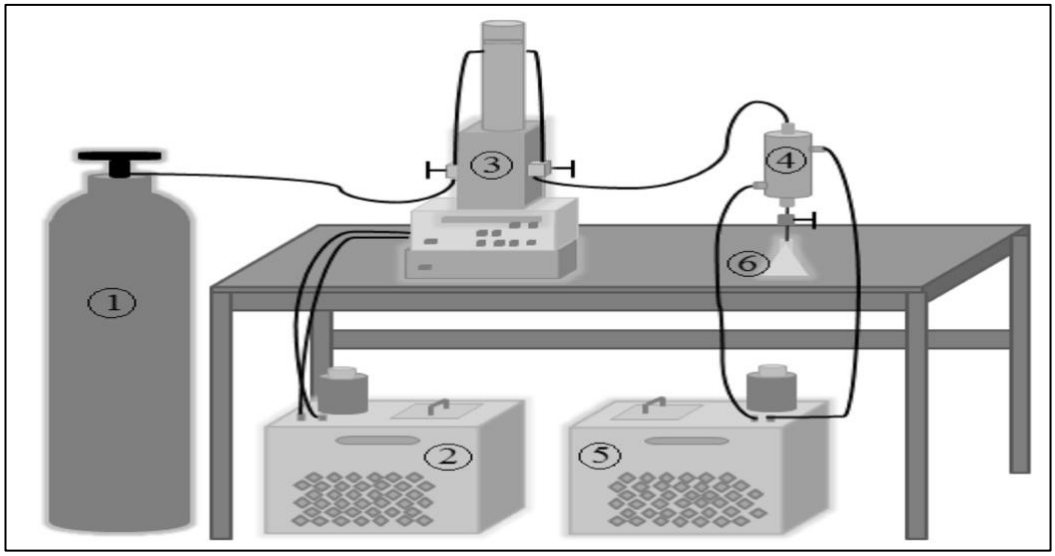


Figure 2.20: Experimental setup used by Argenta et al. (2017). Carbon dioxide cylinder (1), cooling bath (2), high pressure pump (3), extractor (4), heating bath (5), extracted sample (6) (Argenta et al., 2017).

The research described illustrates the great industrial applications of SFE processes as they generally offer much faster extraction times with lowered environmental impact when compared with traditional hydrometallurgical processes. A future, very useful, area of application which has not been explored to date, is the recovery of selected metals from battery recycling operations. The increasing demand for Co, Ni and Li from recycled batteries offers huge opportunities for application of gas phase and $ScCO_2$ extraction processes.

2.8 Summary

This literature review covered the fundamentals of gold chemistry. This was done to better understand how zero-valent gold can be extracted from solid media such as tailings. A range of pre-treatment and leaching techniques that can be used for processing refractory gold ores, were also evaluated to provide the reader with a more wholistic view of gold processing. The leaching section aimed to provided readers with a better understanding of how gold can undergo dissolution.

The pre-treatment section was included to give the reader a broader understanding of how one can go about using pre-treatment methods to aid in treating refractory ores.

Finally, the literature covered the basic principles behind supercritical fluid extraction as well as identified commercially available ligands and modifiers. The top performing ligands according to Mawire (2019), namely [Hbet][TF_2N] and HFA, will be tested against AcAc since it is readily available and costs less than the ligands identified by Mawire (2019). The ligands listed above will be used in conjunction with supercritical CO_2 and TBP-HNO_3 for the extraction of Au from low-grade, refractory gold tailings.

3 Experimental

The following chapter will describe the gold bearing material used in this research, the chemicals used, the preparation methods for synthesizing reagents, the experimental procedures, experimental set up, the analytical techniques applied and finally discuss the supercritical extraction experiments that were conducted in this research.

3.1 Gold bearing materials

Two gold bearing samples were used in the research: tailings from the recovery of gold following mining, and a nugget of gold (purchased from SA Precious metals, purity of 99.9%).

The tailings were collected from the DRD Gold plant (ERGO). The ore used in this research is not the same sample as that used in previous research (Mawire, 2019; Ali, 2021) conducted by our group. However, the ERGO plant tailings come from the same source, that being the Witwatersrand basin. The similarities between the plant tailings used in this research and those used by Mawire (2019) and Ali (2021) will be discussed in section 4.1.

3.1.1 Tailings from gold processing at ERGO

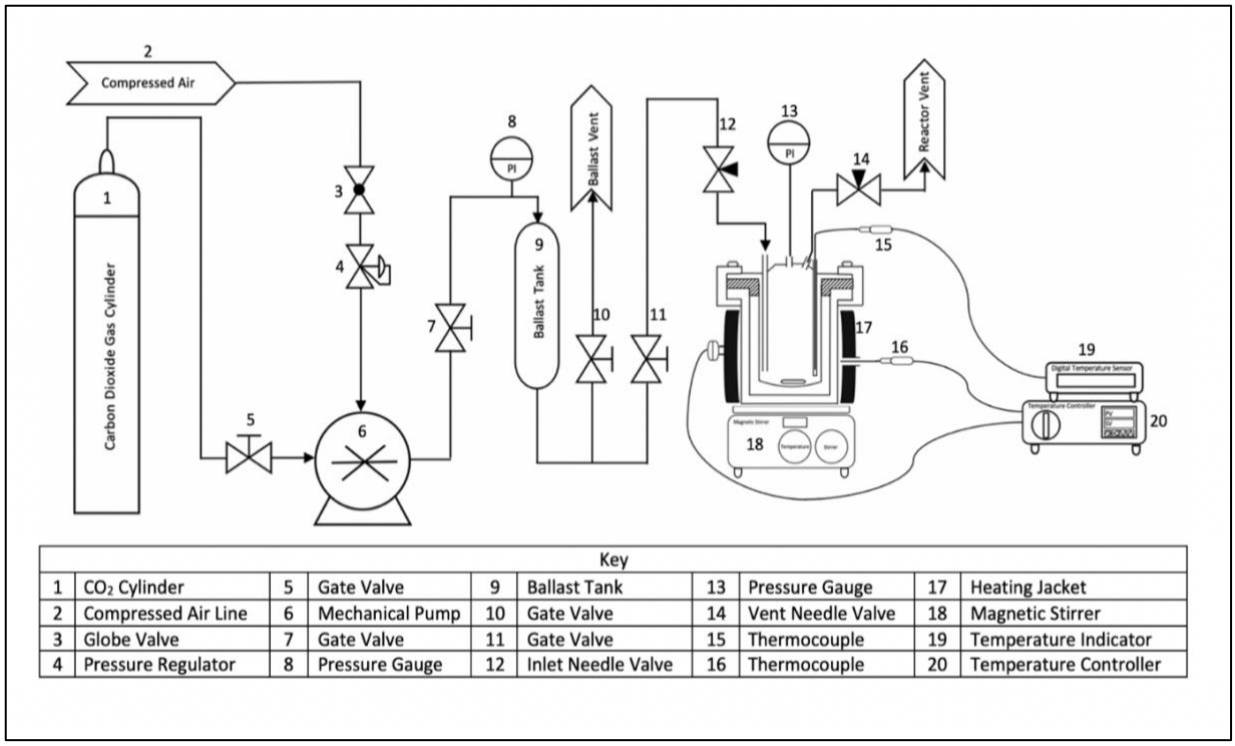
A sample of gold tailings was received from the DRD Gold plant on the East Rand (ERGO) at the outset of the project. The gold content of the ore, determined by fire assay (DRD Gold), was about 0.17 g/t. Representative sub-samples were split from the initial sample. The sample (10 kg) was split into ten representative sub-samples of about 1 kg in a Jones riffler. The split was repeated for each of the 1 kg sub-samples. Sub-samples of 100 g were collected and bagged. These 100 g sub-samples were then divided into two 50 g samples by taking approximately 5 g of material with a spatula at a time, all the time mixing the sub-sample. Three of these 50 g sub-samples were chosen for material characterization. The material was characterized using X-ray diffraction (XRD), X-ray fluorescence spectrometry (XRF), atomic absorption spectroscopy (AAS), inductively coupled plasma atomic emission spectroscopy (ICP-OES) and inductively coupled plasma–mass spectrometry (ICP-MS) (see Section 3.4 for descriptions of the analytical techniques used).

3.1.2 Pure gold nugget

A pure gold nugget (99.9%) was purchased from SA Precious metals and used in a series of supercritical gold extraction experiments. After each experiment the gold nugget was cleaned with ethanol and then cleaned further in an ultrasonic bath to remove any remailing solid residue that may have been on the gold's surface.

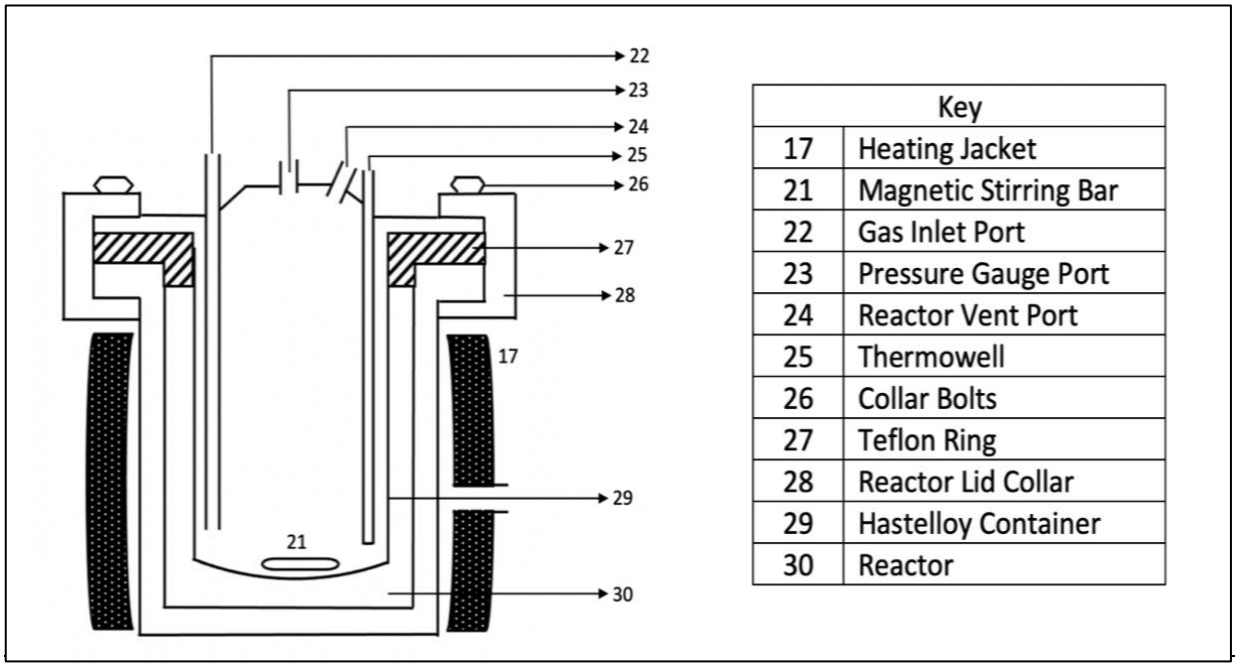
3.2 Experimental apparatus and operating procedure

As part of the research, a supercritical unit was designed and constructed with the assistance of Ultravision. The experiments require supercritical conditions, and this is achieved by pressurising CO_2 using a mechanical pump (see Figure 3.1, point 6). The pump is driven by compressed air, which allows the pump to compress the CO_2. The compressed CO_2 is stored in a ballast tank and the compression continued until the ballast tank contained highly pressurised CO_2 (roughly 100 Bar). The experiments require the high pressure CO_2 to be heated, as it needs to become a supercritical fluid. The heating is achieved through the use of a heating jacket (see Figure 3.1, point 17). The heating jacket is controlled using a controller, and the feedback temperature is read using a thermocouple located inside the heating jacket. The reactor temperature is measured using a thermocouple located in the thermowell. A batch reactor is used, meaning that the reactor is loaded prior to heating and pressurising. The reactor has a Teflon seal (Figure 3.2, point 27) to prevent leaks from occurring. The system is continually stirred, through the use of a magnetic stirrer (see Figure 3.1, point 18).



Key									
1	CO_2 Cylinder	5	Gate Valve	9	Ballast Tank	13	Pressure Gauge	17	Heating Jacket
2	Compressed Air Line	6	Mechanical Pump	10	Gate Valve	14	Vent Needle Valve	18	Magnetic Stirrer
3	Globe Valve	7	Gate Valve	11	Gate Valve	15	Thermocouple	19	Temperature Indicator
4	Pressure Regulator	8	Pressure Gauge	12	Inlet Needle Valve	16	Thermocouple	20	Temperature Controller

Figure 3.1: Supercritical fluid extraction experimental setup, adapted from Mawire (2019).



Key	
17	Heating Jacket
21	Magnetic Stirring Bar
22	Gas Inlet Port
23	Pressure Gauge Port
24	Reactor Vent Port
25	Thermowell
26	Collar Bolts
27	Teflon Ring
28	Reactor Lid Collar
29	Hastelloy Container
30	Reactor

Figure 3.2: Supercritical fluid reactor, adapted from Mawire (2019).

The operating procedure for the Supercritical Unit is as follows:

Step 1: The ballast tank is pressurized the night before to give the system time for the pressure to reach steady state.

Step 2: The reactor is preheated to 40°C to reduce the time needed to reach the required conditions for a test.

Step 3: The ligand is mixed with 20 mL of the oxidant and added along with the sample (a bead of gold or several grams of tailings) in the Hastelloy bucket. With the reactor at temperature, the bucket is placed into the reactor.

Step 4: A Teflon ring is seated on the lip of the Hastelloy bucket to prevent the reagents from creeping out and into the stainless-steel reactor.

Step 5: The reactor is sealed: the lid is seated and the collar fastened; the bolts on the collar are tightened with a torque wrench in the same diagonal pattern to ensure that tightening is even and not too tight.

Step 6: The exhaust valve is closed and the CO_2 inlet valve opened. The reactor is pressurized to 30−40 Bar below the required pressure, then checked for leaks (with soapy liquid).

Step 7: There being no leaks, the reactor is brought to the desired pressure and temperature for the experimental run. The magnetic stirrer is switched on and the test begins. The control of temperature and pressure is maintained by controlling the temperature of the heating jacket and by the injection of CO_2 into the reactor.

Step 8: Thirty minutes before an experiment is due to end, the stirrer is switched off to give the two liquid phases time to separate. Phase separation reduces the amount of liquid that can escape when the reactor is depressurized at the end of the test.

Step 9: To cool gas leaving the reactor during depressurization, ice bags are placed over the exhaust pipe. A tube at the end of the pipe collects condensate.

Step 10: Once the system is depressurized, the reactor is opened, the reactants and products removed and stored for analysis. In tests conducted with samples of tailings, the pregnant solution is separated from the residue in a Büchner funnel connected to a vacuum pump. The residue is washed three times with ethanol. The residue and wash are then analysed.

3.3 Chemicals used and Reagent Preparations

The following chemicals were used in the experiments: hexafluoroacetylacetone (98%) (HFA), acetylacetone (≥99%) (AcAc), bis (trifluoromethane)sulfonimide lithium salt (99.95%), tributyl phosphate (97%) (TBP), betain hydrochloride (≥99%), nitric acid (65%) (HNO_3), hydrogen peroxide (30%) (H_2O_2), gold (99.9%) and carbon dioxide technical (dry). The reagents were purchased from Sigma-Aldrich.

Two reagents needed to be prepared, the adduct (TBP-HNO_3) and the ionic liquid ([Hbet][TF_2N]).

The adduct used in this study was $TBP(HNO_3)_{0.7}(H_2O)_{0.7}$. Others had used this complex successfully to dissolve gold (see Mawire 2019 and Wang & Wai 2005). The adduct was prepared according to a recipe followed by Mawire (2019). The tailings contain very low amounts of gold ($5.6x10^{-6}$ g / 20 g of tailings) thus in theory very small amounts of the adduct was required. However, these small amounts of adduct make it difficult to separate the solids and liquids after the experimental run. Thus 20 mL of the adduct was used in each experiment, this also ensured that there was an excess as side reactions can occur with minerals such as pyrite. The adduct was prepared in 50 mL batches (enough for two experiments). The adduct was prepared by mixing approximately 42.57 mL of TBP (97% purity) with 7.41 mL of HNO_3 (65% purity). Mawire's method included mixing the TBP and HNO_3 for 15 minutes. The mixture was then centrifuged to separate the TBP-HNO_3 adduct from the rest of the mixture. The adduct was separated using a pipette.

The synthesis of [Hbet][TF_2N] has been reported in literature (Mawire 2019; Mori et al., 2015; Volia et al., 2019). The following procedure can be used to synthesize 40 g of [Hbet][TF_2N] (Mawire, 2019; Mori *et al., 2015*; Volia *et al*., 2019). 15.58 g of HbetCl and 28.85 g of $LiTf_2N$ were added to 20 mL of deionized water. The mixture was stirred at room temperature for 1 hour and then refrigerated overnight. The [Hbet][TF_2N] was then separated from the aqueous phase and washed several times using a few milliliters of deionized water, as impurities such as lithium and chloride were present. To test whether the impurities (LiCl) had been removed, the aqueous phase was dosed with silver nitrate ($AgNO_3$). If Cl^- ions were still present, a white precipitate (AgCl)

formed. The [Hbet][TF_2N] washing process needed to be repeated until no precipitation occurred when adding $AgNO_3$ to the aqueous phase. The remaining [Hbet][TF_2N] still contained water. Mawire (2019) heated up the [Hbet][TF_2N] to 110°C to remove any remaining water.

3.4 Analytical Techniques Used

3.4.1 XRF Major

XRF was performed on the tailings sample to determine its mineral characteristics. The XRF major and trace elemental analyses were performed at The University of the Witwatersrand. The XRF major elemental analysis was conducted using a Panalytical X-ray fluorescence spectrometer. The analyses were performed at an instrument setting of 50 kV and 50 mA. A Johnson Matthey Spectrolflux 105 was used to fuse the major elements together and fusing was conducted at 1000°C using 0.35 g of the tailings and 2 g of flux. The calibration standards used were certified international reference materials, namely the NIM series and the USGS series. Elements with a mass percentage greater than 5% are considered to have a precision of 1%, whereas elements with a mass percentage smaller than 5% are considered to have a precision of 5%.

3.4.2 XRF Trace

The trace elemental analysis was performed using a Philips PW2404 x-ray spectrometer. A Moviol solution biner was added to a sample of the tailings and pressed pellets were made. The pellets were used in determining the quantity of trace elements in the ore. The precision of readings was reported as follow: 1% for elements that are present at levels greater than 100 ppm and 10% for elements which are present in the range between 10 and 100 ppm. The precision of the results was determined using counting time as a basis. This analysis used the same reference materials as those used in the XRF major analyses.

3.4.3 XRD

XRD was conducted using a Bruker D2 phaser and the peaks in the diffractogram were identified using Profex (an open-source software). The analysis was performed using a cobalt anode with a wavelength of 1.79 Å, a range of 2 Theta from 5-80 degrees in 0.0274 degree steps.

3.4.4 Micro-Raman spectroscopy

Micro-Raman spectroscopy (μRS) was used to establish the presence of pyrite in the tailings sample. The analysis was performed by the School of Physics at the University of the Witwatersrand, using a LabRam HR. A 2D mapping of the tailings was done, the grid of which was 600 μm × 600 μm with 41 points on each side. This gives a dense map of 1681 points; the measurement interval was set to 15 μm and a laser with a diameter of 1 μm was used. The accumulation time that was used for each data point was 5 seconds, thus the mapping process took roughly 2.5 hours. A reference sample from the RRUFF data base (University of Arzona) was used, the RRUFFID of which is R050190.

3.4.5 AAS

AAS was used to analyse the gold content of pregnant leach solutions from the ore characterization experiments. The instrument used for the analysis was an Agilent Technologies 200 Series AA. A wavelength of 242.8 nm was used, and calibration standards were prepared from a standard gold solution (Agilent Technologies – Gold AA Standard: 1000 μg/mL Au in 20% HCL).

3.4.6 ICP-OES and ICP-MS

Gold analyses of solutions were performed using inductively coupled plasma atomic emission spectroscopy (ICP-OES) and inductively coupled plasma–mass spectrometry (ICP-MS) at the University of Johannesburg. The instruments used for the analyses were a Spectro Arcos ICP-OES and a PerkinElmer NexION 300X quadrupole-ICP-MS. Calibration standards for both ICP-MS and ICP-OES were

prepared using single element standards from Inorganic Ventures and Ultraspec. The analysis solution samples were prepared by first filtering the liquid samples and then diluting it to the analysis concentrations. When conducting the analyses using ICP-MS, a 500 μL sample was pipetted from the filtered solutions and then diluted to 10 mL using a 2% HNO_3 solution. The samples analysed using ICP-OES were prepared in an identical manner; however, a 1000 μL sample was diluted to 10 mL using a 2% HNO_3 solution. The instrumentation settings used by each technique are reported in Table 3.1.

Table 3.1: Instrument settings used for ICP-MS and ICP-OES.

Instrument	Settings	
PerkinElmer NexION 300X quadrupole-ICP-MS	Nebulizer Gas Flow	0.865 L/min
	Auxiliary Gas Flow	1.4 L/min
	Plasma Gas Flow	17 L/min
	ICP RF Power	1500 W
	Analog Stage Voltage	-2100 V
	Pulse Stage Voltage	1500 V
	Discriminator Threshold	7
	Deflector Voltage	-8.25 V
	Quadrupole Rod Offset (QRO)	-12.5 V
	Cell Entrance Voltage	-17 V
	Cell Exit Voltage	-38 V
	Cell Rod Offset	-16.5 V
	Axial Field Voltage	475 V
	Cell Gas A (Helium)	4 mL/min
Spectro Arcos ICP-OES	Plasma Power	1400 W
	Pump Speed	30 Rpm
	Coolant Flow	12 L/min
	Auxiliary Flow	1 L/min
	Nebulizer Flow	0.8 L/min
	Strategy	Standard

3.5 Supercritical Gold Extraction Experiments

The supercritical gold extraction experimental work consisted of the initial preparation of liquid leach solutions from a [Hbet][TF_2N], TBP-HNO_3 and $ScCO_2$ system, additional experimental work consisting of a range of experiments to explore alternative extraction solutions to [Hbet][TF_2N] and TBP-HNO_3 in $ScCO_2$, and gold extraction from the DRD Gold ERGO tailings.

3.5.1 Initial extractions in [Hbet][TF_2N], TBP-HNO_3 and $ScCO_2$

Initially, two liquid samples were prepared to develop a method for analysing the pregnant leach solution obtained from $ScCO_2$ extraction of gold with [Hbet][TF_2N] and TBP-HNO_3. The experimental conditions used to prepare the samples are given in Table 3.2.

Table 3.2: Gold extraction in [Hbet][TF2N], TBP-HNO_3 and $ScCO_2$.

Experiment	Ligand (1 mL)	Oxidant (20 mL)	Temperature (°C)	Pressure (Bar)	Time (hours)	Mass of Au (mg)
1	[Hbet][TF_2N]	TBP-HNO_3	40	100	4	26.5
2	[Hbet][TF_2N]	TBP-HNO_3	80	100	4	26.5

3.5.2 Evaluation of different gold extraction solutions in supercritical CO_2

After the initial experiments were conducted additional screening experiments were performed to determine which ligand-oxidant combinations were the most promising. The top two best performing ligands from Mawire's (2019) work were selected ([Hbet][TF_2N] and HFA) and were compared to a cheaper non-fluorinated β-diketone (AcAc) (see Table 3.3). A gold nugget was used in these experiments to act as a source of zero valent gold, this ensured that the system had an excess amount of gold. The extracted amount of gold was determined by ICP-MS and ICP-OES. As a first measurement, ICP-OES was used, and if the gold levels fell below the detection limits of the instrument a subsequent measurement was made using the ICP-MS. The detection limits when using ICP-MS and ICP-OES are approximately 0.01 mg/kg and 20 mg/kg, respectively. These limits are higher than what one would normally expect

as Au is not as easily detected as other more 'sensitive' elements. The sample matrices were also very complex, i.e. high total dissolved solids in an aqueous-organic mixture, resulting in a higher detection limits.

Table 3.3: Screening experiments of the different ligand-oxidant systems.

Experiment	Ligand (3 g)	Oxidant (20 mL)	Temperature (°C)	Pressure (Bar)	Time (hours)
1	AcAc	6.34 M HNO_3	80	100	8
2	HFA	6.34 M H_2O_2	80	100	8
3	[Hbet][TF_2N]	6.34 M HNO_3	80	100	8
4	AcAc	6.34 M H_2O_2	80	100	8
5†	None	6.34 M HNO_3	80	100	8
6	HFA	6.34 M HNO_3	80	100	8
7	[Hbet][TF_2N]	6.34 M H_2O_2	80	100	8
8†	None	6.34 M H_2O_2	80	100	8

† experiment was conducted using 23 mL of the oxidant

The top two performing ligands were then used in further work to determine the effect of varying the temperature on the amount of gold extracted (see Table 3.4).

Table 3.4: Experiments to determine the effect that changing temperature has on the system.

Experiment	Ligand (3 g)	Oxidant/Adduct (20 mL)	Temperature (°C)	Pressure (Bar)	Time (hours)
1	AcAc	6.34 M HNO_3	90	100	8
2	AcAc	6.34 M HNO_3	100	100	8
3	AcAc	6.34 M H_2O_2	90	100	8
4	AcAc	6.34 M H_2O_2	100	100	8
5	HFA	6.34 M HNO_3	100	100	8
6	HFA	6.34 M H_2O_2	100	100	8

Thereafter, experiments were performed to determine the effect of ligand to oxidant volumetric ratios on gold extraction at the obtained best ligand-oxidant-temperature condition. Experiments were performed at 100°C, 100 Bar for 8 h at AcAc : HNO_3 volumetric ratios of 1:1, 1:0.5, 1:6.45 and 1:0.

The molar ratio (the total reagent volume was kept at 23 mL) of ligand to oxidant was varied for the AcAc:HNO_3 supercritical extraction system. This was done in an attempt to better understand the possible stoichiometric equation that could describe the reaction between the gold, ligand and oxidation. The experiments were performed at 100°C, 100 Bar for 8 h at AcAc:HNO_3 molar ratios of 0:1, 1:0.65, 1:1, 1:1.3 and 1:4.22.

The influence of the concentration of the oxidant, HNO_3, on gold extraction was also determined. The experiments were all conducted using 9.1 mL of AcAc and 13.9 mL of HNO_3 at different concentrations (0; 3.00; 4.50 and 6.34 M).

3.5.3 Extraction of Gold from DRD Gold Ergo tailing

Finally, experiments were conducted on the DRD Gold plant tailings, prepared in section 3.1.1. Three representative samples (roughly 50 g each) were mixed together and further separated into smaller sub-samples (roughly 11.20 g each). The tailings sample was added to the AcAc:HNO_3 (1:1 molar ratio) supercritical CO_2 extraction system at 100°C at 100 Bar for 8 hours. The experiment was performed in duplicate. The experiments used the best operating conditions, within the studied ranges. The liquid samples were analysed using ICP-MS and the solid residue was digested and then analysed using ICP-MS.

4 Results and Discussion

The following chapter presents and discusses the results of all experimental work. It includes the results of the ore characterization as well as the results for the initial experiments conducted using the tributyl phosphate-nitric acid adduct (TBP-HNO_3). The procedure developed to test the pregnant solution after supercritical fluid extraction, using the TBP-HNO_3, will be discussed. The results from the screening experiments for the different ligand-oxidant combinations will then be presented and discussed. The best ligand-oxidant combination was then used in further experiments to determine what effect changing parameters such as the temperature, ligand to oxidant concentration and oxidant concentration had on the supercritical extraction process. Finally, the best conditions for gold extraction, using the pure gold sample, were applied to some low-grade gold tailings from the DRD Gold plant. These results are presented and discussed.

4.1 Characterisation of the Ergo tailings sample

The mineral chemical composition of the ERGO tailing sample is presented in Tables 4.1 and 4.2. From the XRF analysis (see Table 4.1) it is observed that the primary minerals present are silica based. This is supported by the results of the XRD analysis that show that the sample is predominantly made up of quartz, muscovite and chlorite (see Figure 4.1). The elements ranging from Al – Na (see Table 4.1) occur in silicate minerals, which accounts for about (or less than) 13%. The loss on ignition is associated with the loss in mass of the sample as volatiles, water vapour, S and C are removed through heating the sample up. The ore should have very little to no volatiles present. This means that the most likely source of the LOI is from water vapour, C and S. The LOI accounts for roughly 1% of the mass loss, this coupled with the low Fe_2O_3 found in the chemical analysis (around 3%) suggests that there is very little FeS_2 present in the ore.

Table 4.1: Chemical composition of tailings†.

Species	[mass%]‡	Relative uncertainty‡‡
SiO_2	83.75 ± 0.93	1.11
Al_2O_3	6.98 ± 0.07	1.03
Fe_2O_3	3.36 ± 0.04	1.19

K_2O	1.23 ± 0.03	2.48
MgO	0.78 ± 0.01	1.49
CaO	0.40 ± 0.02	5.73
TiO_2	0.37 ± 0.02	5.41
Na_2O	0.14 ± 0.02	16.90
P_2O_5	0.04 ± —	—
Cr_2O_3	0.04 ± —	—
MnO	0.03 ± —	—
NiO	0.01 ± 0.01	86.60
LOI	1.49 ± 0.24	16.27
Total	98.62 ± 0.97	0.98

† Composition measured by XRF

‡ Uncertainties are of type A (statistical—based on the standard deviation of three measurements). They assume a normal distribution and are expressed at the 95% confidence level.

‡‡ The relative uncertainty (%) for each element is calculated as follows: $\frac{2*Standard\ deviation\ of\ the\ readings}{Average\ Mass\ Percentage} * 100$.

The trace elements (see Table 4.2) at ppm levels will reside in trace minerals as well as in solid solution with other minerals. The trace elemental analysis did not include Au which will be discussed later.

Table 4.2: XRF trace element analysis†.

Species	[ppm]‡	Relative uncertainty‡‡
Cr	255.32 ± 5.33	2.09
Ba	223.21 ± 0.56	0.25
Zr	144.80 ± 2.06	1.42
Ni	82.46 ± 3.54	4.29
Zn	70.92 ± 7.81	11.01
V	47.76 ± 7.46	15.63
Co	42.13 ± 2.38	5.65
Rb	35.96 ± 1.53	4.26
Sr	30.79 ± 0.96	3.12
Cu	30.52 ± 5.74	18.82
Pb	29.01 ± 1.89	6.53
U	24.14 ± 3.70	15.32
Y	11.55 ± 0.97	8.40
Ga	7.68 ± 0.57	7.48
Sc	6.75 ± 2.43	36.09
Th	6.71 ± 1.93	28.81

Nb	5.36 ± 0.65	12.10
Mo	0.98 ± 1.02	104.15

† Composition measured by XRF

‡ Uncertainties are of type A (statistical—based on the standard deviation of three measurements). They assume a normal distribution and are expressed at the 95% confidence level.

‡‡ The relative uncertainty (%) for each element is calculated as follows: $\frac{2*Standard\ deviation\ of\ the\ readings}{Average\ Mass\ Percentage} * 100$.

To identify the minerals, present in the tailings, an XRD scan was performed, and the results can be seen in Figure 4.1.

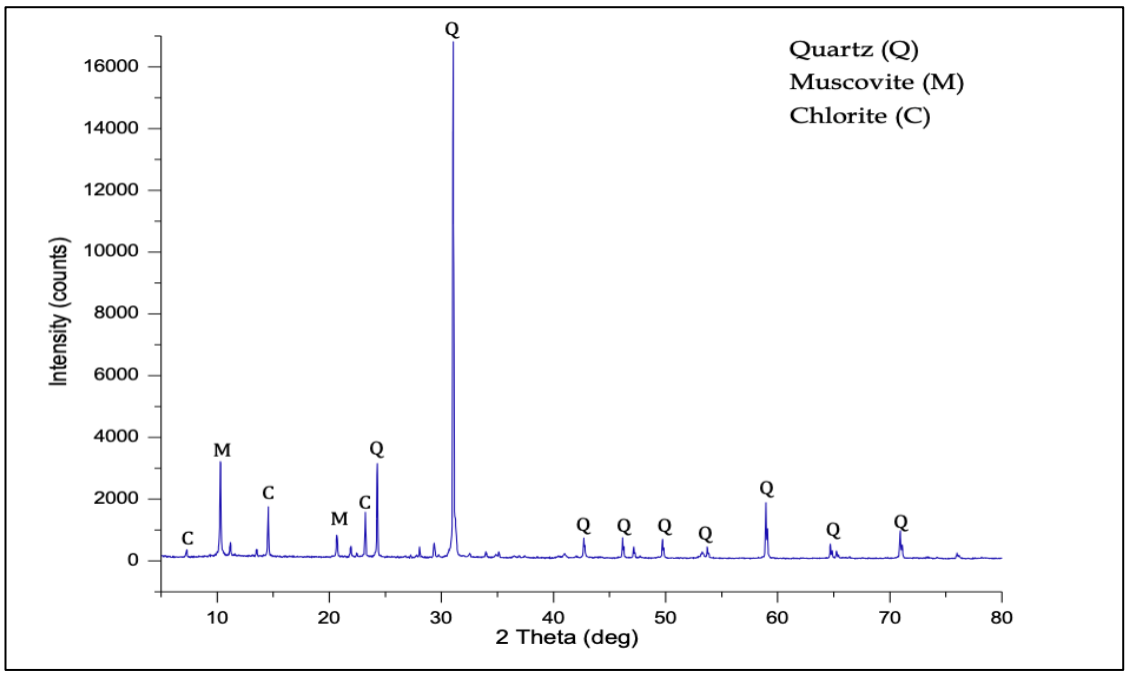


Figure 4.1: XRD diffractogram of the DRD Gold plant tailings [Cobalt anode - wavelength of 1.79 Å, 2 Theta range: 5-80 degrees and steps 0.0274 degrees].

The XRD diffractogram (see Figure 4.1) shows that the tailings is predominantly made up of quartz (SiO_2), along with some muscovite ($KAl_2(Si_3Al)O_{10}(OH,F)_2$) and chlorite ($(Mg,Fe)_6(Si,Al)_4O_{10}(OH)_8$), (chemical formulae for muscovite and chlorite were used from Ali (2022) and Mawire (2019)). Pyrite (FeS_2) peaks could not be identified, and this is due to there being such low amounts present in the tailings.

Micro-Raman spectroscopy (μRS) was used to establish the presence of pyrite in the sample as pyrite could not be confirmed using XRD as mentioned above. The test confirmed the presence of pyrite in the ore sample (see Figure 4.2), and this is important as gold is locked up in refractory minerals such as pyrite and electrum. However, only 4 pyrite particles were identified in the sample. This is a testament to the low-grade nature of the DRD gold tailings.

These results are similar to those found in previous research conducted by Mawire (2019) (see Figure 4.1 in his thesis) and Ali (2021) (see Figure 3.2 in his thesis). Mawire (2019) and Ali (2021) determined (using XRD) that the tailings were predominately quartz, with minor amounts of chlorite and muscovite. There were also trace amounts of pyrite, pyrophyllite and microcline in the tailings.

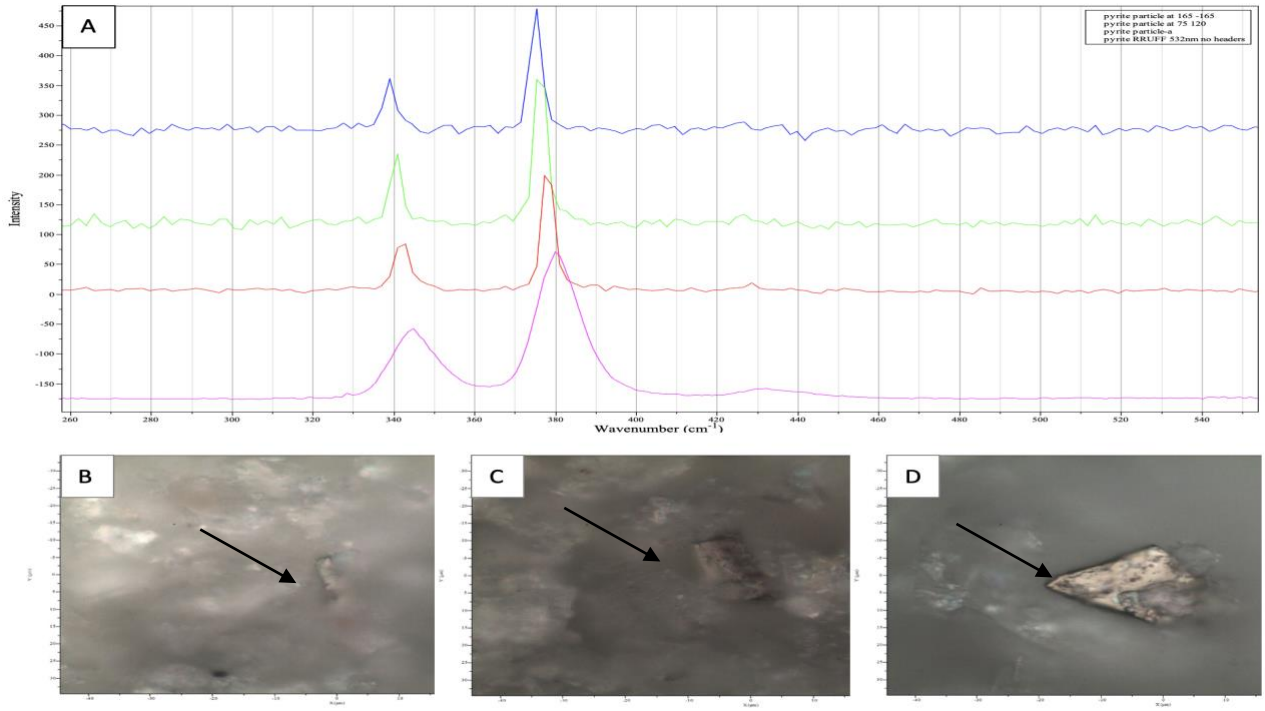


Figure 4.2: Micro-Raman spectra of three particles of pyrite (A–D). Figure A contains the identified pyrite spectrum. The blue, green and red spectra were produced from the pyrite particles identified in Figures B, C and D respectively (see the arrows). The pink spectrum is a reference pyrite sample from the RRUFF data base.

Ergo plant data reported the tailings to contain 0.17 g/t of residual gold (Arshir Narain, personal communications, March 2021). Consequently in 20 g of sample—the maximum mass of sample to be tested in this project—there should be approximately

3.4×10^{-6} g of gold. Owing to the low gold concentration, an attempt was made to determine whether AAS or ICP-OES could be used when determining how much gold is extracted after each 20 g experiment. This was done by using microwave digestion to digest 1 g of each sub-samples in 20 mL of aqua regia.

The digested samples were analysed for their gold content using AAS and ICP-OES. The measurements fell below the detection levels of AAS and ICP-OES. The digestion was repeated with a 20 g sample. Even here the measurements fell below the detection limits of AAS. Larger samples were not tested as the reactor used in this research has a small rector bed; meaning that even if Au was extracted, the amount could not be determined by AAS or ICP-OES. The small reactor bed size means that there is a limit to the quantity of ore that can be used. If too much ore is loaded into the reactor, then the solid to liquid ratio ultimately suffers.

ICP-MS can measure trace elements at very low detection limits. Three of the sub-samples, prepared earlier (see chapter 3.1.1), were mixed, and then split into 12 smaller sub-samples in a small Jones riffler. Two sub-samples were digested using a strong acid, this was done in triplicate. Three masses of tailings were used in each digestion, namely 0.1, 0.15 and 0.2 g. The leach solution was then analysed by ICP-MS (see Table 4.3). The level of gold in the sample of tailings is 0.28±0.07 g/t, and this is significantly different to that determined by DRD Gold. This grade will be used in the research.

Table 4.3: Au in the sample of DRD Gold tailings tested.

Sub-Sample	Mass (g)	Au (mg/kg)	Total Au in sample (mg/kg)	Average Au in each sub-sample (mg/kg)
Sample 1—Test 1	0.1001	1.349	0.337	
Sample 1—Test 2	0.1542	1.577	0.256	0.295
Sample 1—Test 3	0.2014	2.346	0.291	
Sample 2—Test 1	0.1034	1.037	0.251	
Sample 2—Test 2	0.1521	1.536	0.252	0.260
Sample 2—Test 3	0.2038	2.263	0.278	
Average				$0.28 \pm 0.07^{\dagger}$

† Calculated as 2 times standard deviation of the 6 readings, which, if the uncertainties are normally distributed, equates to an uncertainty at the 95% confidence level.

4.2 Feasibility of gold extraction using [Hbet][TF_2N], TBP-HNO_3 and $ScCO_2$

It is well-established from literature that tributyl phosphate (TBP) can act as a ligand and an additive to increase the solubility of HNO_3 in $ScCO_2$, which it does by forming an adduct, TBP-HNO_3 (Wang & Wai 2005; Mawire 2019, Prabhat et al., 2016; Wuhau et al., 2010). The adduct, namely TBP-HNO_3, is an ideal oxidising agent when trying to oxidise zero valent metals as the TBP allows the HNO_3 to be carried by the $ScCO_2$ to the reaction interface. Mawire (2019) showed that gold could successfully be extracted from a low-grade gold tailings sample in $ScCO_2$ using TBP-HNO_3 as an oxidant with various ligands. As a continuation of his work, this study investigated the feasibility of using TBP-HNO_3 as an adduct and the possible safety implications thereof. Work done by Mawire (2019) identified the analysis of the liquid phase as a challenge as it formed a biphasic liquid and analysis with AAS and ICP was not possible.

To establish a method to analyse for gold , pure gold in the form of gold shavings were used. A liquid product sample was prepared at 100 Bar and 80°C after 4 hours , with the reactor initially charged with 1 mL of the betaine bis(trifluoromethylsulfonyl)imide ([Hbet][TF_2N]), 26.5 mg Au and 20 mL of the TBP-HNO_3.

The liquid product sample was sent to CM Solutions for analysis. The company has expertise on how to break down the organic compounds in the sample to allow for gold analysis using ICP. The analysis protocol involved taking 1 mL of the $ScCO_2$ gold extraction sample containing organic compounds and adding it to 20 mL of concentrated nitric acid. The sample was brought to boiling point and left until all brown fumes dissipated. Then 5 mL of concentrated perchloric acid ($HClO_4$) was added to the sample to digest any remaining organic material and left until no white perchloric acid fumes were being produced. Thereafter the sample was cooled and 5 mL of aqua regia was added. Once digestion was complete (brown nitric fumes stopped), the treated solution was made up to 50 mL and analysed for Au using ICP. It was found that the gold in solution was very low at this dilution and hence the sample was concentrated to 10 mL. At this final volume, gold could easily be detected. The Au in solution was 0.27 mg/L and interestingly, ICP analysis also detected iron (Fe) in the solution at a concentration of 113 mg/L. The most likely source of Fe in

solution could be from corrosion of the Hastelloy liner or the stainless steel reactor lid during the experiment.

During the development of the analysis protocol, a safety concern was raised. The strong smell of TBP and other digestion vapours were detected despite wearing a respiratory mask and working in a fume hood. The digestion solution was also very volatile during the preparation steps. It is known that TBP, according to its safety data sheet (MSDS), is "suspected of causing cancer", posing a safety risk. CM solutions also advised the group that they were not willing to analyse any samples of this nature any further. Further analysis of experiments conducted using the TBP was discontinued. As the amount of gold extracted in an experiment was too little to measure confidently without using AAS or ICP, the solid gold shavings could not be weighed and the extracted mass of gold determined by difference. Determining extraction in this way easily produced relative uncertainties at the 95% confidence level of ± 100%, if not more.

In addition to the challenges experienced analysing the liquid sample, it was also observed that when increasing the [Hbet][TF_2N] amount to 2 mL in the reactor, a white precipitate formed. This was seen for extractions at 100 Bar - 40°C, and 100 Bar - 80°C after 4 hours (26.5 mg Au in 20 mL of the TBP-HNO_3). The precipitates from both experiments were analysed using single-crystal X-ray diffraction and it was found that both had the same unit cell and thus were the same compound (see Figure 4.1 for the identified structure).

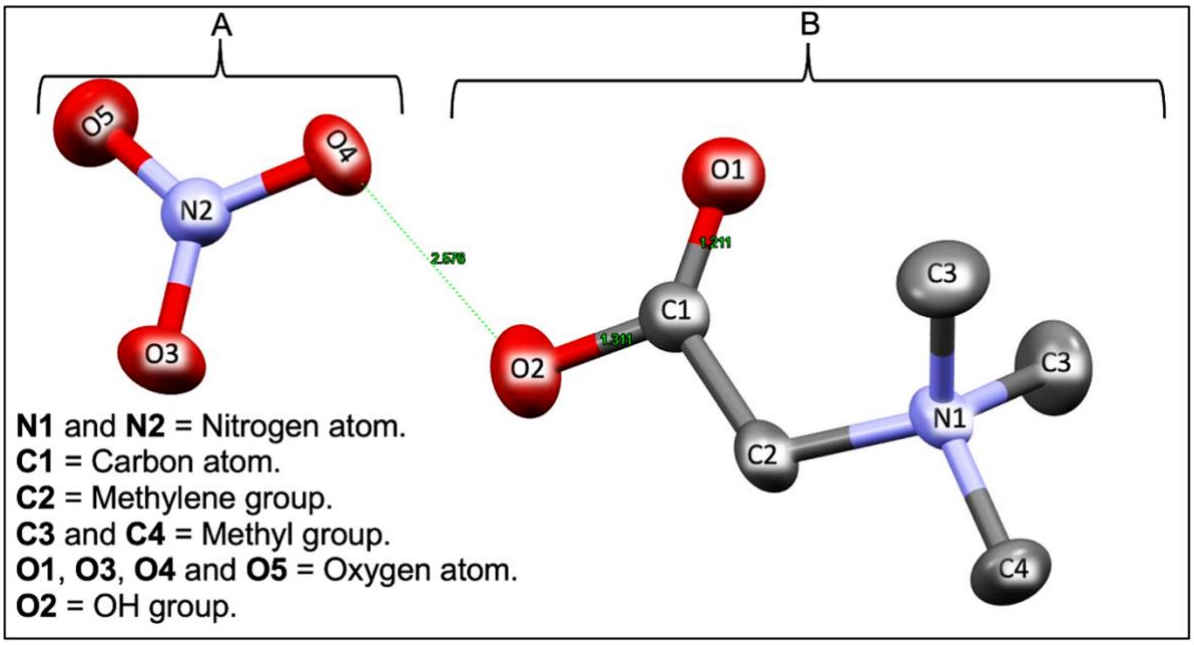


Figure 4.3: Molecular structure of crystalline precipitate (Trimethylammonioacetic acid nitrate).

The identified compound (seen Figure 4.3) is known as trimethylammonioacetic acid nitate (betaine nitric acid). The molecule consists of a nitrate molecule (part A) that is bonded to an OH group (through hydrogen bonding) in the carboxylic acid group (part B). The formation of this complex has been reported by Haussühl (1989). It was developed as part of Haussühl's research which looked at growing large single crystals of betaine adducts from aqueous solutions. The formation of the betaine nitric acid adduct means that the [Hbet][TF_2N] is sensitive to the nitric acid in the SFE process. Thus, the IL is undergoing a side reaction with the nitric acid. This introduces an inexpedience as it means that [Hbet][TF_2N] and HNO_3 are being consumed, thereby reducing the amount of reagent available for Au extraction.

The use of [Hbet][TF_2N] and TBP-HNO_3 as extractants in a supercritical gold extraction system pose safety as well as operational challenges which was not foreseen by Mawire (2019). As a result, it was decided to consider alternative extraction mixtures (ligand and oxidant) to apply to the low-grade gold sample from DRD gold.

4.3 Developing a new SFE process without using Tributyl phosphate (TBP)

The results from the TBP experiments lead to a re-evaluation of the process developed by Mawire (2019). TBP aids in solubilising HNO_3 in $ScCO_2$. Removal of the TBP from the supercritical extraction mixture therefore has mass transfer implications. Consequently, different options were identified and considered, these included:

i. Finding a suitable replacement Lewis base for TBP, one that aids in solubilising HNO_3 in $ScCO_2$.
ii. Finding a suitable acid that can be used in the $ScCO_2$ extraction process to oxidise gold.

A literature review showed that TBP was the only proposed solubilising agent in supercritical metal extraction and hence it was decided to pursue option (ii).

Mawire (2019) identified H_2O_2 as an oxidant that is capable of working in the $ScCO_2$ extraction process. Mawire (2019) compared extraction results for the H_2O_2 system to that of a system using HNO_3 in its undissolved form. It is important to understand how changes to the reagent solubilities can affect the reactions/transport phenomena that take place in a supercritical extraction system.

Figure 4.4 (a) and (b) illustrate the possible interactions during the SFE process when using the TBP-HNO_3 adduct (soluble oxidant) and an insoluble oxidant (HNO_3/H_2O_2) in $ScCO_2$ respectively.

The following steps occur during the process and are presented in Figure 4.4a:

1. The adduct/ soluble oxidant (i.e. non-polar acid) dissolves in the $ScCO_2$.
2. The adduct/ soluble oxidant is carried by the $ScCO_2$ to the reaction sites. Due to the fluid-like nature of the $ScCO_2$, the adduct/ soluble oxidant can penetrate into any cracks in the ore accessing hard to reach reaction sites.

The HNO_3 in the adduct or the soluble oxidant provides the oxidation potential needed to convert Au^0 into either Au^{+1} or Au^{3+}.

3. The ligand, also transported to the reaction sites in a similar fashion, reacts with the oxidized gold and forms a gold complex.
4. If the gold complex is soluble in $ScCO_2$ then the complex diffuses back into the bulk solution. If not, the ligand stays dispersed in the stirred liquid phases.

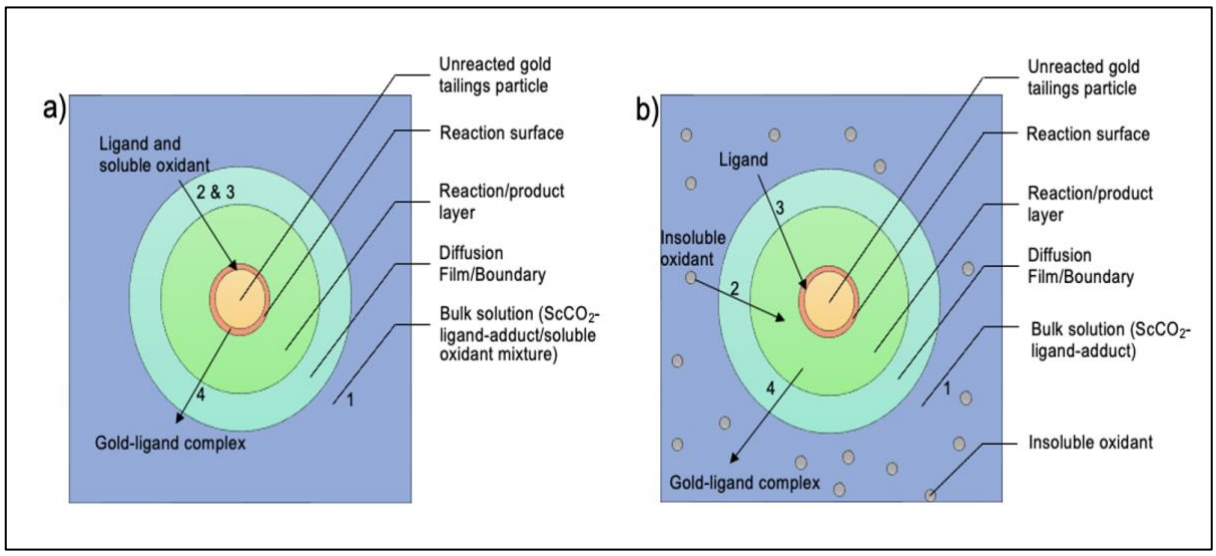


Figure 4.4: Possible transport steps in the SFE process.

The steps involved in Figure 4.4b are very similar, except that the insoluble oxidant is not transported as effectively as the ligand-$ScCO_2$ mixture. As mentioned before supercritical fluids have great diffusivity, and other mass transport properties, thus if the oxidant is insoluble then it does not benefit from the enhanced properties of the supercritical fluid (diffusion of the oxidant to the reaction sight may be slower). There will still be a transfer of the gold complex from the aqueous/organic bulk solutions into the SCF, as long as the complex is soluble.

This research followed a fundamental approach to better understand the reactions taking place in the SFE process. Therefore, pure gold was used to limit the rate limiting effect of gauge material in the ore and thus studying a pure gold-ligand-oxidant-$ScCO_2$ system.

One might argue that, in using a solid button of gold, the reaction would be slower because the surface area is smaller. But gold in the tailings has a much smaller surface area—there is only 0.17 g Au/t. Thus by using a solid piece of gold, we have a larger surface area while ensuring that we don't lose any gold when cleaning the reactor. Calculations (see Equations 31-33) were performed to support this hypothesis and they are presented in Table 4.4.

$$Sample\ Volume\ (cm^3) = \frac{Mass\ of\ Au\ in\ the\ sample\ (g)}{Density\ of\ Au\ (g/cm^3)} \quad (31)$$

$$Diameter\ per\ particle\ (\mu m) = 2 * \left(\sqrt[3]{\frac{Sample\ Volume\ (cm^3)}{Number\ of\ Particles} * \frac{3}{4} * \frac{1}{\pi}} \right) * 10000 \quad (32)$$

$$Surface\ Area\ (mm^2) = Number\ of\ Particles * \pi * \left(\frac{Diameter\ (\mu m)}{1000} \right)^2 \quad (33)$$

Table 4.4: Surface area of gold particles assuming a set mass and that particles are spherical.

Assuming 8.8555g of gold			Assuming the sample has a grade of 0.17 g/t and we use 20 g		
Number	diameter [µm]	s. area [mm^2]	Number	diameter [µm]	s. area [mm^2]
1	7832.4	192.7	1	69.6	0.0152
2	6216.5	242.8	2	55.2	0.0191
4	4934.1	305.9	4	43.8	0.0241
8	3916.2	385.4	8	34.8	0.0304
16	3108.3	485.6	16	27.6	0.0383
32	2467.0	611.9	32	21.9	0.0482
64	1958.1	770.9	64	17.4	0.0608
128	1554.1	971.3	128	13.8	0.0766
256	1233.5	1223.7	256	11.0	0.0965
512	979.0	1541.8	512	8.7	0.1216
1024	777.1	1942.5	1024	6.9	0.1532
2048	616.8	2447.4	2048	55	0.1930
4096	489.5	3083.6	4096	4.3	0.2432

The results (see Table 4.4) show that the surface area of the pure gold button is four orders of magnitude greater than the gold contained in 20 g of the tailings. This puts to rest the argument that by using a solid button of gold that we are slowing down the reaction rates, in fact we are most likely speeding up the rate of the reaction.

Experiments were conducted with H_2O_2 to see if it could replace the TBP-HNO_3 adduct. The results were compared to a system where HNO_3 alone was used as the oxidant (mass transfer mechanisms described earlier). Three different ligands were used, namely acetylacetone ($C_5H_8O_2$) (AcAc), hexafluoroacetylacetone ($C_5H_4F_3O_2$) (HFA) and [Hbet][TF_2N] along with HNO_3 (6.34 M) or H_2O_2 (6.34M). The tests were run at 100 Bar, 80°C for 8 h. The solutions were analysed with ICP-MS and ICP-OES and were analysed for Au, Cr, Ni and Fe content. Even though a solid gold nugget was used in the experiments, additional metal analysis was performed to determine if leaching of metals from the reactor took place.

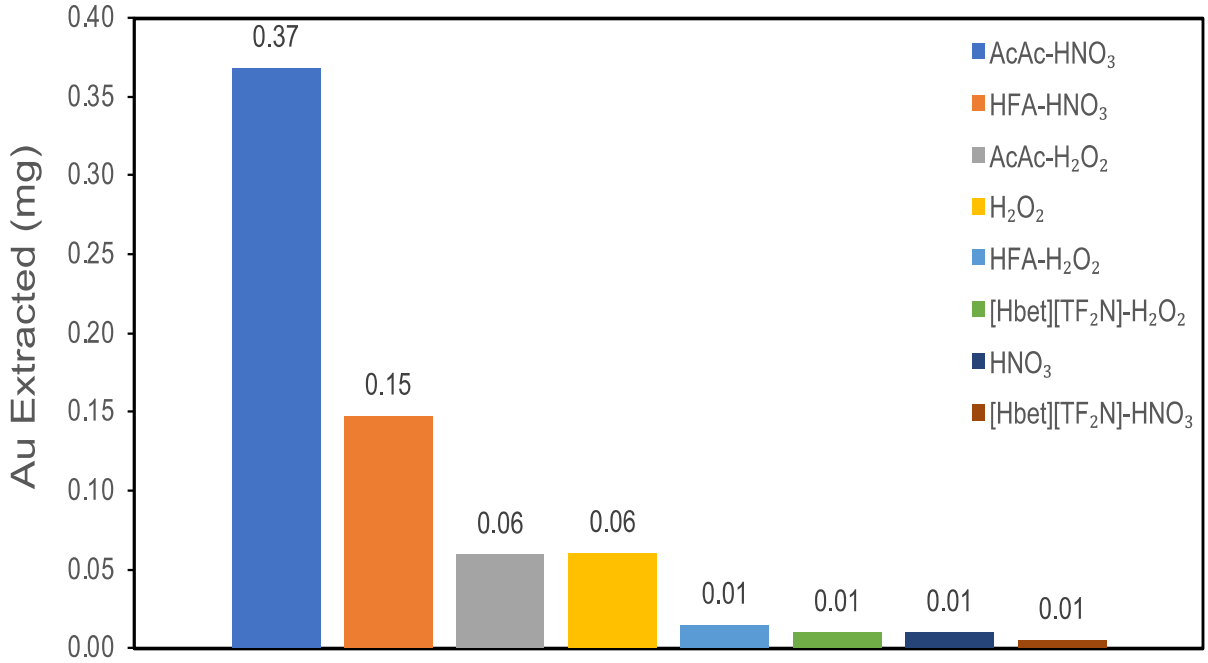


Figure 4.5: SFE of Au in different oxidants (20 mL HNO_3 or H_2O_2) and 3 mL of the ligands (Acetylacetone(AcAc), hexafluoroacetylacetone (HFA) and betaine bis(trifluoromethylsulfonyl)imide ([Hbet][TF_2N])) at 100 Bar, 80℃ for 8 h.

Blank tests, using only HNO_3 or H_2O_2 (see Figure 4.5) and no ligands, were conducted to establish a base Au extraction reading and also to determine if the oxidants had any extraction abilities of their own. The results show that even when just using HNO_3 or H_2O_2 that there was some Au extracted, albeit small amounts, 0.01 and 0.06 mg respectively. These results also show that the H_2O_2, when used alone, extracted more Au than the HNO_3. However, it must be noted that we do not have a standard deviation for the results, thus more research is required to definitively say that H_2O_2 extracts more Au than HNO_3 (when used alone).

The amount of Au extracted does change dramatically when the fluorinated β-diketone (HFA) and non-fluorinated β-diketones (AcAc) were added to the HNO_3 system, however this is not the case for the H_2O_2 system. There was no improved kinetics when AcAc was added to the H_2O_2 system and worse kinetics were observed when HFA was added to the H_2O_2 system. The AcAc-HNO_3 and HFA-HNO_3 systems extracted, 0.37 mg and 0.15 mg respectively. These are orders of magnitudes greater than the systems in which only oxidants were used. The AcAc-HNO_3 and HFA-HNO_3 combinations extracted 35.8 and 13.7 times more Au than the HNO_3 system (based on calculated values).

It is known that the solubilities of fluorinated β-diketones (HFA) in $ScCO_2$ are at least an order of magnitude higher than non-fluorinated β-diketones (AcAc) (Ashrat-Khorassani et al.,1997b). The fluorinated β-diketone used in this research also has a higher thermostability than AcAc (Özel et al, 1997). Taking the above points into consideration, one would expect HFA to extract more Au than AcAc, however this is not observed from the results. The AcAc-HNO_3 system extracted roughly 2.5 times more Au than the HFA-HNO_3 system. Possible explanations for this increased Au extraction could include, (i) that the amount of ligand is so small that the solubility plays no role in the mass transfer as all of the ligand is dissolved in the $ScCO_2$, (ii) the initial molar concentration of AcAc in solution is higher than that of HFA (identical volumes) increasing the chemical kinetics, (iii) side reactions occur that consume the HFA and (iv) another possibility could be that the mass transfer of the reaction products influences the kinetics. At present, it is difficult to say if any of these or other factors contribute to the experimental observations and additional experimental work will have to be conducted.

However, from a cost point of view these results are promising. If one considers that the cost of a reagent influences the economic viability of a process substantially, the price of AcAc and HFA are roughly R1.47/mL and R184.59/mL, respectively (Sigma-Aldrich). The price of AcAc is therefore two orders of magnitude less than that of HFA. This means that by identifying AcAc as an alternative ligand to HFA, that the associated reagent cost has possibly been reduced by two orders of magnitude. The use of fluorinated compounds is also not ideal from an environmental perspective.

The results for the [Hbet][TF_2N]-HNO_3 system shows that it is by far the worst performing system (reported in the figure as 0.01 mg but the calculated value was 0.005 mg). This reinforces the findings of previous experiments that suggested that the [Hbet][TF_2N] is attacked by the HNO_3, producing trimethylammonioacetic acid nitrate. This implies that both [Hbet][TF_2N] and HNO_3 are being consumed by this side reaction, leading to less being available for the oxidation and complexation of Au, resulting in lower Au extractions.

It was observed in Mawire (2019), that the HFA-TBP-HNO_3 system did extract Au. He determined that the [Hbet][TF_2N] -TBP-HNO_3 system extracted more Au than the HFA-TBP-HNO_3 system. However, this is not the case in the current research as this research uses pure gold and no TBP. Mawire (2019) achieved roughly an Au extraction of 77% and 53% after 8 hours, for the [Hbet][TF_2N]-TBP-HNO_3 and HFA-TBP-HNO_3 systems, respectively. This could suggest that the TBP played a greater role in the Au extraction process than initially thought, as it has been shown that the [Hbet][TF_2N] is attacked by the HNO_3 (refer to the crystal formed in Figure 4.3).

Figure 4.6 presents chrome (Cr), Fe and nickel (Ni) extraction results for the HFA and AcAc systems. It can be seen that that there is a general trend of increasing metal extraction when using HFA in the HNO_3 system. This could explain why we see slower gold extraction kinetics for HFA than AcAc as more side reactions occur which consumes the HFA. It also gives merit to the statement that we have made about AcAc possible being more reactive than HFA when extracting Au as the amount of Au extracted using HFA is very small, 0.01 mg.

The trends seen in Figure 4.5 showed that the systems in which concentrated HNO_3 (6.34 M) was used, resulted in greater amounts of Au being extracted. However, this is not the case when looking at metals other than Au, specifically in the HFA system (see Figure 4.6). The use of H_2O_2 as an oxidant, instead of HNO_3, lead to an increase in the amount of Fe, Ni and Cr being extracted with no effect on the amount of Au that was extracted. The amount of Fe, Ni and Cr extracted increased from 8.61, 22.03 and 5.72 mg to 64.28, 47.73 and 23.90 mg, respectively. This means that the reactor metals leach more readily when using the HFA-H_2O_2 system as opposed to the other

systems. Thus, one could possibly use the HFA-H_2O_2 system if the aim is to extract base metals.

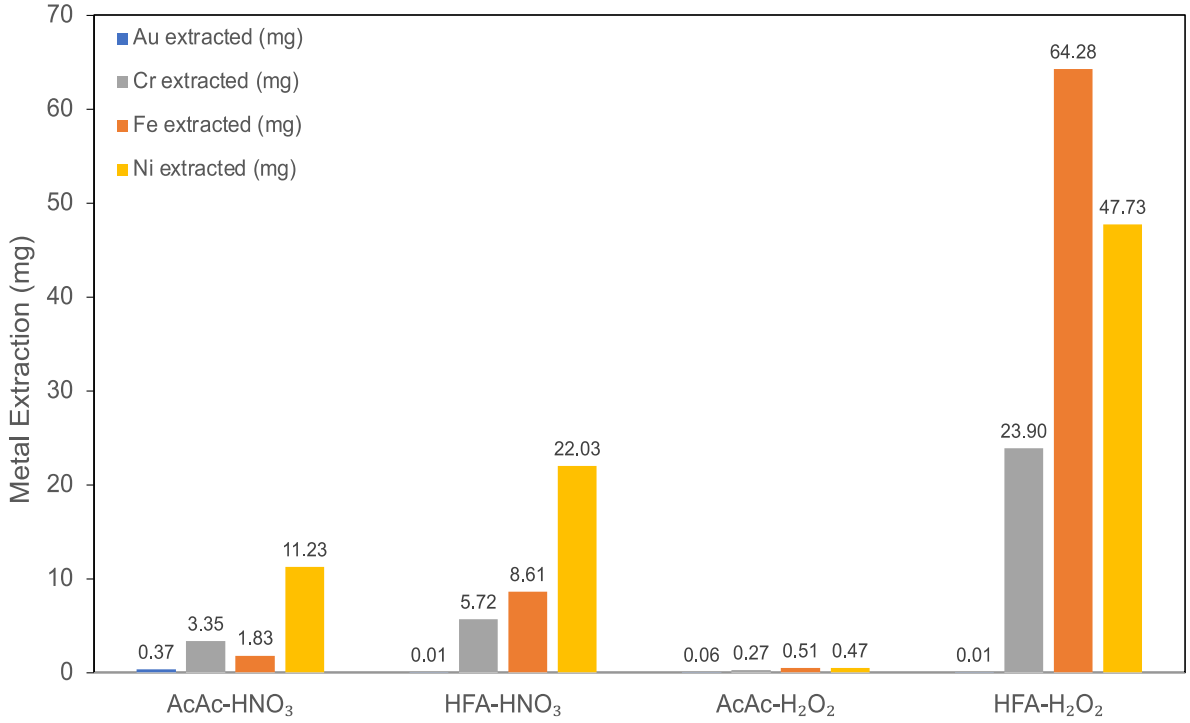


Figure 4 6: Metals extracted using AcAc/HFA with different oxidants after 8 hours at 100 Bar and 80℃.

The effect of temperature on Au extraction was evaluated for the two best performing ligands (with respect to Au extraction), namely the AcAc (see Figures 4.7 and 4.8) and HFA (see Figures 4.9 and 4.10) in different oxidising systems. The temperatures used for these experiments were 80, 90 and 100˚C.

Gold extraction results for the AcAc-HNO_3 and AcAc-H_2O_2 systems are presented in Figures 4.7 and 4.8 below.

Figure 4.7 shows that there is approximately a 63% increase in the amount of Au extracted when operating at 100˚C as opposed to 80˚C. This increase in metal extraction is expected as Mawire (2019) showed that in similar experiments, that the reaction kinetics is a function of temperature. The mass transfer and chemical kinetics in the supercritical environment becomes better as the temperature increases and in doing so increases the rate at which Au is extracted. The increasing trend is also

observed when looking at the amount of Fe, Cr and Ni that are being extracted from the reactor surface by side reactions. Most noteworthy is the amount of Ni that was extracted, it increased from 11.23 mg (80°C) to 18.63 mg (100°C), this is an increase of roughly 66%.

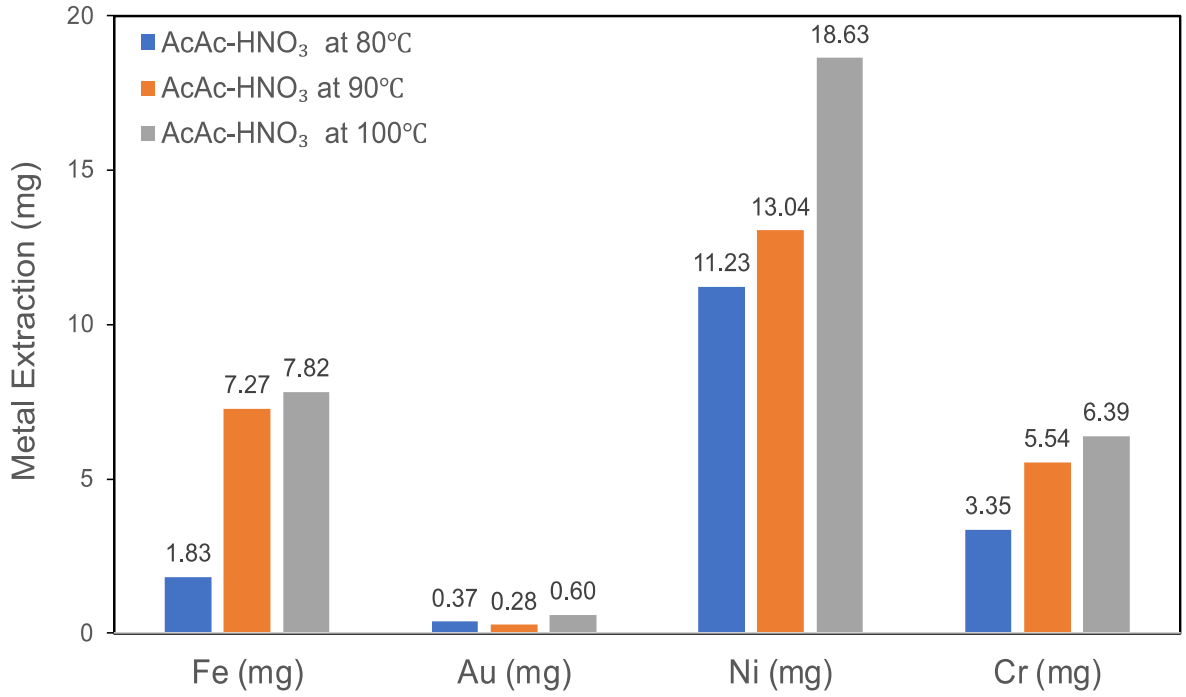


Figure 4.7: AcAc-HNO_3 (20 mL of 6.34 HNO_3 and 3 mL AcAc) metal extraction over a temperature range (80-100°C) for 8 hr at 100 Bar.

The trends observed in Figure 4.8 are similar to those in Figure 4.7. Once again there is an increase in the amount of metal extracted when there is an increase in temperature. When increasing the temperature from 80°C to 90°C, there is a sharp increase in the amount of Au extracted. However, when the temperature increased to 100 °C, the concentration of Au in solution dropped to below 0.03 mg/L. Therefore, it has been reported (see Figure 4.8) as 0 mg as it is below the detection limits of our equipment. The reasons behind this decrease in Au extraction could be due to the disproportionation of H_2O_2 to H_2O and O_2. The disproportionation of H_2O_2 occurs with time under normal conditions, and it is conceivable that an increase in temperature speeds this reaction up. H_2O_2 has a redox potential of +1.776 V whereas O_2 has a lower redox potential of +1.23 V, this means that H_2O_2 is the stronger oxidant (Brown, 2015), thus there is a decrease in the Au extraction as less H_2O_2 is present in the system (due to the side reactions and disproportionation). This means that the

lowered oxidation potential of the system results in the conditions not being favourable to oxidise Au^0 into Au^+/Au^{3+}.

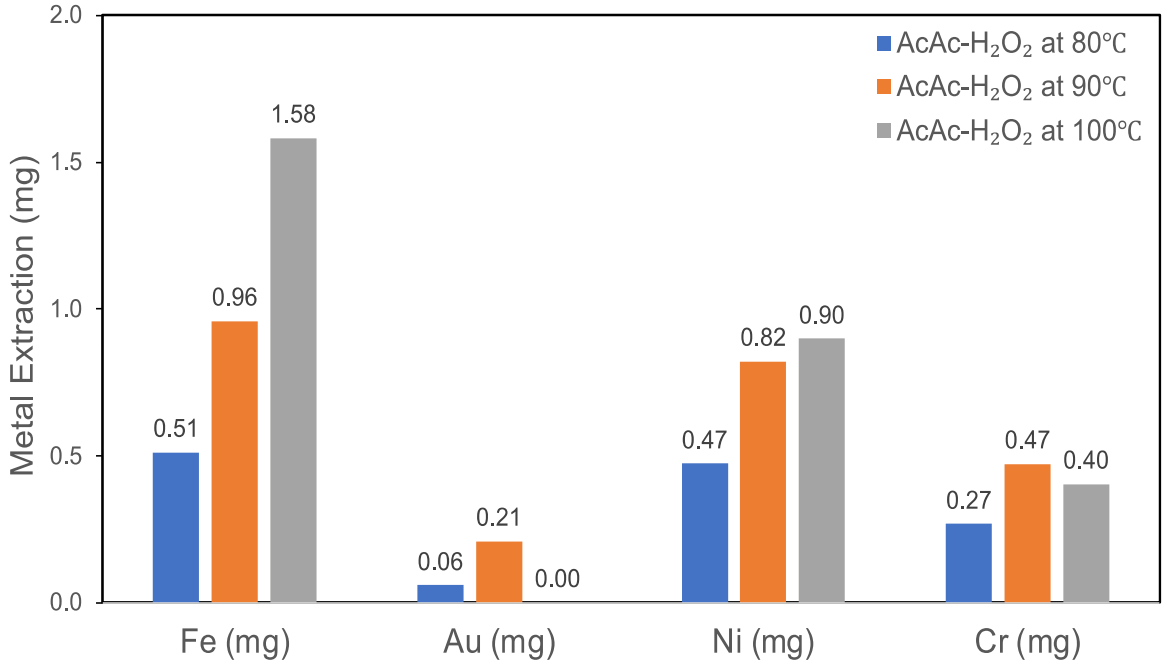


Figure 4.8: AcAc-H_2O_2 (20 mL of 6.34 H_2O_2 and 3 mL AcAc) metal extraction over a temperature range (80-100℃) for 8 hr at 100 Bar.

Gold extraction experiments were also conducted for the HFA-HNO_3 and HFA-H_2O_2 systems, however experiments were only conducted at 80°C and 100°C (see Figures 4.9 and 4.10). The results for both systems show that there is very little change in the amount of Au that is extracted. There are slightly lower amounts of Au being extracted at the higher temperatures, the amount is negligible. However, results show that there is a distinct increase in the amount of Fe, Cr and Ni extracted, in both systems, as the temperature increases. The HFA-HNO_3 system (see Figure 4.9) had the greatest increase in Fe, Ni and Cr extraction as the temperature increased.

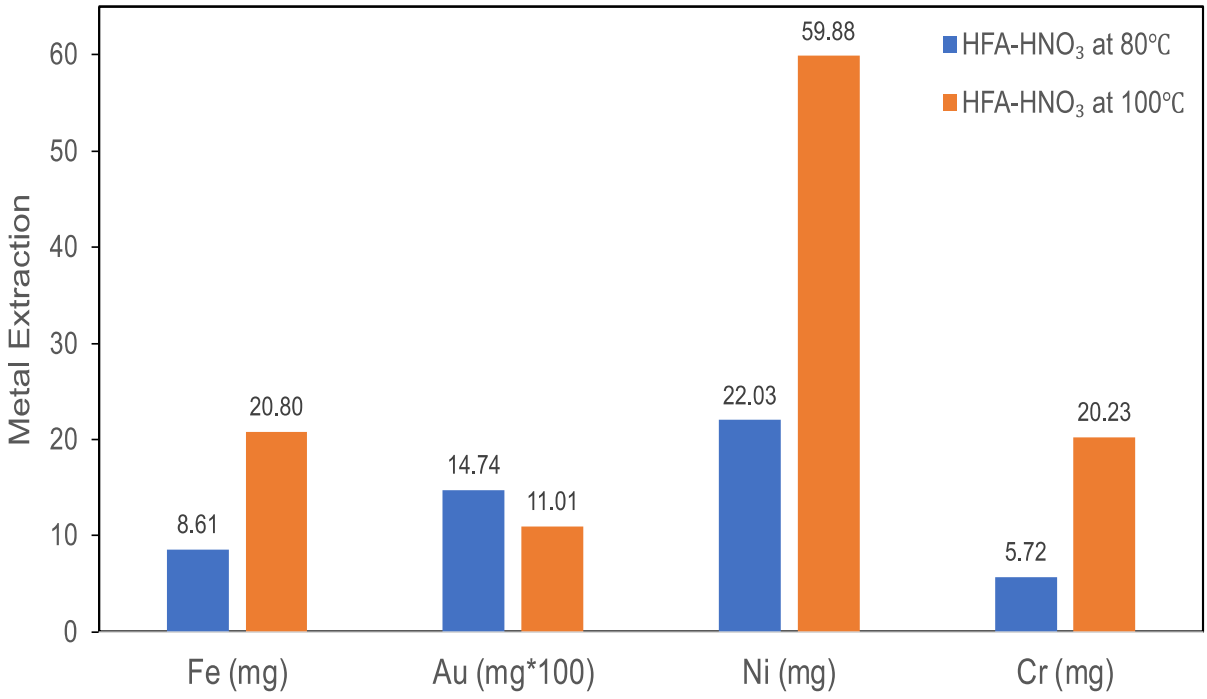


*Figure 4.9: HFA-HNO_3 (20 mL of 6.34 HNO_3 and 3 mL HFA) metal extraction over a temperature range (80-100℃) for 8 hr at 100 Bar (Au is in mg*100 so that the difference can be seen).*

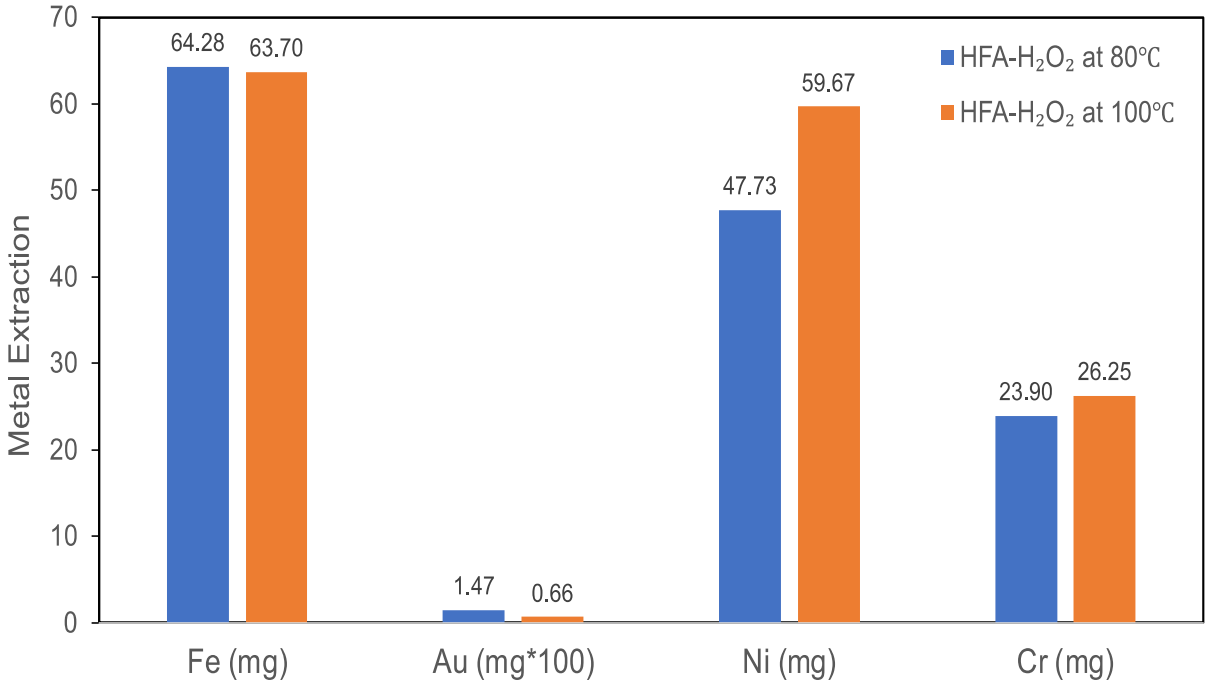


*Figure 4.10: HFA-H_2O_2 (20 mL of 6.34 H_2O_2 and 3 mL HFA) metal extraction over a temperature range (80-100℃) for 8 hr at 100 Bar (Au is in mg*100 so that the difference can be seen).*

4.4 Examining what effect changing operating parameters has on Au extraction.

The experimental results show that the AcAc-HNO_3-100°C system is the most promising system to use for extraction of zero valent Au in supercritical CO_2. The previous experiments used 3 g of the respective ligands. While it is customary to investigate molar ratios, in this particular part of the study we used masses and then volumes as we are looking at the extraction method from a production point of view i.e., the volume of ligand required per unit mass of ore. In later experiments, the molar ratio of ligand to oxidant will be evaluated. The ligand mass was converted to mL for each experiment and then enough oxidant was added to give a total liquid volume of 23 mL. For the AcAc experiments, 3 g is roughly 3 mL and this a 1:6.45 ratio (volume ratio).

The volumetric ratio of AcAc to HNO_3 was varied with the aim of better understanding what effect this would have on the extraction of Au. The results presented in Figure 4.13 show that there is 36.6 times more Au extracted when using a 1:1 volumetric ratio than there is when using the initial 1:6.45 ratio. This result is not unexpected as there is more of the ligand present in the system and thus as the Au oxidises, more of the Au-complex is formed. If there is a shortage of the ligand, then the Au ions revert into zero-valent Au. The results also show that there is almost no Au being extracted when using only AcAc (0.004 mg but rounded to 0 mg in Figure 4.11), this is because zero valent gold is extremely stable and thus does not readily dissolve in aqueous solutions without the presence of an oxidant (Lorösch, 2001).

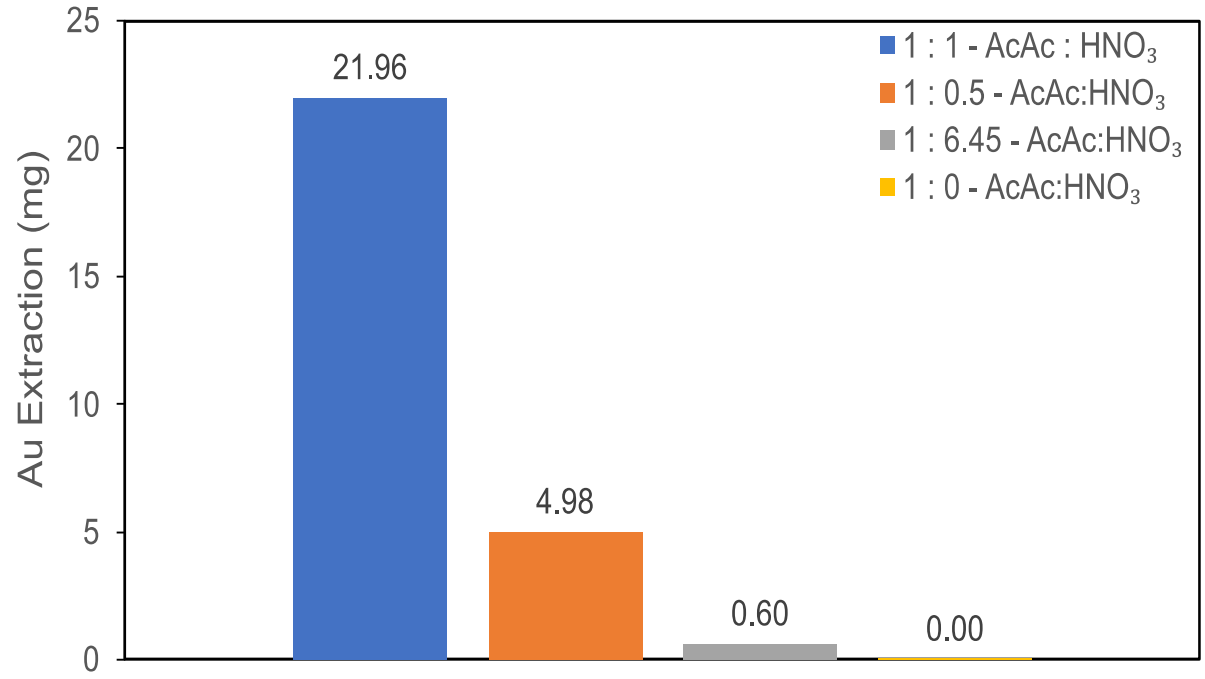


Figure 4.11: Au extracted when varying the volumetric ratio of AcAc to HNO_3 (6.34 M) at 100 Bar and 100℃ for 8 hours.

The extraction of Cr, Fe and Ni in the 1 mL:1 mL ratio system is much lower than those observed when using the other volumetric ratios (see Figure 4.12) and could suggest that 1:1 system is more reactive with respect to Au.

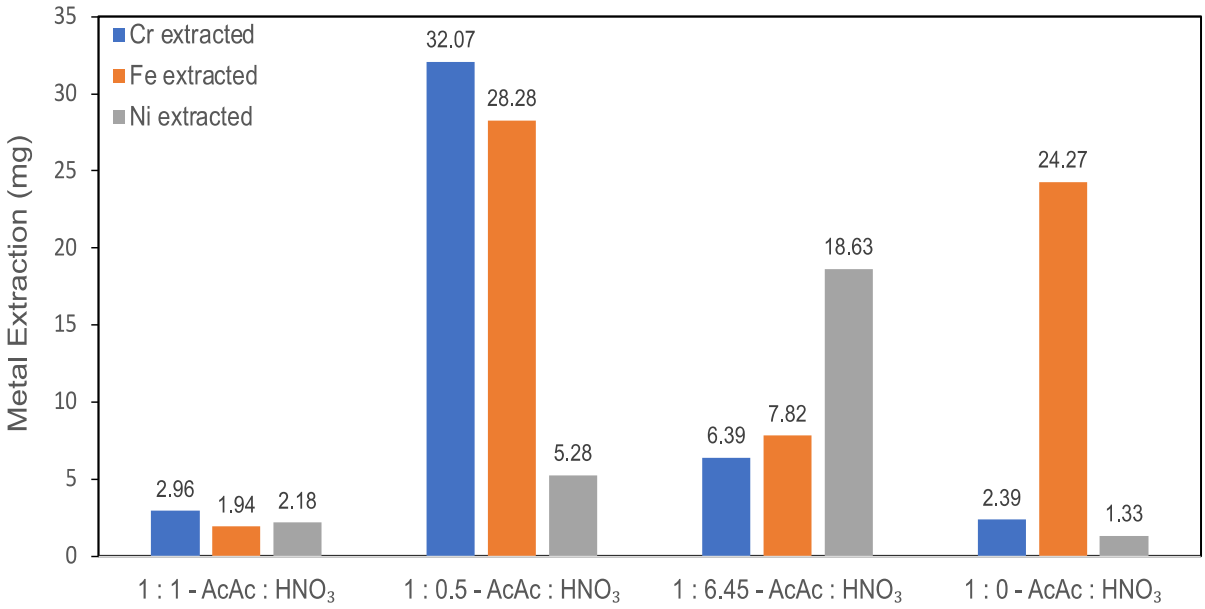


Figure 4.12: Cr, Fe and Ni extracted when varying the ratio of AcAc to HNO_3 at 100 Bar and 100℃ for 8 hours.

Based on the results in Figure 4.12, a 1 mL AcAc : 1 mL HNO_3 volumetric ratio system at 100^{o}C proved to be the highest gold extraction system.

It was observed during the experiments that the seal between the Hastelloy liner and the reactor lid failed due to the elevated temperatures and high pressures. This meant that the SCF was leaking into the stainless-steel reactor and thus high amounts of Fe were extracted as seen in the results above. It was noticed that the Hastelloy container was becoming dull, which is a good indication that there is some form of corrosion taking place (the Fe, Cr and Ni results in all experiments to date provide analytical proof of this). A microscope was used to identify the corrosion and the images can be seen in Figures 4.13 and 4.14.

Figure 4.13 is an image of the Hastelloy container, the surface is rough and if one examines the top right corner of the image, there is a well-defined mark, these are all indications of corrosion. Figure 4.14 is an image taken of the bottom of the stainless-steel reactor, it can be seen that there is pitting present.

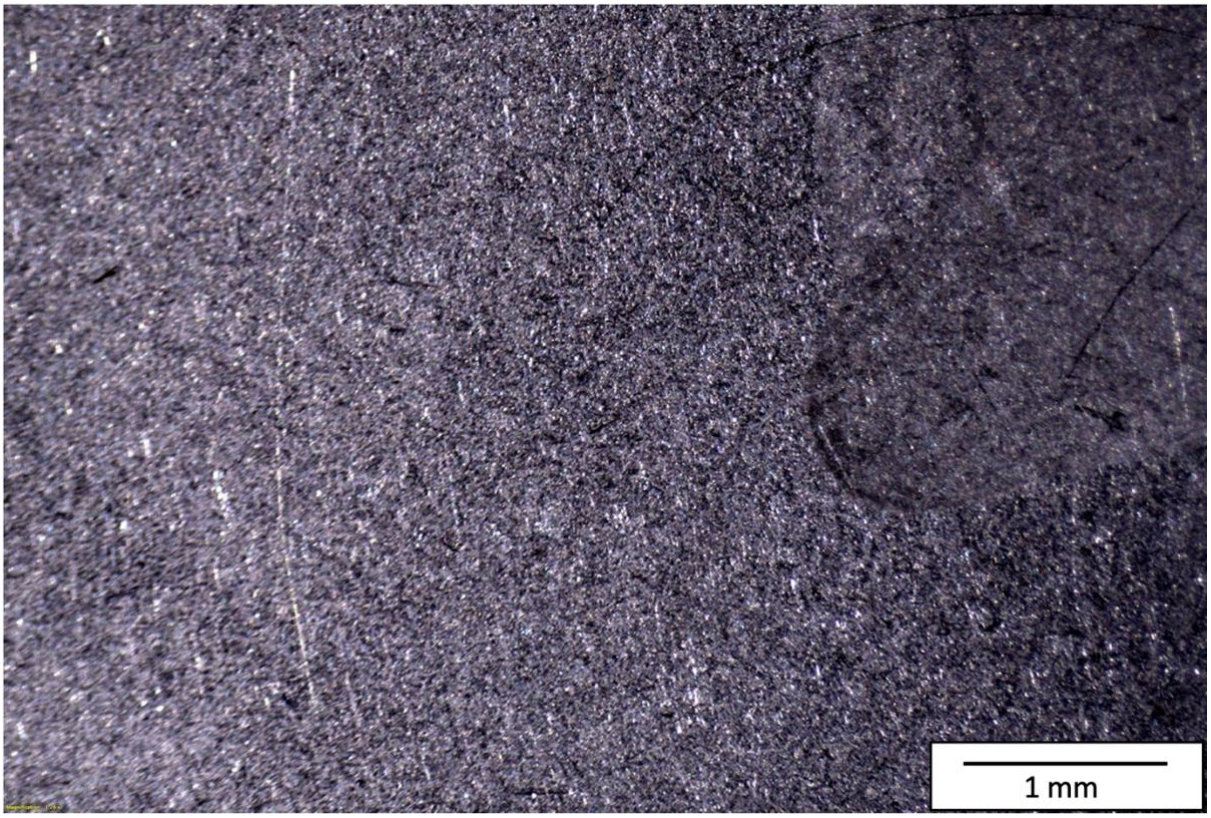


Figure 4.13: Corrosion of the Hastelloy bucket.

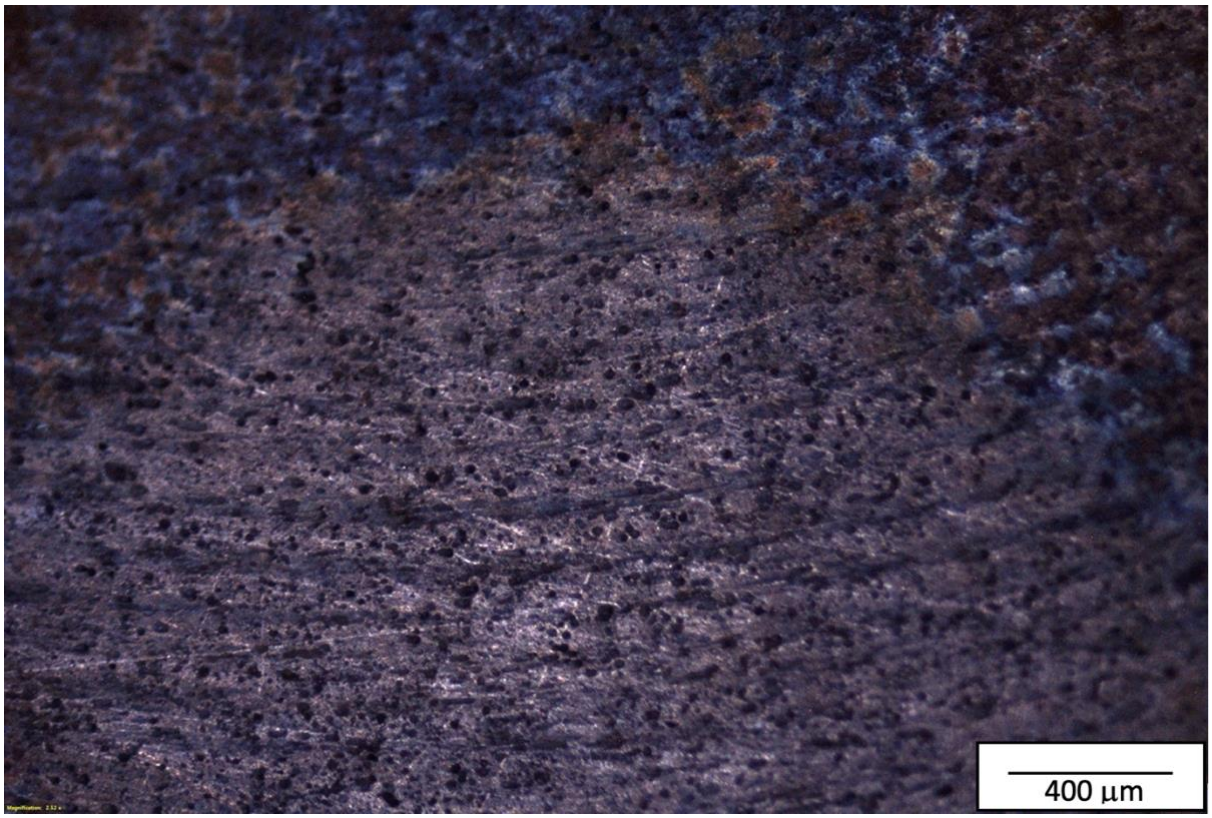


Figure 4.14: Corrosion of the stainless steel reactor.

Hastelloy's are well known for their corrosion resistant properties, however the Hastelloy liner is undergoing substantial corrosive attack under the conditions used in this research. To minimize corrosion of the reactor and prevent consumption of the reagents in the system, the Hastelloy liner was replaced by an inert Teflon liner. Due to the design of the reactor, the thermowell was still exposed to the reaction liquid.

The results from experiments performed in the reactor containing a Teflon liner are presented in Figure 4.15. When using a Teflon liner, the amounts of Cr and Ni that was extracted decreased, by an order of magnitude, from 2.96 mg and 2.18 mg to 0.62 mg (average) and 0.17 mg (average), respectively. This is exactly what was expected, however there was an increase in the amount of Fe that was extracted. The slight increase in Fe extraction could simply be due to more extractant being available to extract Fe from the exposed stainless steel thermowell.

Most noticeably the amount of Au extracted decreased from 21.96 mg to 11.86 mg when using the Teflon liner and was not the expected result. This is a 46% decrease in

Au extraction. It is believed that the decreased Au extraction suggests that the Cr or Ni ions could have an influence on the reaction. However more research needs to be conducted to prove this hypothesis. The Teflon liner eventually buckled due to the high pressures and temperatures within the reactor. The Teflon liner should be designed with expansion in mind or ring supports should be added to prevent buckling.

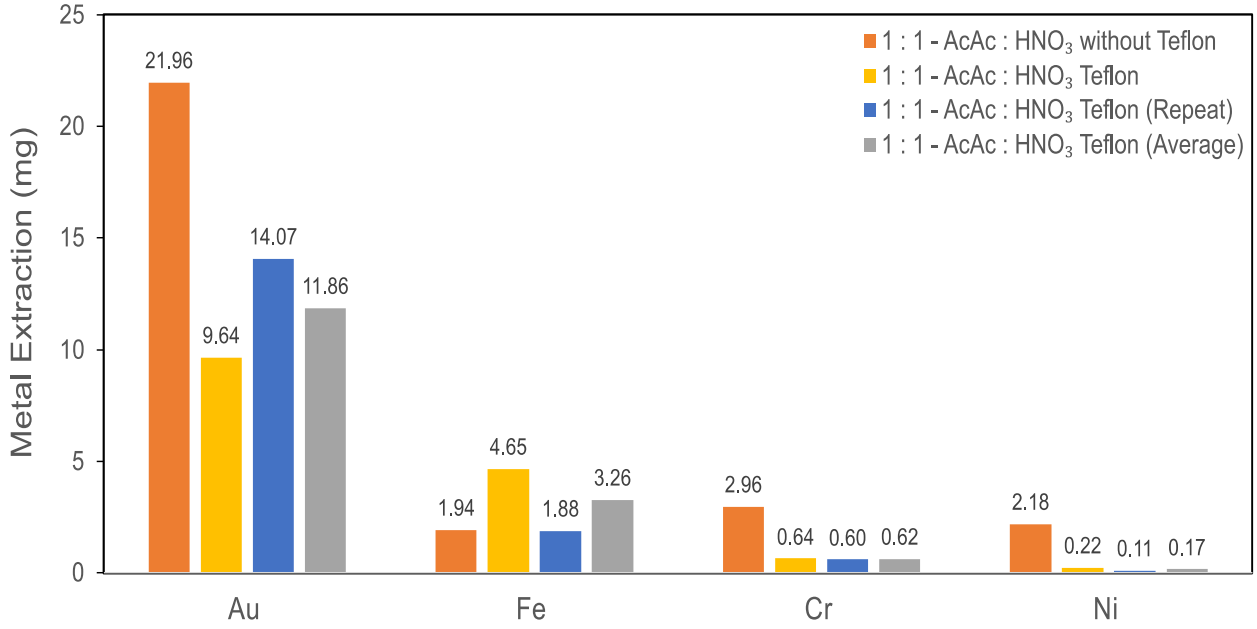


Figure 4.15: Metals extracted when using a Hastelloy bucket vs a Teflon liner at 100 Bar and 100 ℃ for 8 hours.

As mentioned before, one of the aims of this research was to identify the possible reactions that are taking place. One of the most important reactions is the extraction of the zero valent Au, using the HNO_3 and AcAc. As seen in the review of literature, Aqua Regia can be used in the dissolution of zero valent Au. Using this equation as a reference, a reaction is proposed for the extraction of Au using AcAc and HNO_3 (refer to Equation 2). The complex that is formed is assumed to be neutrally charged and not negatively charged like the $AuCl_4^-$ ion in the aqua regia system as seen in Equation 1.

Equation 1

$$Au_{(s)} + HNO_{3\,(aq)} + 4HCl_{(aq)} \rightarrow H(AuCl_4)_{(aq)} + 2H_2O_{(l)} + NO_{(g)}$$

Equation 2

$$Au_{(s)} + 3HNO_{3_{(aq)}} + 3C_5H_8O_{2_{(org)}} \rightarrow Au(C_5H_7O_2)_{3_{(org)}} + 3H_2O_{(aq)} + 3NO_{2_{(g)}}$$

The molar ratio of AcAc to HNO_3 was varied to determine the plausibility of the proposed equation (Equation 2). The total volume of the system was maintained at an overall volume of 23 mL. The results are presented in Figure 4.16 and it can be seen that there is a significant increase in the amount of Au (64.65 mg) that is extracted when the molar ratio of AcAc to HNO_3 is 1:1. The amount of Au extracted decreases when moving away from a 1:1 ratio, this finding sheds light on the possible reaction that could be taking place and in doing so suggests that the proposed reaction is plausible. This of course only holds true if the assumptions made hold true and that the AcAc doesn't decompose leading to the formation of another Au-complex besides the suggested $Au(C_5H_8O_2)_3$.

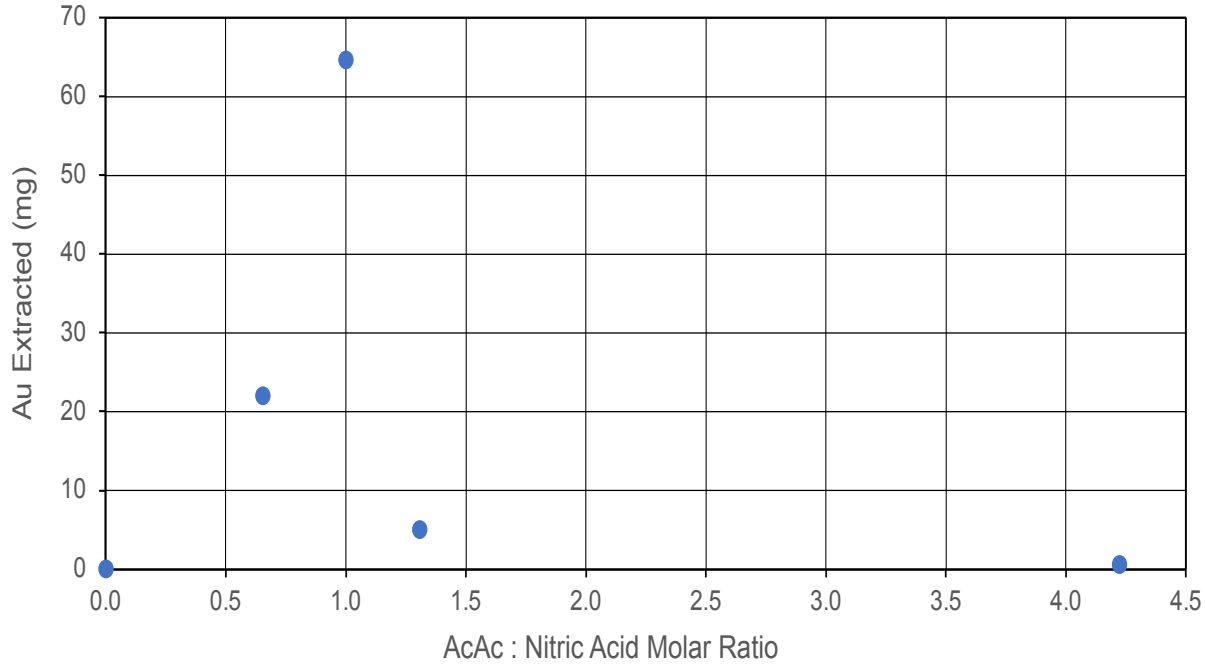


Figure 4.16: Au extracted when changing the molar ratio of AcAc to HNO_3 at 100 Bar and 100℃ for 8 hours.

When using the 1:1 molar ratio with the AcAc and HNO_3 (6.34 M), the volume of AcAc needed is 9.1 mL and HNO_3 is 13.9 mL. This volumetric ratio was used to determine what effect changing the concentration of the oxidant (HNO_3) would have on the

amount of Au extracted. The results from these experiments are presented in Figure 4.17. There is an increasing trend which is exponential in nature. This means that the amount of Au extracted is sensitive to the oxidant concentration.

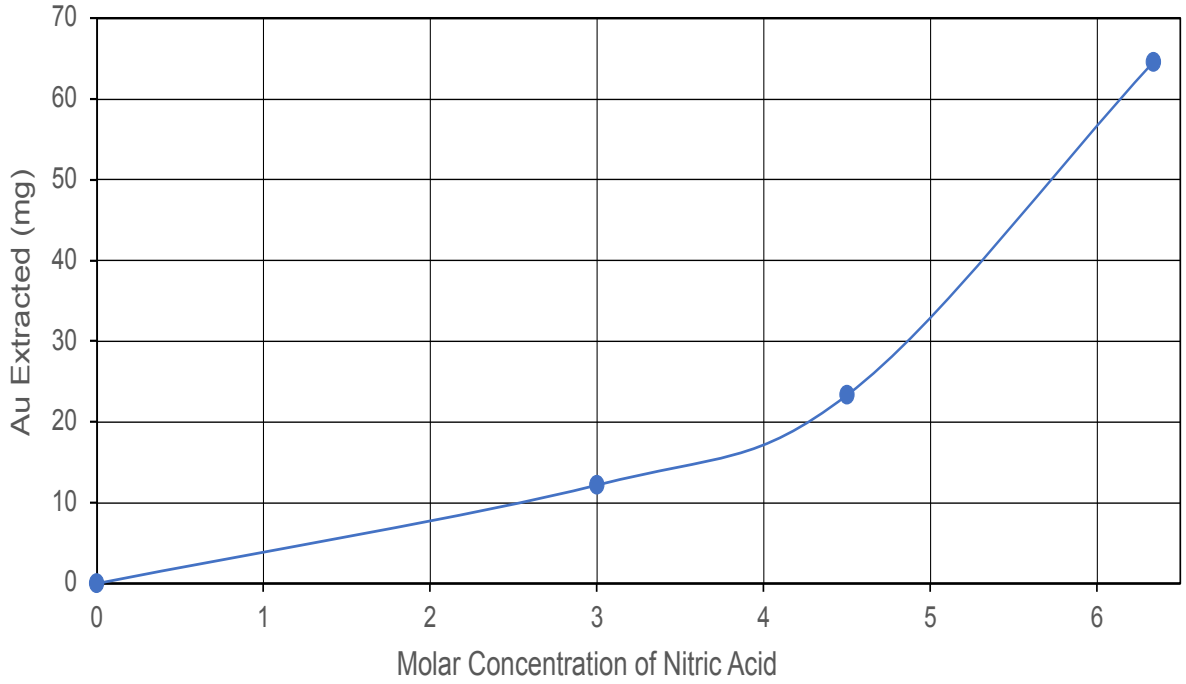


Figure 4.17: The effect of HNO_3 concentration on the extraction of Au at 100 Bar and 100℃ for 8 hours.

The results presented so far (see chapter 4) have proven that Au can be extracted when using the newly developed process.

4.5 Extraction of gold from gold tailings using an AcAc-HNO_3 -$ScCO_2$ system

It has been seen in Chapter 3 that the tailings samples that were prepared are indeed representative of the bulk. Two repeat tests were conducted to test the viability of this process on the DRD Gold tailings. When using ICP-MS to test the amount of Au that was extracted, into the liquid phase, it was determined that there were far higher amounts of Au present than should be in the ore. When calculating backwards the Au content was calculated to be 4.45 g/t (test 1) and 8.40 g/t (test 2). This could be explained by focusing on the ICP-MS analysis technique that was used. Manganese (Mn) has a minor spectral line at 242.794 nm, while the wavelength used to measure the amount of Au is at 242.795 nm. This means that the high readings could be due to

spectral overlap. In other words, some of the Mn that is being extracted from the ore is contributing to the perceived gold content of the solution. The ICP-MS analyst checked the primary spectra line for the two different tests, and he found that test 2 had more Mn than test 1 and this explains why test 2 had a higher Au reading. It may also be due to the fact that no matrix matching was done between the standards used for the calibration curve construction and the samples analysed. Attention to developing an accurate method of analysis would be a requirement for future research. It should be noted that no Mn was present in the preceding samples; therefore, this finding has no impact on the results presented earlier in this chapter.

The results from the pregnant leach solutions are therefore unusable when trying to calculate the percentage of Au that was extracted from the tailings. An alternative was to digest the remaining solids to determine the Au content that remained in the solid and calculate the amount of Au extracted. This was possible as the initial mass of ore that was placed into the reactor was known and the final mass that was recovered after the extraction experiments could be measured. These results are presented in Table 4.5 below.

Table 4.5: Metal analysis of the tailings residue at experimental conditions 100°C, 100 Bar, 8 hours and 23 mL ligand-oxidant solution (1:1 molar ratio).

Experiment	Cr (mg/kg)	Fe (mg/kg)	Ni (mg/kg)	Cu (mg/kg)	Au (mg/kg)
Extract 1 Rep 1	179.50	15854.32	586.50	53.06	0.121
Extract 1 Rep 2	189.21	16004.09	634.36	39.37	0.151
Extract 1 Rep 3	187.41	15931.93	668.69	49.89	0.129
Extract 1 Average†	185.37±10.33	15930.12±148.80	629.85±82.56	47.44±14.33	0.134±0.031
Extract 2 Rep 1	218.59	17326.31	617.09	44.48	0.152
Extract 2 Rep 2	220.30	17103.26	613.32	33.40	0.153
Extract 2 Rep 3	177.61	15342.85	478.57	27.90	0.153
Extract 2 Average†	205.50±48.34	16590.81±2173.00	569.66±157.82	35.26±16.89	0.152±0.001

† Uncertainties are of type A (statistical—based on the standard deviation of three measurements). They assume a normal distribution and are expressed at the 95% confidence level.

The results from Table 4.5 show that there had indeed been some Au extraction. In Chapter 3 it was determined that the amount of Au in the tailings was on average 0.277 mg/kg. The amount of Au extracted in tests 1 and 2 are 0.144 mg/kg and 0.125

mg/kg, respectively. The following equation can be used to calculate the percentage of Au extracted:

$$Percentage\ Au\ extracted = \left(\frac{Au\ initial - Au\ final}{Au\ initial}\right) * 100$$

Thus, it has been determined that 51.62% of the Au was extracted in the first experiment and 45.13% in the second experiment. Both reactions were performed at the same conditions which gives an average Au extraction of 48.38%.

The DRG Gold plant feed has been analysed in previous research (Dworzanowski, 2018) and it was concluded that around 5% of the total gold is present in electrum. Additionally, the remaining 95% is present as free gold (6.5%) or is associated with a variety of minerals, namely in sulphides (54.7%), in silicates (18.8%), in oxides (12%) and in uranium minerals (8%). The DRD Gold leaching process recovers the easily accessible Au (see chapter 1), meaning that the remaining Au is more difficult to access, i.e., it is locked up in refractory sulphides and silicates.

The 48.38% Au extraction illustrates that the process developed in this research is capable of accessing Au which is locked up in refractory minerals. However, it is well known that SiO_2 is very stable and unless there are fractures in the SiO_2, the Au locked within the SiO_2 is likely not accessible when using this process. The reason for saying this is that to break down SiO_2, a strong acid such as hydrofluoric acid is needed. Further investigation is needed to determine whether an ore with a high Au-sulphide association, as opposed to a high Au-SiO_2 association, will lead to higher Au extractions when using the method developed in this research.

5 Conclusion

The research investigated using a supercritical fluid extraction method to extract zero valent gold and applied the method to a refractory mine tailings sample. The proposed extraction solution (oxidant and ligand) is safer than the method proposed by Mawire (2019) as it excludes the use of tributyl phosphate. In terms of the objectives set out for the research, the following conclusions were reached.

5.1 To develop a method to analyse the pregnant leach solution produced in Mawire's (2019) extraction method.

This research identified a technique that can be used to analyse the amount of gold contained in a pregnant TBP-HNO_3-[Hbet][TF_2N] leach solution. The process involves breaking down the organic compounds in the pregnant leach solution using concentrated nitric acid as well as concentrated perchloric acid. Aqua regia was then used to dissolve any gold in solution. Even though the technique works, it has been concluded that it is time consuming and produces harmful vapours when the organic compound (TBP) is digested.

5.2 To determine whether the extraction method proposed by Mawire (2019) is safe.

During the development of the analysis technique, a safety concern was raised. The digestion of the TBP is a volatile process and thus produces very strong vapours. The TBP and other digestion vapours were detected by the analysts, despite wearing respirators and working in a fume hood. According to the safety data sheet for TBP, it is "suspected of causing cancer", which poses a great safety risk to people and the environment. Thus, it can be concluded that the method developed by Mawire (2019) is not safe as it requires the use of a suspected carcinogen. If TBP is used, one must follow strict guidelines for working with carcinogenic substances and put in place additional safety measures.

5.3 To determine if there is an alternative oxidant to the TBP-HNO_3 adduct used in Mawire's (2019) work and if so, investigate the extraction of gold in supercritical CO_2 utilising a new reagent mixture.

This research investigating replacing the TPB-HNO_3 adduct with either HNO_3 (strong acid) or H_2O_2 (weak acid). It was found that the most promising oxidant to use was HNO_3 with β-diketones. The amount of Au extracted when using the HNO_3-β-diketone systems were at least an order of magnitude greater than those of the H_2O_2-β-diketone systems.

5.4 To determine if there is a ligand that can extract more gold than [Hbet][Tf_2N] and HFA.

It was determined that AcAc can be used to extract more gold (in the studied systems) than HFA and [Hbet][Tf_2N]. When comparing the HFA-HNO_3 and AcAc-HNO_3 systems, it was determined that roughly 2.5 times more gold was extracted in the AcAc-HNO_3 system. The results from the research suggest that the zero valent gold is more reactive to AcAc (non-fluorinated β-diketone) than it is when using HFA (fluorinated β-diketone) in a supercritical environment.

5.5 To determine, by applying a more fundamental approach (using pure gold instead of tailings), under what conditions zero valent gold is extracted using supercritical fluids.

The following conditions were evaluated; temperature (80-100^{o}C), HNO_3 concentration (0-6.34 M), volumetric ratio of AcAc : HNO_3 (1 : [0; 0.5; 1; 6.45]), molar ratio of AcAc : HNO_3 (1 : [0; 0.65; 1; 1.38; 4.22]). It can be concluded that under the conditions studied, that the best conditions for zero valent gold extraction occurred after 8 hours, at 100^{o}C, at 100 Bar, a volumetric ratio of 1 AcAc : 1 HNO_3, and a molar ratio of 1 AcAc : 1 HNO_3 (6.34 M) when using the reactor with a Hastelloy liner. At these conditions a maximum of 64.65 mg of gold was extracted (reported in terms of mass extracted as there was a large excess of gold used in the experiments).

It was also observed that the liner underwent corrosion during all of the extraction experiments, indicating side leaching reactions. When a Teflon liner was used, the gold extraction dropped pointing to a possible positive effect of Cr and Ni (some of the extracted metals) on the extraction of gold.

5.6 To apply the new method to a DRD Gold tailings sample.

Using the best operating conditions identified in this research, the new supercritical fluid extraction method was able to extract zero valent gold from the DRD Gold tailings. The average amount of gold that was extracted from the low grade, refractory tailings was 48.38%. This extraction was achieved using a safer reagent (non-carcinogenic).

5.7 Thoughts on the hypothesis.

This research was able to prove the hypothesis set out in the beginning of the paper. The newly developed supercritical fluid extraction method can extract zero valent gold from the refractory DRD Gold mine tailings, and this has been achieved in a safe and efficient manner.

5.8 Recommendations for future research

Future studies should investigate the following:

- The interaction of the Cr and Ni ions in the extraction of gold should be investigated to better understand how their presence influences the amount of gold extracted.
- Investigations into the reactions that are taking place need to be carried out so that one can definitively state what the reaction equations are as well as the structures of the gold-complexes that are being formed.
- The sensitivities of the reagents to one another should be investigated i.e. are there side reactions that are occurring between the reagents, leading to less gold being extracted.
- Studying the reaction mechanisms of gold extraction by determining the influence of the operating parameters on the extraction of gold in an inert reactor.
- Applying the HFA-HNO_3 system to the recycling of battery materials as it was observed that large amounts of Ni were extracted when using this system.

- Adding a reagent collection vessel to the process so that the reactor does not vent straight into the fume hood. If the venting is not controlled properly then products can be lost.

6 References

Ali, I.A (2021). Gas-phase extraction of gold from tailings: insights from density functional theory and the emperical *(MSc Dissertation),* The University of the Witwatersrand, Johannesburg, South Africa.

Altinkaya, P., Mäkinen, J., Kinnunen, P., Kolehmainen, E., Haapalainen, M. & Lundström, M. (2018). Effect of biological pretreatment on metal extraction from flotation tailings for chloride leaching. *Minerals Engineering*, 129, pp. 47-53.

Amankwah, R.K. & Ofori-Sarpong, C. (2011). Microwave heating of gold ores for enhanced grindability and cyanide amenability. *Minerals Engineering*, 24, pp. 541-544.

Argenta, A.B., Reis, C.M., Mello, G.P., Dotto, G.L., Tanabe, E.H. & Bertuol, D.A. (2017). Supercritical CO_2 extraction of indium present in liquid crystal displays from discarded cell phones using organic acids. *The Journal of Supercritical* Fluids, 120, pp. 95-101.

Ashraf-Khorassani, M., Combs, M.T. & Taylor, L.T. (1997a). Review-Supercritical fluid extraction of metal ions and metal chelates from different environments. *Journal of Chromatography A*, 774, pp. 37-49.

Ashraf-Khorassani, M., Combs, M.T. & Taylor, L.T. (1997b). Solubility of metal chelates and their extraction from an aqueous environment via supercritical CO_2. *Talanta*, 44, pp.755-763.

Britannica (2020). South Africa- Gold Mining. [Online] Available at: https://www.britannica.com/place/South-Africa/Gold-mining [Accessed 18 March 2020].

Brown, T.L., LeMay, H.E., Bursten, B.E., Murphy, C.J., Woodward, P.M. & Stolzfus, M.W. (2015). Appendix E: Standard Reduction Potentials at 25°C. In, *Chemistry The Central Science, 13TH Edition (*pp.1143*).* Pearson

CEIC (2020). South African Gold Production (Data and Charts,1990-2019). [Online] Available at: https://www.ceicdata.com/en/indicator/south-africa/gold-production
[Accessed 18 March 2020].

de Carvalho, L.C., da Silva, S.R., Giardini, R.M.N., de Souza, L.F.C. & Leão V.A. (2019). Bio-oxidation of refractory gold ores containing stibnite and gudmundite. *Environmental Technology & Innovation*, Volume 15, Article 100390.

Ding, X., Liu, Q., Hou, X. & Fang, T. (2017). Supercritical Fluid Extraction of Metal Chelate: A Review. *Critical Reviews In Analytical Chemistry*, 47, pp.99-118.

DRDGold (2019). *2019* Annual Integrated Repor*t.* South Africa*:* DRDGold Limited.

Dworzanowski, M. (2018). A mineralogical investigation into the nature and deportment of gold in ERGO flotation feed and concentrate. *The University of The Witwatersrand – School of Chemical and Metallurgical Engineering* [PowerPoint Slides].

Erkey, C. (2000). Supercritical carbon dioxide extraction of metals from aqueous solutions: a review. *Journal of Supercritical Fluids*, 17, pp.259-287.

Fraser, K.S., Walton, R.H. & Wells, J.A. (1991). Processing Of Refractory Gold Ores. *Minerals Engineering*, 4, pp. 1029-1041.

Friend, W.Z. & Wise, E.M. (1964). Chapter 10: Corrosion Resistance of Gold. In Wise, E.M. (Ed), *Gold: Recovery, Properties and Applications* (pp. 180-202). Canada: Van Nostrand.

Ghoreishi, S.M., Hedayati, A. & Ansari, K. (2016). Experimental investigation and optimization of supercritical carbon dioxide extraction of toxic heavy metals from solid waste using different modifiers and chelating agents. *The Journal of Supercritical Fluids,* 117, pp. 131-137.

Glennon, J.D., Harris, S.J., Walker, A., McSweeney, C.C. & O'connell, M. (1999). Carrying gold in supercritical CO2. *Gold Bulletin,* Volume 32, pp. 52-58.

Harris, D.C. (1990). I. Fundamental aspects of gold deposits: The Mineralogy of gold and its relevance to gold recoveries. *Mineralium Deposita*, 25, S3 – S7.

Heiser, J. (2014). Business model innovation ensuring success for DRDGold in the declining gold mining industry (Masters Thesis)., Stellenbosch: Stellenbosch University.

Hongwu, Y., Zhixian, Z., Mingrui, Z., Xianxin, Z. & Boyang, R. (1991). Solvent Extraction of Gold(III) by Benzo-15-Crown-5 and Characterization of the Crystalline Extracted Complex. *Polyhedron*, 10, pp.1025-1029.

Janisch, P.R. (1986). Gold in South Africa. *Journal Of The South African Institute Of Mining And Metallurgy, Vol.* 86, Issue 8, pp. 273-316.

Joung, S.N., Yoon, S.J., Kim, S.Y & Yoo, K.P. (2000). Extraction of lanthanide ions from aqueous solution by modified supercritical CO_2: tri-n-butylphosphate+CO_2 and bis-2-ethylhexyl phosphoric acid+CO_2. *Journal of Supercritical Fluids,* 18, pp. 157-166.

Kaksonen, A.H., Perrot, F., Morrios, C., Rea, S., Benvie, B., Austin, P. & Hackl, R. (2014). Evaluation of submerged bio-oxidation concept for refractory gold ores. *Hydrometallurgy*, 141, pp. 117-125.

Knez, Ž., Pantić, M., Cör, D., Novac, Z. & Hrnčič, M. (2019). Are supercritical fluids solvents for the future?. *Chemical Engineering and Processing: Process Intensification, Volume* 14, Article 107532.

La Brooy, S.R., Linge, H.G. & Walker, G.S. (1994). Review Of Gold Extraction From Ores. *Minerals Engineering*, 7, pp. 1213-1241.

Laintz, K.E., Wai, C.M., Yonker, C.R. & Smith, R.D. (1991). Solubility of Fluorinated Metal Diethyldithiocarbamates in Supercritical Carbon Dioxide. *Journal of Supercritical Fluids,* 4, pp. 194-198.

Li, K. & Xu, Z. (2019). A review of current progress of supercritical fluid technologies for e-waste treatment. *Journal of Cleaner Production,* 227, pp. 794-809.

Lin, Y., Smart, N. & Wai, C. (1995). Supercritical fluid extraction and chromatography of metal chelates and organometallic compounds. *Trends in Analytical Chemistry,* 14, pp. 123-132.

Liu, K., Zhang, Z. & Zhang, F. (2016). Direct extraction of palladium and silver from waste printed circuit boards powder by supercritical fluids oxidation-extraction process. *Journal of Hazardous Materials*, 318, pp. 216-223.

Lorösch, J. (2001). Process and Environmental Chemistry of Cyanidation.: Degussa AG.

Lurie, J. (2013). Chapter 9: South African Stratigraphy. In, *South African Geology for Mining, Metallurgical, Hydrological and Civil Engineering* (pp.44-55). Johannesburg: Lupon Publishing.

Marsden J.O. & House, C.I. (2006). The Chemistry of Gold Extraction (2nd Edition). USA: Society for Mining, Metallurgy, and Exploration.

Mawire, G.T. (2019). Supercritical extraction of gold from refractory ores *(MSc Dissertation),* The University of the Witwatersrand, Johannesburg, South Africa.

Meng, N., Jiang, D., Liu, Y., Gao, Z., Cao, Y., Zhang, J., Gu, J. & Han, Y. (2016). Sulfur transformation in coal during supercritical water gasification. *Fuel*, 186, pp. 394-404.

Minerals Council South Africa, 2020. *Gold (Key Facts and Figures/Gold mining in South Africa).*[Online] Available at: https://www.mineralscouncil.org.za/sa-mining/gold [Accessed 18 March 2020].

Muir, A., Mitchell, J., Flatman, S. & Sabbagha, C. (2005). A practical guide to re-treatment of gold processing residues. *Minerals Engineersing,* Issue 18, pp. 811-824.

Nicoli, N. (1995). The Crisis in South African Gold Mining. *World Development,* 23, pp. 857-868.

Nicol, M.J., Fleming, C.A. & Paul, R.L. (1987). Chapter 15: The Chemistry of the Extraction of Gold. In Stanley, G.G. (Ed.), *The Extractive Metallurgy of Gold in South Africa* (pp. 831-905).South Africa: South African Institure of Mining and Metallurgy.

Nanthakumar, B., Pickles, C.A. & Kelebek, S. (2007). Microwave pretreatment of a double refractory gold ore. *Minerals Engineering*, 20, pp. 1109-1119.

Nwaila, G., Becker, M., Ghorbani, Y., Petersen, J., Reid, D.L., Bam, L.C., de Beer, F.C., & Franzidis, J-P. (2013). A Geometallurgical Study of the Witwatersrand Gold Ore at Carletonville, South Africa. In: *The Second AUSIMM International Geometallurgy Conference.* Brisbane: pp. 75-83.

Olubambi, P.A. (2009). Influence of microwave pretreatment on the bioleaching behaviour of low-grade complex sulphide ores. *Hydrometallurgy*, 95, pp.159-165.

Özel, M.Z., Burford, M.D., Clifford, A.A., Bartle, K.D., Shadrin, A.S., Smart, N.G. & Tinker, N.D. (1997). Supercritical fluid extraction of cobalt with fluorinated and non-fluorinated β-diketones. *Analytical Chimica Acta*, 346, pp. 73-80.

Pitchaiah, K.C., Sujatha, K., Deepitha, J., Ghosh, S. & Sivaraman, N. (2019). Recovery of uranium and plutonium from pyrochemical salt matrix using supercritical fluid extraction. *The Journal of Supercritical Fluids*, 147, pp. 194-204.

Prabhat, P., Rao, A., Kumar, P. & Tomar, B. (2016). Supercritical fluid extraction and purification of uranium from crude sodium diuranate. *Hydrometallurgy*, 164, pp. 177-183.

Pretorius D.A. (1974). The Nature of The Witwatersrand Gold-Uranium Deposits. *University of The Witwatersrand – Economic Geology Research Unit. Information Circular No.* 86.

Reisdörfer, G., Bertuol, D. & Tanabe, E. (2020). Extraction of neodymium from hard disk drives using supercritical CO2 with T organic acids solutions acting as cosolvents. *Journal of CO2 Utilization,* 35, pp. 277-287.

Sengers, J.M.H. (2000). Supercritical Fluids: Their Properties and Applications. In Kiran, E., Debenedetti, P.G. & Peters, C.J. (Eds.), *Supercritical Fluids: NATO Science Series, Series E: Applied Sciences, volume 366* (pp. 1-29). Netherlands: Kluwer Academic Publishers

Shamispur, M., Yamini, Y. & Hasan, J. (2001). Solubility of large crown ethers in supercritical carbon dioxide. *Fluid Phase Equilibria*, 186, pp. 39-46.

Silwa, W. & Deska, M. (2008). Calixarene Complexes with Soft Metal Ions. *Arkivoc, 2008(i),* pp. 87-127. Retrieved from: [https://www.researchgate.net/publication/225163654_Calixarene_Complexes_with_Metal_Ions] Accessed: 23/04/2020

Smart, N.G., Carleson, T., Kast, T., Clifford, A.A., Burford, M.D. & Wai, C.M. (1997). Review–Solubility of chelating agents and metal-containing compounds in supercritical fluid carbon dioxide. *Talanta*, 44, pp. 137-150.

Steed, J.W. (2001). First- and second-sphere coordination chemistry of alkali metal crown ether complexes. *Coordination Chemistry Reviews*, 215, pp. 171-221.

Syed, S. (2012). Recovery of gold from secondary sources-A review. *Hydrometallurgy*, 115-116, pp. 30-51.

Tomioka, O., Enoiuda, Y. & Yamaoto, I. (2000). Cleaning of materials contaminated with metal oxides through supercritical fluid extraction with CO2 containing TBP. *Progress in Nuclear Energy,* 37, Issue 1-4, pp. 417-422.

Wai, C.M., Wang, S., Liu, Y., Lopez-Avila, V. & Beckert, W.F. (1996). Evaluation of dithiocarbamates and β-diketones as chelating agents in supercritical fluid extraction of Cd, Pd and Hg from solid samples. *Talanta*, 43, pp. 2083-2091.

Wai, C.M. & Wang, S. (1997). Review - Supercritical fluid extraction: metals as complexes. *Journal Of Chromatography A*, 785, pp. 369-383.

Wang, J.S. & Wai, C.M. (2005). Dissolution of Precious Metals in Supercritical Carbon Dioxide. *Industrial and Engineering Chemistry Research*, 44, pp. 922-926.

Wang, J. & Zhuang, S. (2020). Cesium separation from radioactive waste by extraction and adsorption based on crown ethers and calixarenes. *Nuclear Engineering and Technology*, 52, pp. 328-336.

Wuhua, D., Pijia, C. & Yongjun, Z. (2010). Extraction of rare earth elements from their oxides using organophosphorus reagent complexes with HNO_3 and H_2O in supercritical CO_2. *Journal of Rare Earths*, 28, pp. 221- 226.

Xue, T. & Osseo-Asare, K. (1985). Heterogeneous equilibria in the Au-CN-H_2O and Ag-CN-H_2O systems. *Metallurgical Transactions B*, 16, pp. 455-463.

Yan, M., Hantoko, D., Kanchanatip, E., Zheng, R. & Zhong, Y., 2020. Valorization of sewage sludge through catalytic sub- and supercritical water gasification. *Journal of the Energy Institute.*

Yannopoulos, J.C (1991a). Chapter 2: Physical and Chemical Properties of Gold. In, *The Extractive Metallurgy of Gold* (pp.11-21). USA: Van Nostrand Reinhold.

Yannopoulos, J.C. (1991b). Chapter 5: Treatment of Refractory Gold Ores. In, *The Extractive Metallurgy of Gold* (pp.79-114). USA: Van Nostrand Reinhold.

Yannopoulos, J.C. (1991c). Chapter 8: Cyanidation of Gold Ores. In, *The Extractive Metallurgy of Gold* (pp.141-170). USA: Van Nostrand Reinhold.

Yannopoulos, J.C. (1991d). Chapter 9: Alternative leaching reagents for gold. In, *The Extractive Metallurgy of Gold* (pp.171-184). USA: Van Nostrand Reinhold.